



NTNU – Trondheim
Norwegian University of
Science and Technology

Estimation of Extreme Response

- in a Jack-up Platform by Application of
Stochastic Methods

Lars Holterud Aarsnes

Marine Technology

Submission date: June 2015

Supervisor: Sverre Kristian Haver, IMT

Co-supervisor: Jørgen Amdahl, IMT

Norwegian University of Science and Technology
Department of Marine Technology

Lars Holterud Aarsnes

Estimation of Extreme Response

... on a Jack-up Platform by Application of Stochastic Methods

Master of Science

Trondheim 10/06/2015

Supervisor: Professor II Sverre Haver

Norwegian University of Science and Technology

Faculty of Engineering Science and Technology

Department of Marine Technology



NTNU – Trondheim
Norwegian University of
Science and Technology

MASTER THESIS 2015

for

Stud. Techn. Lars Holterud Aarsnes

Estimation of Extreme Response for a Jack-up Platform

Estimering av ekstremrespons for en oppjekkbar plattform

Background

Jack-up structures are frequently used for drilling operations. The natural period of jack-ups are rather large – often well into the wave frequency range. The natural period depends heavily on the water depth and the sea bed conditions. For good quality sea bed conditions, the jack-up can be modelled as fixed to the sea bed if bucket or piled foundation are used. For a spudcan type foundation a fixed connection at sea bed will be too optimistic. For very soft sea bed conditions, a conservative approach will be to model the jack-up as pinned to the sea bed. In this thesis the base case solution should be a realistic level of fixity, but consequences of uncertainties related to degree of fixity shall be investigated.

Since the largest natural period is likely to be well inside the wave frequency range, the jack-up motions and structural response will be significantly affected by dynamics. A reasonable estimate of the quasi-static load and corresponding response can be calculated using the design wave approach based on a Stokes 5th order wave profile. A question in this connection is what parameters shall be used to define the design Stokes 5th profile? This question shall be discussed and a recommendation regarding the wave characteristics shall be made.

The estimation of the dynamics effects is a greater challenge. Various approaches that can be adopted shall be discussed, but focus shall be placed on the equivalent dynamic amplification factor, EDAF. EDAF is defined as the factor that may be used to multiply the q-probability quasi-static load/load effect in order to obtain a reasonable estimate of the q-probability dynamic load effect. In general, the q-probability response is most consistently estimated using a long-term response analysis. An alternative approach for complicated response problems is to apply the metocean contour method. It is recommended to adopt this method for the present study.

The necessary weather information will be given by the Norwegian hindcast data base, NORA10, which contains weather characteristics every 3 hours from 1957 – 2014.

The work is proposed carried out in the following steps:

1. Establish the wave climate description for a Southern North sea position from 57 years of hindcast data.
2. Establish the finite element model for USFOS simulations. Ensure that USFOS work as expected and perform an eigenvalue analysis. Discuss the consequence of the estimated natural periods with respect to predicting the extreme responses for design. Indicate the uncertainty band for the natural periods due to uncertainties in the degree of fixity of platform legs to sea bottom.
3. Discuss the methodology for obtaining adequate estimates of the q-probability responses of the structure based on the quasi-static q-probability load using Stokes 5th regular wave. The dynamics are accounted for by the EDAF factor or an equivalent acceleration field.
4. Estimate the q-probability quasi-static response values for various directions. Select worst direction and calculate quasi-static q-probability values for overturning moment (OTM) and deck displacement (DD). The present standard approach is to define the q-probability Stokes 5th order wave profile by the q-probability wave height, h_q , and the most unfavorable wave period with a 90% confidence interval. The approach suggested by the coming revision of the N-003 is to define the design wave profile by the q-probability wave crest height and the associated mean wave period. Investigate the consequences of replacing the present definition with the new recommendation.
5. Describe the linear Gaussian surface process and approximations used regarding wave kinematics above the mean free surface. Discuss how one can account approximately by inaccuracies in the present formulation.

The future recommendation will be to use a second order surface process. Although a linear Gaussian surface elevation is used in this thesis discuss briefly the advantages achieved by introducing a second order surface process.

6. Estimate EDAF for the selected heading. This includes finding the worst sea state on the q-probability $H_s - T_p$ contours - both for quasi-static response - and dynamic response analysis. Estimate the percentile in the quasi-static q-probability 3-hour extreme value distribution of the worst sea state that agrees with the q-probability quasi-static value obtained with the Stokes 5th order wave. Is the EDAF sensitive to the percentiles that is adopted for this estimation?

7. Establish q-probability characteristic response for design. Discuss uncertainties that can affect the results. Establish the acceleration field that can be used in quasi-dynamic analysis.
8. Discuss sources of uncertainties in the analysis.
9. Present how it is possible to perform a full long-term analysis of jack-up response. If time permits illustrate the long-term analysis. One may select a course resolution of the sea state space in order to perform the required number of 3-hours simulations.
10. Conclusions and recommendations for future work

The candidate may of course select another scheme as the preferred approach for solving the requested problem. He may also consider other subjects than those mentioned above.

The work may show to be more extensive than anticipated. Some topics may therefore be left out after discussion with the supervisor without any negative influence on the grading.

The candidate should in his report give a personal contribution to the solution of the problem formulated in this text. All assumptions and conclusions must be supported by mathematical models and/or references to physical effects in a logical manner. The candidate should apply all available sources to find relevant literature and information on the actual problem.

The report should be well organized and give a clear presentation of the work and all conclusions. It is important that the text is well written and that tables and figures are used to support the verbal presentation. The report should be complete, but still as short as possible.

The final report must contain this text, an acknowledgement, summary, main body, conclusions, suggestions for further work, symbol list, references and appendices. All figures, tables and equations must be identified by numbers. References should be given by author and year in the text, and presented alphabetically in the reference list. The report must be submitted in two copies unless otherwise has been agreed with the supervisor.

The supervisor may require that the candidate should give a written plan that describes the progress of the work after having received this text. The plan may contain a table of content for the report and also assumed use of computer resources. As an indication such a plan should be available by end of March.

In the thesis the candidate shall present his personal contribution to the resolution of problems within the scope of the thesis work.

Theories and conclusions should be based on mathematical derivations and/or logic reasoning identifying the various steps in the deduction.

The original contribution of the candidate and material taken from other sources shall be clearly defined. Work from other sources shall be properly referenced using an acknowledged referencing system.

The report shall be submitted in two copies:

- Signed by the candidate
- The text defining the scope included
- In bound volume(s)

Drawings and/or computer prints which cannot be bound should be organised in a separate folder.

The report shall also be submitted in pdf format along with essential input files for computer analysis, spreadsheets, MATLAB files etc in digital format.

Ownership

NTNU has according to the present rules the ownership of the thesis. Any use of the thesis has to be approved by NTNU (or external partner when this applies). The department has the right to use the thesis as if the work was carried out by a NTNU employee, if nothing else has been agreed in advance.

Thesis supervisor

Adjunct professor: Sverre Haver

Co-suprvisor: Prof. Jørgen Amdahl

Deadline: June 10 , 2015

Trondheim, January 10, 2015

Sverre Haver

Preface

This thesis concludes my five years of studying Marine Technology at the Norwegian University of Science of Technology. The thesis investigates the extreme response in a jack-up platform, based on stochastic theories, and deals with different methods of accounting for the dynamic effects on the response. The scope was formulated by Adjunct Professor Sverre Haver and the thesis combines a mixture of statistics and marine engineering. I have really enjoyed these last six months working with the thesis and I have deepened my knowledge of statistics, applied engineering, second-order wave theory and structural response. I also learnt the programming language python in the process and I assume I will benefit from this in the future.

I've written the thesis as simple as possible and a non-professional reader should be able to understand what is being investigated, but it is still a technical report and basic knowledge of engineering is required to understand the methodology and background theory. After reading this thesis it should be evident that dynamic effects cause larger responses on the platform due to the motions of the structure. A reader with an engineering background should learn that this is because of the nonlinear drag forces from the Morison equation and that the stiffness and damping matrixes are time dependent. The dynamic effects apply because of the structure's low stiffness and thus high eigenperiod. All the responses are calculated based on stochastic methods and how this works requires knowledge of basic statistical theory.

First of all I want to thank my supervisor Adjunct Professor Sverre Kristian Haver for his guidance and advice during my both my project and master thesis. Sverre has always been very positive, helpful and quick to respond to any issue I've raised. I also want to thank my co-supervisor Professor Jørgen Amdahl for all his help and discussions regarding USFOS related problems. A special thanks to staff in DNV GL for supplying the finite-element models and for answering all my questions thoroughly and GustoMSC, the owner of the models, for allowing me to use the models and publish the thesis. I would like to express that I appreciate all the professors and classmates I've had during my five years at NTNU and UFRJ. I have learned a lot from all of you and I had a great time studying with you. Finally, I would like to thank my friends and family for all the support and interest they have shown in my studies during these years.

Trondheim, June 10th, 2015



Lars Holterud Aarsnes

Preface

Abstract

This thesis investigates different stochastic methods for estimating the extreme response on a jack-up platform in the North Sea. The extreme response of jack-ups is often heavily affected by dynamics and thus dynamic effects must be accounted for. In this thesis the *Equivalent Dynamic Amplification Factor* (EDAF) has been calculated based on time domain simulations of sea states decided by the Environmental Contour Method.

A metocean report was created based on 57 years of hindcast data of the Ekofisk-field, with a focus on finding the extreme sea states and waves. The long-term variation of the environment is described by the joint probability distribution of *significant wave height* (H_s) and *spectral peak period* (T_p). The environmental contour lines in the T_p - H_s plane have been constructed based on their annual probability of exceedance. Estimates for the 100 and 10 000 year largest crests and wave heights were found using their respective Forristall distributions. These results are used as input for the extreme response analyses.

For structures acting quasi-statically it is common practice to estimate the extreme response by using the Design Wave Method. Previously the Stoke 5th wave was designed based on the extreme wave height, but using the extreme crest with the same return period gives larger responses. The crest height should therefore be the deciding parameter of the Design Wave Method.

Long-term analysis of the dynamic response based on an all sea states approach has been illustrated and conducted using time domain simulations in the nonlinear finite element program USFOS. The extreme response for deck displacement, base shear and overturning moment was calculated based on annual probabilities of exceedance of 10^{-2} and 10^{-4} .

The focus of the thesis has been on using the Environmental Contour Method to calculate the extreme (Gumbel) distribution for both static and dynamic response. The EDAFs and the α -percentiles were found by comparing the Gumbel distribution with the responses of the Design Wave Method and the Long-Term Analysis.

The time domain simulations in USFOS are based on linear (Airy) wave theory and Wheeler stretching is used to account for wave kinematics up to the free surface. By comparing the static time domain simulations with Stokes 5th regular waves in USFOS, the results show that Wheeler stretching doesn't adequately account for higher order wave kinematics and hence cannot correctly predict the extreme response. This means that second order wave theory should be used for drag-dominated structures such as jack-ups in regard to extreme response estimation.

Abstract

Sammendrag

Denne masteroppgaven undersøker forskjellige stokastiske metoder for å estimere ekstremrespons i en oppjekkbar plattform i Nordsjøen. Oppjekkbar plattform er ofte sterkt påvirket av dynamiske effekter og dette må medregnes i ekstremresponsanalyser. I denne oppgaven blir *ekvivalent dynamisk forsterkningsfaktor* (EDAF) beregnet ved hjelp av tidsplananalyser bestemt ved Konturlinjemetoden.

Basert på femtisyv år med værdata for Ekofiskfeltet sør i Nordsjøen, er en havmiljøbeskrivelse laget med formålet å finne de mest ekstreme sjøtilstandene og bølgetoppene. Langstidsvariasjonene til havmiljøet er beskrevet ved hjelp av den kombinerte sannsynlighetsfunksjonen for *signifikant bølgehøyde* (H_s) og spektral topp-perioden (T_p). Konturlinjene in H_s - T_p planet har blitt funnet basert på deres årlige sjanse for overskridelse og estimater for 100-års og 10 000-års bølgetopp og bølgehøyde er funnet ved hjelp av deres respektive Forristall-fordelinger. Disse verdiene har blitt brukt som inndata for ekstremresponsanalysene.

For strukturer som reagerer kvasistatisk på ytre påføringslaster er det vanlig på beregne ekstremresponsen ved hjelp av Designbølgemetoden. Dette gjøres ved at en Stokes 5te grads bølge bestemmes slikt at enten bølgetoppen har riktig returperiode eller bølgehøyden har riktig returperiode for å finne kvasistatisk respons med tilsvarende returperiode. Disse to metodene har blitt sammenlignet og ved å bruke riktig bølgetopp for designbølgen, blir det en mer korrekt representasjon av ekstremresponsen.

En langtid responsanalyse basert på å inkludere alle bidrag fra alle sjøtilstander (all sea states approach) har blitt illustrert og utført i tidsplanet ved hjelp av det ikke-lineære elementmetodeprogrammet USFOS. Ekstremresponsen for dekkforskyvning, skjærkraft og veltemoment har blitt beregnet basert på en årlig sannsynlighet for overskridelse på 10^{-2} og 10^{-4} .

Hovedfokuset har på å bruke konturlinjemetoden til å finne Gumbel-ekstremfordelingen for både statisk og dynamisk respons. EDAF og α -persentil har deretter blitt regnet ut ved å sammenlikne med den kvasistatiske Designbølgemetoden og dynamisk Langtidsanalyse.

Tidsplansimuleringer i USFOS er basert på lineær bølgeteori og bruker Wheeler-strekking for å estimere bølgekinematikken opp til den frie overflaten. Ved å sammenlikne statiske langtidssimuleringer med harmoniske Stokes 5te bølger viser det seg at lineær teori med Wheeler ikke gir et tilstrekkelig estimat for høyere ordens bølgekinematikk med tanke på ekstremrespons. Dette betyr at andre ordens bølgeteori burde brukes ved ekstremresponsestimering for friksjonskraft(drag)-dominerte strukturer.

Contents

1	INTRODUCTION.....	1
1.1	OBJECTIVE.....	2
1.2	SCOPE AND LIMITATIONS.....	3
1.3	OUTLINE.....	3
2	DESIGN FRAMEWORK AT NORWEGIAN CONTINENTAL SHELF.....	5
2.1	SITE.....	6
2.2	GOVERNING RULES AND REGULATIONS.....	7
2.2.1	<i>Ultimate Limit State</i>	9
2.2.2	<i>Accidental Damage Limit State</i>	10
3	FINITE ELEMENT MODEL FOR USFOS.....	11
3.1	SPRING CONNECTIONS.....	12
3.2	DAMPING.....	13
3.3	LEG HYDRODYNAMIC PROPERTIES.....	15
3.4	EIGENVALUE ANALYSIS.....	15
3.5	FINDING THE WORST WAVE HEADING.....	18
3.6	DECK DISPLACEMENT OF NODE 209.....	20
3.7	SUMMARY.....	20
4	METOCEAN REPORT.....	21
4.1	SCATTER OF HS AND TP.....	21
4.2	MARGINAL DISTRIBUTION OF SIGNIFICANT WAVE HEIGHT.....	24
4.3	CONDITIONAL DISTRIBUTION OF SPECTRAL PEAK PERIOD GIVEN HS.....	30
4.4	DISTRIBUTION OF WAVE HEIGHTS.....	34
4.5	DISTRIBUTION OF WAVE CRESTS.....	36
4.6	ENVIRONMENTAL CONTOUR LINES.....	39
4.7	SUMMARY.....	41
5	ESTIMATION OF EXTREME RESPONSE.....	45
5.1	DESIGN WAVE METHOD (QUASI-STATIC RESPONSE).....	47
5.2	THE PRINCIPLES OF TIME DOMAIN SIMULATIONS.....	51
5.3	UNCERTAINTIES IN TIME DOMAIN SIMULATIONS.....	52
5.3.1	<i>Air Gap Analysis</i>	52
5.3.2	<i>Stokes 5th vs Static Time Domain Simulation</i>	53
5.3.3	<i>Error in Reaction Overturning Moment in USFOS</i>	58
5.3.4	<i>Surface Elevation and Wave Kinematics</i>	60
5.3.5	<i>USFOS Uncertainties</i>	68

Contents

5.4	ACCOUNTING FOR DYNAMIC EFFECTS	73
5.4.1	<i>Dynamic Amplification Factor</i>	73
5.4.2	<i>Equivalent Dynamic Amplification Factor</i>	74
5.4.3	<i>Equivalent Acceleration Field</i>	75
5.5	LONG-TERM ANALYSIS	75
5.5.1	<i>Selecting Sea States for Extreme Response Simulations</i>	77
5.5.2	<i>Extreme Response Distribution</i>	78
5.5.3	<i>Maximum Response</i>	81
5.5.4	<i>Relative Contribution to Extreme Response for each Sea State</i>	83
5.6	ENVIRONMENTAL CONTOUR METHOD.....	85
5.6.1	<i>Calculating the Most Unfavourable Sea State</i>	87
5.6.2	<i>Distribution of Maximum Response</i>	90
5.6.3	<i>Results</i>	91
5.7	SENSITIVITY STUDIES	95
5.7.1	<i>Number of Seeds in Sea State Selection</i>	95
5.7.2	<i>Number of Seeds in Most Unfavorable Sea State</i>	96
5.7.3	<i>Relative Velocity</i>	98
5.7.4	<i>Increased Drag Coefficient to Account for Higher Order Effects</i>	99
5.8	SUMMARY	102
6	CONCLUSIONS AND FURTHER WORK	103
6.1	CONCLUSION	103
6.2	RECOMMENDATIONS FOR FURTHER WORK.....	103
7	REFERENCES	I

Figures

FIGURE 2-1: LOCATION OF ASSUMED SITE (EKOFISK) FOUND BASED ON GPS-COORDINATES. THE MAP IS FROM WWW.MAPS.GOOGLE.COM 6

FIGURE 3-1: THE FINITE ELEMENT MODEL OF CJ70, WHICH WAS SIMULATED IN USFOS 11

FIGURE 3-2: THE EFFECT OF DAMPING AS A PERCENTAGE OF CRITICAL DAMPING ON A HARMONIC LOAD. LOAD DESCRIBED BY THE FUNCTION: $e^{-\gamma t} \cdot \cos(\omega_0 t - \alpha)$, WHERE γ IS THE PERCENTAGE OF CRITICAL DAMPING. 14

FIGURE 3-3: BASE SHEAR MAXIMUM FOR EQUAL STOKES 5TH WAVES WITH DIFFERENT WAVE HEADINGS, WHERE THE RESPONSE IS DIVIDED BY THE AVERAGE OF THE WHOLE SAMPLE FOR EASIER COMPARISON. 19

FIGURE 3-4: OVERTURNING MOMENT MAXIMUM FOR EQUAL STOKES 5TH WAVES WITH DIFFERENT WAVE HEADINGS, WHERE THE RESPONSE IS DIVIDED BY THE AVERAGE OF THE WHOLE SAMPLE FOR EASIER COMPARISON. 19

FIGURE 3-5: PLATFORM DECK OF CJ70, WITH THE CENTER (NODE 209) USED FOR FINDING THE DECK DISPLACEMENT. 20

FIGURE 4-1: LEFT: ORIGINAL TP-HS PAIRS FOR EACH SEA STATE. SHOWING HOW LOGARITHMIC SPACING CAUSES TP VALUES TO GROUP. RIGHT: COMPARISON OF CORRECTED (BLUE) AND ORIGINAL (RED) TP-HS PAIRS 22

FIGURE 4-2: FINAL SCATTER SHOWING HS-TP PAIRS USING THE CORRECTED VALUES FOR TP..... 23

FIGURE 4-3: HINDCAST DATA FOR HS COMPARED WITH THE FITTED LOGNORMAL AND 2-PARAMETER WEIBULL DISTRIBUTIONS. THE VERTICAL YELLOW LINE IS THE FINAL CUT-OFF VALUE FOR $H=H(=2.8)$ DECIDED BY USING THE LEAST MEAN SQUARE ERROR METHOD. BOTH THE LOGNORMAL AND THE WEIBULL HAVE BEEN LINEARIZED IN THIS REPRESENTATION USING THEIR RESPECTIVE FUNCTIONS..... 28

FIGURE 4-4: FINAL CUMULATIVE PROBABILITY DISTRIBUTION FOR HS. DISTRIBUTED BY USING THE LONOWE MODEL. ESTIMATES FOR ULS AND ALS SIGNIFICANT WAVE HEIGHTS ARE INCLUDED AS VERTICAL LINES IN THE PLOT, AT 12.9 M AND 16.3 M RESPECTIVELY..... 29

FIGURE 4-5: WEIBULL LINEARIZATION OF FIGURE 4-4. SHOWING THE DISTRIBUTION OF SIGNIFICANT WAVE HEIGHTS FOR THE SITE..... 30

FIGURE 4-6: PLOT OF MEAN AND VARIANCE OF LN(TP) FOR EACH GROUP OF HS AND THE FITTED FUNCTION (RED).. 32

FIGURE 4-7: CUMULATIVE DISTRIBUTION OF TP GIVEN HS WITH A 90% CONFIDENCE BOUND FOR THE TP INTERVAL, ALSO SHOWING THE SIGNIFICANT WAVE HEIGHT FOR ALS AND ULS. ORIGINAL DATA SET SHOWN IN BLACK..... 33

Figures

FIGURE 4-8: CUMULATIVE FORRISTALL DISTRIBUTION OF THE 3 HOUR MAXIMUM WAVE HEIGHT, BOTH REGULAR AND LINEARIZED WITH RESPECT TO THE UPPER WEIBULL-PART OF THE DISTRIBUTION.35

FIGURE 4-9: THE CUMULATIVE FORRISTALL DISTRIBUTION OF THE 3-HOUR MAXIMUM CREST HEIGHT BOTH FOR REGULAR AND LINEARIZED WEIBULL DISTRIBUTION.38

FIGURE 4-10: ENVIRONMENTAL CONTOUR LINES IN THE GAUSSIAN SPACE (LEFT) AND IN THE HS-TP PLANE WITH SEA STATE POPULATION (RIGHT)41

FIGURE 4-11: FINAL CONTOUR LINES IN THE HS-TP PLANE FOR ULS(TEAL) AND ALS (RED) TOGETHER WITH THE ORIGINAL HINDCAST DATA (BLACK)43

FIGURE 5-1: SURFACE ELEVATION OF STOKES 5TH REGULAR WAVE WITH HEIGHT 20 M AND PERIOD 15 SECONDS...48

FIGURE 5-2: WAVE KINEMATICS OF A 20 METER HIGH, 15 SECOND PERIOD STOKES 5TH WAVE FROM USFOS. COLLECTED 1.5 SECONDS BEFORE THE CREST WHEN THE WAVE WAS 10 METERS HIGH. WAVE DIRECTION IS 180 DEGREES (ALONG THE NEGATIVE X-AXIS). FROM THE LEFT: HORIZONTAL VELOCITY, VERTICAL VELOCITY, HORIZONTAL ACCELERATION AND VERTICAL ACCELERATION.....48

FIGURE 5-3: STOKES 5TH HORIZONTAL VELOCITY UNDERNEATH THE CREST OF A 20 METER HIGH STOKES 5TH WAVE..58

FIGURE 5-4: THE REACTION BASE SHEAR AND REACTION OVERTURNING MOMENT FOR USFOS. THE MOMENT HAS A NON-ZERO MEAN VALUE AROUND WHICH IT OSCILLATES59

FIGURE 5-5: GRAPHICAL ILLUSTRATION OF WHEELER STRETCHING, FIGURE FROM THE USFOS THEORY-MANUAL, (SINTEF, 2010).64

FIGURE 5-6: HORIZONTAL VELOCITY FOR LINEAR WAVE THEORY WITH WHEELER STRETCHING AS FOUND IN USFOS FOR WAVE WITH A CREST OF 11.5 METERS. THE DIRECTION IS THE NEGATIVE X-DIRECTION.....64

FIGURE 5-7: DETAILED COMPOSITION OF EXTREME WAVES, SHOWING EACH OF THE CONTRIBUTIONS FROM LINEAR, SUM-FREQUENCY AND DIFFERENCE FREQUENCY. FIGURE FROM (STANSBERG, 1998)67

FIGURE 5-8: HORIZONTAL VELOCITY UNDERNEATH A LARGE CREST. MEASUREMENTS (DOTS), LINEAR BASED ON FREE WAVES ONLY (SOLID LINE) AND SECOND ORDER (DOTTED LINE). FIGURE FROM (JOHANNESSEN, 2008)68

FIGURE 5-9: USFOS SPOOL TO PEAK WAVE COMMAND. FIGURE FROM (SINTEF, 2010)69

FIGURE 5-10: ILLUSTRATORY FIGURE EXPLAINING THE DIFFERENCE BETWEEN FAST FOURIER TRANSFORM AND EQUAL AREA PROJECTION OF FREQUENCIES IN THE SPECTRUM, TAKEN FROM (SINTEF, 2010).....73

FIGURE 5-11: THE SELECTED SEA STATES (GREEN) FOR THE LONG-TERM ANALYSIS OF RESPONSE, TOGETHER WITH THE CONTOUR LINES FOR ULS (TEAL) AND ALS (RED) IN THE TP-HS PLANE.78

Figures

FIGURE 5-12: THE LOCATION PARAMETER, $\alpha(hs, tp)$, FOR THE GUMBEL DISTRIBUTION OF EXTREME RESPONSE FOR EVERY VALUE OF HS AND TP FOR BASE SHEAR [N]. CREATED BY INTERPOLATION, USING THE RADIAL BASIS FUNCTION WITH 18 SELECTED SEA STATES (CIRCLES) AS INPUT. TEAL AND RED CONTOUR LINES ARE FOR ULS AND ALS, RESPECTIVELY.....80

FIGURE 5-13: THE SCALE PARAMETER, $\beta(hs, tp)$, FOR THE GUMBEL DISTRIBUTION OF EXTREME RESPONSE FOR EVERY VALUE OF HS AND TP FOR BASE SHEAR [N]. CREATED BY INTERPOLATION, USING THE RADIAL BASIS FUNCTION WITH 18 SELECTED SEA STATES (CIRCLES) AS INPUT. TEAL AND RED CONTOUR LINES ARE FOR ULS AND ALS, RESPECTIVELY.....81

FIGURE 5-14: RELATIVE CONTRIBUTION TO THE PROBABILITY OF THE RESPONSE EXCEEDING THE LIMIT STATES FOR DECK DISPLACEMENT GIVEN THE SEA STATES PARAMETERS OF HS AND TP. SHOWN TOGETHER WITH THE RESPECTIVE ENVIRONMENTAL CONTOURS FOR ULS (UPPER) AND ALS(LOWER)84

FIGURE 5-15: RELATIVE CONTRIBUTION TO THE PROBABILITY OF THE RESPONSE EXCEEDING THE LIMIT STATES FOR BASE SHEAR GIVEN THE SEA STATES PARAMETERS OF HS AND TP. SHOWN TOGETHER WITH THE RESPECTIVE ENVIRONMENTAL CONTOURS FOR ULS (UPPER) AND ALS(LOWER)85

FIGURE 5-16: ZOOMED IN VERSION OF THE CONTOUR LINES SHOWING THE FIVE INITIAL SEA STATES AND THE 6TH, ADDITIONAL, SEA STATE (SLIGHTLY DARKER) FOR ULS AND ALS. THE FIRST SEA STATE IS PLACED AT THE EIGENPERIOD, WHICH IS 8 SECONDS.....88

FIGURE 5-17: EXTREME DISTRIBUTION OF DECK DISPLACEMENT FOR ULS FROM ENVIRONMENTAL CONTOUR.....92

FIGURE 5-18: EXTREME DISTRIBUTION OF BASE SHEAR FOR ULS FROM ENVIRONMENTAL CONTOUR.....92

FIGURE 5-19: EXTREME DISTRIBUTION OF OVERTURNING MOMENT FOR ULS FROM ENVIRONMENTAL CONTOUR .93

FIGURE 5-20: EXTREME DISTRIBUTION OF DECK DISPLACEMENT FOR ALS FROM ENVIRONMENTAL CONTOUR93

FIGURE 5-21: EXTREME DISTRIBUTION OF BASE SHEAR FOR ALS FROM ENVIRONMENTAL CONTOUR94

FIGURE 5-22: EXTREME DISTRIBUTION OF OVERTURNING MOMENT FOR ALS FROM ENVIRONMENTAL CONTOUR..94

FIGURE 5-23:COMPARISON OF RESULTING GUMBEL EXTREME BASE SHEAR DISTRIBUTION FOR THE WORST SEA STATE FOR ULS USING THE ORIGINAL 30 SEEDS (TEAL), 30 NEW SEEDS (RED) AND THE TWO SAMPLES COMBINED INTO OF CONTAINING 60 SEEDS (BLUE).....97

FIGURE 5-24: COMPARISON OF HORIZONTAL VELOCITY AT A WAVE CREST (11.5 METERS AND 15.6 SECOND PERIOD) BETWEEN STOCHASTIC TIME DOMAIN SIMULATION AND REGULAR STOKES 5TH ORDER WAVE. WAVE HEADING IS IN THE NEGATIVE X-DIRECTION.....101

Figures

Tables

TABLE 2-1: SUMMARY OF SITE INFORMATION	6
TABLE 2-2: SUMMARY OF LIMIT STATES USED IN THIS THESIS	9
TABLE 2-3: ACTION FACTORS FOR ULS SCENARIOS.....	10
TABLE 3-1: STIFFNESS MATRIX FOR LINEAR SPRINGS TO GROUND FOR THE CJ70 FEM MODEL	12
TABLE 3-2: DAMPING RATIOS AS PERCENTAGE OF CRITICAL DAMPING	15
TABLE 3-3: EQUIVALENT DRAG AND INERTIA COEFFICIENTS FOR THE CJ70 FEM-MODEL USED IN USFOS.....	15
TABLE 3-4: COMPARISON OF EIGENPERIODS USING DIFFERENT SEA BED CONNECTIONS	16
TABLE 3-5: VISUALIZATION OF THE FIRST EIGENMODES WITH EIGENVALUES FOR CJ70 CALCULATED USING USFOS.	17
TABLE 3-6: COMPARISON OF EIGENMODES FOR CJ70 USING THE TWO DIFFERENT METHODS.....	18
TABLE 4-1: HINDCAST DATA FILE,	21
TABLE 4-2: PARAMETERS FOR THE LONOWE HYBRID DISTRIBUTION OF Hs.....	29
TABLE 4-3: THE SIGNIFICANT WAVE HEIGHT DESCRIBING ULS AND ALS.....	30
TABLE 4-4: PARAMETERS FOR MEAN AND VARIANCE FUNCTIONS IN THE DISTRIBUTION OF Tp GIVEN Hs.....	33
TABLE 4-5: EXTREME SEA STATES AND THEIR CORRESPONDING VALUES FOR Hs AND Tp	34
TABLE 4-6: PARAMETERS FOR THE FORRISTALL CREST DISTRIBUTION	38
TABLE 4-7: PARAMETERS FOR THE JOINT MODEL OF ALL-YEAR, OMNIDIRECTIONAL Hs AND Tp.....	42
TABLE 4-8: EXTREME SEA STATES AND THEIR CORRESPONDING VALUES FOR Hs AND Tp	42
TABLE 4-9: WAVE HEIGHTS CALCULATED FROM THE FORRISTALL WAVE HEIGHT DISTRIBUTION AND BASED ON NORSOK RECOMMENDATIONS	42
TABLE 4-10: WAVE CRESTS CALCULATED USING FORRISTALL CREST DISTRIBUTION BASED ON SECOND ORDER WAVE THEORY AND CALCULATED AS A FACTOR OF WAVE HEIGHT	42
TABLE 5-1: RESULTING RESPONSES CALCULATED WITH DESIGN WAVE METHOD USING STOKES 5 TH WAVE BASED ON CREST HEIGHT FROM FORRISTALL CREST DISTRIBUTION AND THE MEAN SPECTRAL PEAK PERIOD.	50
TABLE 5-2: RESULTING RESPONSES CALCULATED WITH DESIGN WAVE METHOD USING STOKES 5 TH WAVE BASED ON WAVE HEIGHT FROM FORRISTALL WAVE HEIGHT DISTRIBUTION AND 90% CONFIDENCE BAND OF PERIODS. ...	50
TABLE 5-3: COMPARISON OF THE TWO METHODS FOR ESTIMATING THE DESIGN WAVE RESPONSE. THE RESULT IS PRESENTED AS THE FACTOR, BY WHICH CREST-METHOD IS LARGER THAN THE HEIGHT-METHOD.	51

Tables

TABLE 5-4: SUMMARY OF ALL THREE DIFFERENT WAVES PICKED FROM THE SHORT-TERM TIME DOMAIN (BLUE) SIMULATION AND COMPARED AGAINST STOKES 5TH WITH BOTH EQUAL HEIGHT (GREEN) AND EQUAL CREST (RED) FOR SURFACE ELEVATION, DECK DISPLACEMENT, BASE SHEAR AND OVERTURNING MOMENT.56

TABLE 5-5: SUMMARY OF ALL THREE DIFFERENT WAVES PICKED FROM THE SHORT-TERM TIME DOMAIN (BLUE) SIMULATION AND COMPARED AGAINST STOKES 5TH WITH BOTH EQUAL HEIGHT (GREEN) AND EQUAL CREST (RED) FOR SURFACE ELEVATION, DECK DISPLACEMENT, BASE SHEAR AND OVERTURNING MOMENT.57

TABLE 5-6: COMPARISON OF OVERTURNING MOMENT FROM USFOS WITH ROUGH OVERESTIMATION BASED ON THE BASE SHEAR59

TABLE 5-7: DRAG COEFFICIENT TO BE USED FOR SIMULATIONS ACCORDING TO NORSOK 003.65

TABLE 5-8: DISTRIBUTION TABLE OF WHICH OF THE LARGEST WAVE CREST (DESCENDING ORDER) GAVE THE MAXIMUM RESPONSE FOR EACH SEED. IN TOTAL 60 SEEDS FOR DYNAMIC ANALYSIS USING Hs 12.9 AND Tp 16.0..... 70

TABLE 5-9: NUMBERED SEA STATES USED FOR THE LONG-TERM ANALYSIS AND THEIR CORRESPONDING Hs AND TP PARAMETERS.77

TABLE 5-10: RESULTS FROM THE LONG-TERM DYNAMIC ANALYSIS OF THE CJ70-PLATFORM FOR BOTH ULS AND ALS83

TABLE 5-11: THE FIVE SELECTED SEA STATES ALONG THE CONTOUR LINES FOR ULS AND ALS87

TABLE 5-12: CHARACTERISTIC RESPONSE FOR ULS FOR EACH SEA STATE, BASED ON 20 SEEDS USING THE 5 LARGEST WAVE ELEVATIONS. THE LARGEST RESPONSES ARE DISPLAYED IN BOLD.89

TABLE 5-13: CHARACTERISTIC RESPONSE FOR ALS FOR EACH SEA STATE, BASED ON 20 SEEDS USING THE 5 LARGEST WAVE ELEVATIONS. THE LARGEST RESPONSES ARE DISPLAYED IN BOLD.89

TABLE 5-14: COMPARISON OF 30 NEW SEEDS FOR THE TWO SEA STATES THAT SHOWED THE SAME DYNAMIC RESPONSE FOR DECK DISPLACEMENT IN THE SCREENING STUDY90

TABLE 5-15: SUMMARY OF PARAMETERS OF THE WORST SEA STATES FOR ENVIRONMENTAL CONTOUR METHOD ...90

TABLE 5-16: RESULTING EQUIVALENT DYNAMIC AMPLIFICATION FACTORS FOUND USING THE ENVIRONMENTAL CONTOUR METHOD FOR ULS AND ALS. THE ALPHA-PERCENTILE HAS BEEN FOUND FROM THREE DIFFERENT METHODS, THE QUASI-STATIC DESIGN-WAVE, DYNAMIC LONG-TERM ANALYSIS AND THE OLD PROCEDURE OF USING AN α -PERCENTILE OF 90.95

Tables

TABLE 5-17: COMPARISON OF WHICH SEA STATE IS SELECTED AS THE MOST UNFAVORABLE FOR THE ULTIMATE LIMIT STATE USING 2 SETS OF 10 DIFFERENT SEEDS AND ALSO THE COMBINED (WHICH IS ASSUMED CORRECT) 20 SEEDS. BOLD NUMBERS SIGNIFY AN ERROR.96

TABLE 5-18: COMPARISON OF WHICH SEA STATE IS SELECTED AS THE MOST UNFAVORABLE FOR THE ACCIDENTAL DAMAGE LIMIT STATE USING 2 SETS OF 10 DIFFERENT SEEDS AND ALSO THE COMBINED (WHICH IS ASSUMED CORRECT) 20 SEEDS. BOLD NUMBERS SIGNIFY AN ERROR.96

TABLE 5-19: COMPARISON OF THE CHARACTERISTIC RESPONSE FOR THE TWO DIFFERENT SAMPLES OF THE LARGEST MAXIMUM FROM 30 SEEDS98

TABLE 5-20: COMPARISON OF THE CHARACTERISTIC RESPONSE WHEN USING RELATIVE VELOCITY TO ACCOUNT FOR VISCOUS DAMPING AND WITHOUT. FOR ULS, SEA STATE #4 AND FOR ALS SEA STATE #2 FROM THE ENVIRONMENTAL CENTER METHOD HAS BEEN USED. THE SAME 30 SEEDS WERE USED FOR ALL SIMULATIONS.98

TABLE 5-21: DRAG COEFFICIENT OF THE ORIGINAL MODEL USED IN TIME DOMAIN SIMULATION WITH LINEAR WAVE THEORY AND THE ALTERED DRAG COEFFICIENT FOR STOKES 5TH REGULAR WAVE.....99

TABLE 5-22: RESULTING STOKES 5TH RESPONSE FOR ORIGINAL TIME DOMAIN DRAG COEFFICIENTS AND REDUCED VALUES:100

TABLE 5-23: RESULTING EDAFS AND ALPHA-PERCENTILES FOR THE DIFFERENT METHODS102

Nomenclature

α	Gumbel/Weibull Parameter
α_1	Rayleigh Damping Coefficient
α_2	Rayleigh Damping Coefficient
β	Gumbel / Weibull Parameter
$\Delta\omega$	Frequency Change
ϵ	Dimensionless wave amplitude
ϕ	Velocity Potensial
γ	Peakedness factor
λ	Damping Ratio
μ	Mean Value
ω	Angular frequency
ρ	Water density
σ	Standard Deviation
ζ	Surface Elevation
ALS	Accidental Damage Limit State
C	Damping Matrix
C_D	Drag Coefficient
C_M	Inertia (Mass) Coefficient
DAF	Dynamic Amplification Factor
EAP	Equal Area Method
EDAF	Equivalent Dynamic Amplification Factor
F	Force
$f(x)$	Probability Density Function
$F(x)$	Cumulative Probability Distribution
$F_{X_{3h}}(x)$	Cumulative Distribution Function of Largest 3hour Maximum
FFT	Fast Fourier Transform

Nomenclature

g	Gravitational acceleration
H_s	Significant Wave Height
K	Stiffness Matrix
M	Mass Matric
m	Mass
MSL	Mean Surface Level
N	Number of Waves
N	Number of Maxima
N	Number of Simulations
PDF	Probability Density Function
q	Annual Probability of Exceedance
r	System Response
T	Wave Period
t	Time
T_p	Spectral Peak Period
u	Velocity in x-direction
ULS	Ultimate Limit State
x	Stochastic Variable, response
x_c	Characteristic load
x	Displacement
\dot{x}	Time Derivative of Response
\ddot{x}	Second Time Derivative of Response
X_q	Max Annual Response
x_{dyn}	Dynamic Response
x_{sta}	Static Response

1 Introduction

Offshore oil production now occurs in some of the harshest areas of the world where the platforms are exposed to loads from wind, current and waves simultaneously. An accurate estimation of the extreme response ensures safety for both the workers and the environment. The limit state design method is used on the Norwegian Continental Shelf and the platform's responses must be found in accordance with the rules and regulations of NORSOK N-003. For the extreme response it's the Ultimate Limit State (ULS) and the Accidental Damage Limit State (ALS) conditions that must be satisfied. ULS covers the environmental loads that have a return period of 100 years and the ALS loads have return period of 10 000 years.

Waves generally cause the largest responses and thus a correct wave load estimation is essential for a reliable platform design. The long-term variety of the wave climate can be described statistically using hindcast data and can be assembled in a metocean report. Sea state characteristics from the metocean report can be used in combination with a wave spectrum to find the largest surface elevations and the corresponding wave periods for ULS and ALS. Then finite element software is used to calculate the resulting response of the platform from the wave loads.

It is impossible to create an exact mathematical representation of the sea surface since it is irregular and continuously changing but by using theories of stochastic processes, it is possible to describe the sea statistically. It is common to split the overall variation in two parts; long-term variability of the environment and the short-term variability of the surface. The short-term variation in the North Sea is can be assumed to be following the JONSWAP-spectrum.

Dynamic effects must be accounted for when estimating the extreme response of certain platforms, such as jack-ups, since they have natural periods in the wave period range. The response of the jack-up will not depend purely on the largest wave, but the wave period also has a large impact due to the dynamic behavior. The large natural periods are due to the low stiffness of the structure and this results in larges motions so that the response cannot be calculated as static. The damping and inertia effects must be solved in the time domain since these aren't constant due to the large motions.

The consequences of this is increased response due to second-order wave kinematics. The horizontal velocity in the crest is significantly increased because of higher order effects that linear wave theory omits. Drag dominated structures, such as jack-ups, are extra sensitive to this velocity increase since it directly affects the Morison-loads that govern the extreme response.

Introduction

Stochastic, nonlinear, time domain analyses directly account for the important effects of dynamics on a structures behavior. An all sea states, long-term analysis is the preferable approach to estimate the extreme response, but this can be very time consuming and it can be difficult to establish an accurate model for the conditional distribution of the 3-h maximum for all sea states. Other, approximate methods to estimate the response include the Design Wave Method and the Environmental Contour Method. The common responses to estimate are base shear, overturning moment and deck displacement of the platform.

The dynamic amplification factor (DAF) can be used to account for the difference between the static and dynamic response for structures with low eigenperiods ($>2s$). For a drag-dominated structure with larger eigenperiods, the highest wave does not necessarily cause the largest response and thus more complex analyses must be used. Under such circumstances the equivalent dynamic amplification factor (EDAF) must be introduced. EDAF is the factor between the characteristic (extreme) quasi-static response and the characteristic dynamic response. The contour line method can be used to calculate the EDAF based on the probability distribution of the static and dynamic extreme responses.

1.1 Objective

The aim of this thesis is to estimate the governing responses for design of a particular jack-up located at a specific site in the southern North Sea. A long-term description of the wave climate at the site must first be established by creating a metocean report based on hindcast data for the site. The metocean report is then used for input to the extreme response analysis which is conducted in the nonlinear finite element software USFOS. The finite element model used for the USFOS-simulations must be validated and uncertainties in the analysis discussed.

The metocean report need to contain all the important information for the extreme response analysis. This includes the join-probability distribution of H_s and T_p , environmental contour lines and the extreme wave height and wave crests.

The extreme response must be calculated using the worst wave heading based on a quasi-static Stokes 5th analysis. The time domain simulations should also be validated by comparison with Stokes 5th. Different ways of accounting for dynamic effects should be discussed with a focus on finding the EDAF. The EDAF can be calculated using the Environmental Contour method and an adequate α -percentile. The α -percentile can be estimated from quasi-static Stokes 5th response or from the Long-Term analysis.

1.2 Scope and Limitations

The metocean report was generated based on 57 years of continuous 3-hour sea states. All hindcast data has been assumed omnidirectional such that probability distribution of the significant wave height is independent on the direction. The metocean report can be viewed as independent of seasonal changes and is generated with the purpose of examining the q-annual probability of exceedance. It has been assumed that climate change doesn't affect the hydrodynamic conditions at the site such that they are the same now as 57 years ago.

The focus of this thesis is on the extreme response due to wave loads, so neither the effect of wind nor current has been considered. The analysis only estimates the response of one specific jack-up, (CJ-70) in the elevated/operational state at a depth of 110 meters. The direction that showed the largest response based on a deterministic Stokes 5th wave analysis was used for all other analyses. The time domain simulations are based on first-order (linear) waves using Wheeler stretching to account for some of the kinematics and a drag coefficient scaled according to NORSOK. The response calculations are nonlinear and done in USFOS. No wave on deck impact is assumed and by comparing the air gap to the 10 000 year largest crest height this is a safe assumption.

1.3 Outline

After discussions with my supervisor, Professor II Sverre Haver, it was decided to not to follow the IMRAD (Introduction, Method, Results and Discussion) outline directly. Instead, the general introduction is followed by two distinct and separate parts: Chapter 4 Metocean Report and Chapter 5 Estimation of Extreme Response. This is since the theories behind Metocean and Response Estimation are quite different and the results of the first part (Metocean) are used as input for the second part (Extreme response estimation) of the thesis.

In Chapter 5, there is a description of the platform's location and the rules and regulations governing jack-ups in the North Sea. Then the finite element model of the jack-up is presented, together with some of the initial analyses. These include finding the eigenvalues and the worst direction since they were prerequisites for some of the other analyses later in the report.

In Chapter 4, the metocean report is presented in the way it was conducted. First the background theory, then the method and finally the results are presented for each section. At the end of the chapter, a section summarizes results for improved readability.

Introduction

The Extreme Response Estimation in Chapter 5, is more extensive and starts by describing the simpler quasi-static problem that can be solved using the Design Wave Method. The following two sections describe the background theory of time domain simulations and how to account for dynamics when undertaking extreme response estimations. Section 5.3 mentions some of the uncertainties and possible inaccuracies in the results due to the software used and the assumptions made. Finally in Section 5.4 (Long-Term Analysis) and Section 5.6 (Environmental Contour Method) the two methods and their results are presented.

It was decided to structure the thesis in this way in order to increase the readability of the report and provide a continuous flow when reading. This was achieved by successively: 1) presenting the problem, 2) showing the methodology and 3) presenting the final results and discussing them.

The thesis investigates two separate parts where the first one acts as input for the second one. Accordingly the results of the Metocean Report were needed before it was possible to start working on the Extreme Response Estimation.

Appendix A contains all extra analysis data that it was decided not to include in the main part of the report. Appendix B describes the computational tools, Python (for scripting) and USFOS for finite element simulations.

2 Design Framework at Norwegian Continental Shelf

Waves generally cause the largest contribution to the most extreme responses and thus a correct wave load estimation is essential for a reliable platform design. The most accurate way to estimate the extreme response, is by a long-term response analysis. The long-term distribution of response is given by: (Baarholm et al., 2010)

$$F_{x_{3h}}(x) = \iint_{h_s t_p} F_{X_{3h}|H_s T_p}(x|h_s, t_p) f_{H_s T_p}(h_s, t_p) dt_p dh_s \quad (1)$$

Where $F_{X_{3h}|H_s T_p}(x|h, t)$ describes the short-term response given the sea state characteristics H_s and T_p and $f_{H_s T_p}(h_s, t_p)$ describes the long-term environmental variation.

The first step in order to estimate the extreme response in a jack-up is to describe the long-term wave climate. Therefore, a typical jack-up site in the North Sea was selected and hindcast data from the location was used to generate a metocean report (see Chapter 4). It is required that the metocean data is collected for the exact site or an even harsher location to avoid underestimation of the responses. For unrestricted service, the 100 year wave may be set to 32 meters, but this thesis investigates a specific site, Ekofisk, (as described in Section 2.1). For the North Sea it is common to assume the sea state characteristics constant for durations of up to three hours. The sea states are usually described by their Significant Wave Height (H_s) and spectral peak period (T_p). H_s is the average height of the 1/3 largest waves in the sample. The spectral peak period is the period associated with the most energetic waves in the spectrum.

In Section 2.2, some of the rules and regulations governing design of jack-ups in the North Sea are described. DNVs recommended practice for Self-Elevating Units, RP-C104 (DNV, 2012) covers Jack-ups. The rules described in NORSOK-N003, Actions and Action Effects (NORSOK, 2007) are governing for the design analysis and are based on the principle of Limit States (which is further described in Sections 2.2.1 and 2.2.2).

The programming language *Python* has been used to calculate all the statistical properties, using self-made scripts implemented with functions from open source *Python* packages. The output from these scripts have been used as input to the nonlinear finite element software *USFOS*. Post-processing of *USFOS* results was also done in *Python*. All figures in this thesis have been plotted by self-written python scripts, unless stated otherwise. Some tables have been processed in *Excel*

for better readability. More information about both *Python*, scripts and *USFOS* can be found in Appendix B.

2.1 Site

The location of the jack-up was chosen to be representative for a typical site in the southern part of the North Sea. This location is suitable for jack-ups and the depth of 110 meters was chosen since this is currently one of the deeper used for jack-ups. The metocean report is based on the total wave hindcast collected from the coordinates: Latitude N 56.31, Longitude E 3.41. This is in the area of the Ekofisk-field. The metocean report uses the total wave height from both the wind sea and the swell sea, but wind forces and currents are neglected in this report to explicitly investigate the extreme wave responses. The method used for collecting the hindcast data was the WAM10 wave model, which is further described in (Wamdi, 1988). Also see Section 4.1 for the methods used to extract examine the data. The file containing hindcast data was received on a file : ‘*NS_south_WAM10_5631N_0341E.txt*’ The hindcast data dates back to the 1.st of September 1957 and has continuously collected 166 053 sea states, each lasting 3 hours, until the 30.th of June 2014.

Table 2-1: Summary of site information

Location	Southern North Sea Ekofisk-field
Latitude	N 56.31
Longitude	E 3.41
Depth	110 m
Waves	From hindcast (WAM10)
Wind	0 m/s
Current	0 m/s



Figure 2-1: Location of assumed site (Ekofisk) found based on GPS-coordinates. The map is from www.maps.google.com

The long-term variation can be described by sea states lasting from 20 min to 3 hours depending on the location. For the North Sea, the H_s and T_p parameters of a sea state can be assumed continuous for 3 hours at a time. H_s is the average of the 1/3 largest waves. T_p is the spectral peak period which is found as the peak of the wave spectrum. The long-term variability of the environment is further described in Chapter 4

The short-term statistics can be described using a spectrum based on the values of H_s and T_p from the long-term variability. For the North Sea it is common to use the JONSWAP spectrum and in this thesis a peakedness parameter of 3.3 has been used, (see Subsection 5.3.5).

2.2 Governing Rules and Regulations

On the Norwegian continental shelf it is common practice to design offshore installations based on the limit states design method. The structure is then designed as to withstand all the environmental impacts during its life time, even in a damaged condition. The design analysis usually focuses on the elevated state of the jack-up, while accidents often occur during installation, retrieval or transit (DNV, 2012). Strict rules apply to the design of the elevated state based on thorough analyses and safety factors are also used to ensure sufficient strength of the structure. The transit state can be harder to model and analyze and also human errors can cause dangerous situations. This thesis investigates the jack-up in the elevated state (operation and survival) which is where the extreme response is likely to occur since the jack-up should not be operating in the other states (installation, retrieval or transit) during a severe storm. This thesis is investigating the effect of waves and according to RP-C104 the wave loads on jack-ups should be calculated using the Morison Equation.

$$F = F_D + F_I = \frac{1}{2} \rho C_D D v|v| + \rho C_I a A \quad (2)$$

Where:

$\rho =$ density of sea water

$a =$ particle acceleration

$v =$ particle velocity

$A =$ Cross section area of leg

$D =$ cross sectional dimension perpendicular to flow direction

$C_D = \text{drag (shape) coefficient}$

$C_I = \text{Inertia (mass) coefficient}$

For the extreme response the majority of the contribution comes from the drag part of the equation.

The response is found by solving the dynamic equation of equilibrium, which is given by:

$$m\ddot{r} + c\dot{r} + kr = F \quad (3)$$

Where

$m = \text{mass}$

$c = \text{damping}, c = c(r)$

$k = \text{stiffnes}, k = k(r)$

$r = \text{displacement of the structure}$

This is further described and discussed in the chapter covering extreme response (Chapter 5) and the section on principles of time domain analysis (Section 5.2). The three main considerations when calculating the response is whether to do an analysis that is:

- Static or dynamic
- Linear or nonlinear
- Deterministic or stochastic

Static analysis can be conducted for very stiff platforms where dynamic effects are insignificant, however jack-ups are in general so flexible that the dynamic effects must be accounted for.

A linear analysis means that equation of equilibrium has been simplified by linearizing the stiffness and damping coefficients. This method should be used carefully because linearization of drag forces introduces uncertainties, especially since the estimation of damping is uncertain (DNV, 2012),

The difference between a deterministic and stochastic analysis is that the deterministic only uses regular (harmonic) waves. The fluid kinematics are described according to the most accurate wave theory (typically Stokes 5th waves are used). A regular wave analysis can be well suited for extreme response analysis with low eigenperiods, but not for rigorous fatigue assessments (DNV, 2012). A stochastic analysis uses irregular waves created as a sum of multiple harmonic wave components.

For Jack-ups the dynamic effects play a large part so a stochastic nonlinear dynamic is the preferable approach. However, it can be very time consuming using an all sea states approach(see Section 5.4) and other methods such as the environmental contour method (see Section 5.6) should be considered too.

A limit state is a condition which a structure cannot exceed in order to fulfill its design criteria. Many offshore structures are designed using the limit states design method, and are therefore constructed to withstand all responses likely to occur during its design life. Common limit states are the *Serviceability Limit State (SLS)*, *Ultimate Limit State (ULS)*, *Accidental Damage Limit State (ALS)* and the *Fatigue Limit State (FLS)*. For marine structures on the Norwegian Continental Shelf these values have to be in accordance with N003 (NORSOK, 2007). This thesis is concerned with the extreme responses on an offshore jack-up platform and will therefore investigate ULS and ALS for the metocean loads. Metocean loads can be anything from wind, waves, current, snow, ice, and earthquakes etc., but in this thesis only the effect of waves is investigated.

The safety factor used for system design is supposed to account for both aleatoric (statistic) and epistemic (systematic) uncertainties. Aleatoric variability can for example be the highest wave crest during a one year period. This variability cannot be eliminated by creating better models since it can never be predicted with certainty. Epistemic uncertainty can be reduced by having more data for previous instances of the variable such that estimating statistical parameters is more accurate.

Table 2-2: Summary of Limit States used in this thesis

Limit State Name	Ultimate	Accidental Load
Abbreviation	ULS	ALS
q-probability of exceedance	10^{-2}	10^{-4}
Years	100	10 000

2.2.1 Ultimate Limit State

The Ultimate Limit State is to make sure that all expected loads can be resisted with an adequate safety margin. ULS is usually applied on a component basis. For environmental loads the ULS values are corresponding to an annual exceedance of 10^{-2} (NORSOK, 2007). The ultimate limit states are usually checked for two different scenarios; a) When permanent and variable actions are governing b) when environmental loads are governing. The factors for each of these scenarios are shown in Table 2-3.

Table 2-3: Action factors for ULS scenarios

Action Combinations	Permanent Actions	Variable Actions	Environmental Actions
A	1.3	1.3	0.7
B	1.0	1.0	1.3

For this report action combination b) is most relevant since characteristic environmental loads on a jack-up is being estimated. For ULS the characteristic load, x_c , is defined as the one corresponding to an annual exceedance of 10^{-2} , which means a statistical probability of occurring once every 100 years. Further references to ULS in this thesis will generally refer to its 10^{-2} annual probability of exceedance.

2.2.2 Accidental Damage Limit State

The Accidental Damage State is a safety measure to ensure that the integrity of the structure is not compromised, even during an accidental damage scenario. The accidental loads are found with a probability corresponding to 10^{-4} annual exceedance, which corresponds to once every 10 000 years. The ALS is supposed to account for the risk of damage during collisions, fires and explosions, but also the 10 000 year environmental loads, which are to be investigated in this report. Also there can be situations where there is a bad behaving problem. This is mostly when there is wave on deck impact for the platform. To ensure this doesn't occur, the annual probability of wave on deck should be less than 10^{-4} . Further references to ALS in this thesis will generally refer to its 10^{-4} annual probability of exceedance.

3 Finite Element Model for USFOS

Two different jack-up models were considered for this thesis, both designed by the engineering company GustoMSC and classified by DNV GL. The models were received from DNV GL and publication was approved by GustoMSC. The two jack-ups were CJ62 and CJ70. Both of them are harsh environment, three legged, cantilever type jack-up drilling platforms, but differ in size and are also modelled differently for FE-analysis. After some initial analyses, it was concluded to continue with the larger of the two, CJ70. The main reason was that it has higher eigenperiods and also its modeling is simpler and thus more simulations could be done in less time.

CJ70 is the largest GustoMSC jack-up with a spacing of 70 meters between the centers of its cantilever legs. It is designed for a depth of up to 150 meters on the Norwegian Continental Shelf. The legs are triangular, open truss using x-braces. In the finite element model, the legs have been modelled as simplified beams using equivalent hydrodynamic properties as the original.

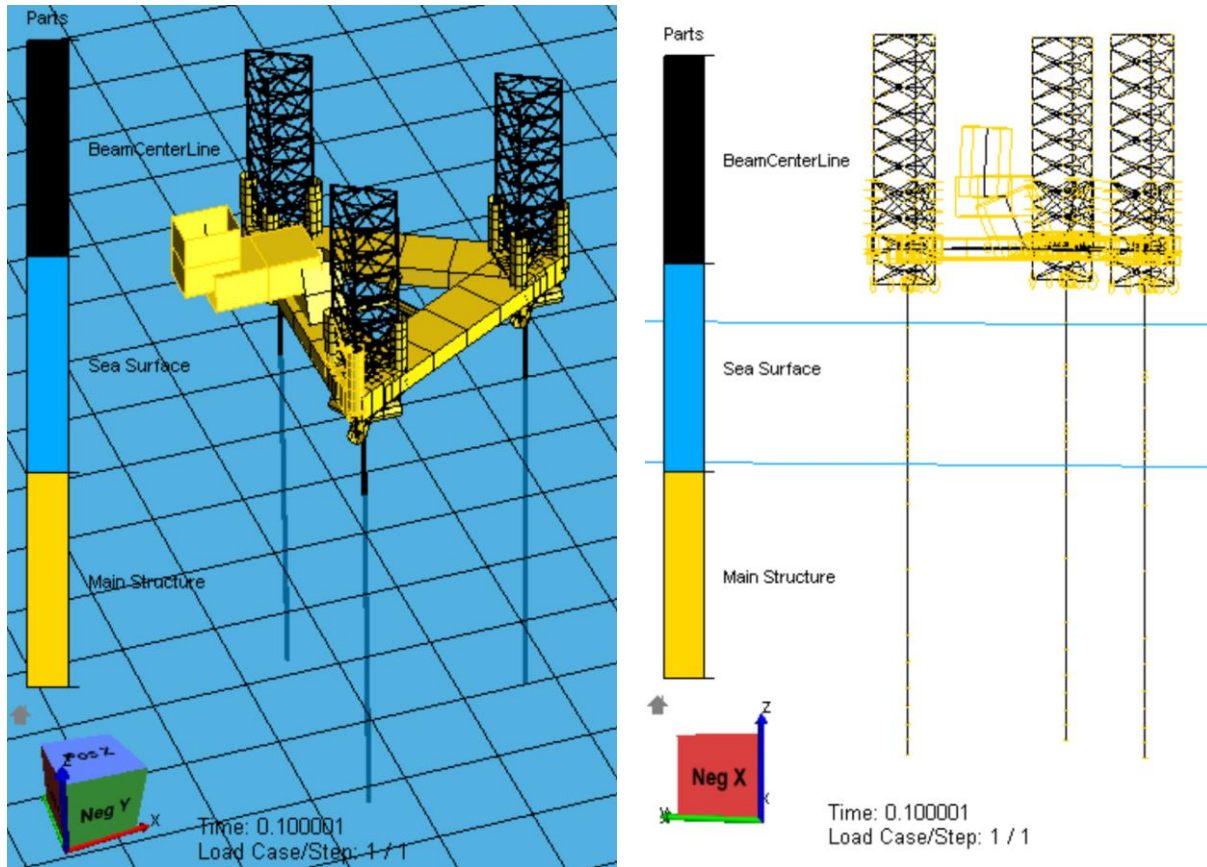


Figure 3-1: The finite element model of CJ70, which was simulated in USFOS

Figure 3-1 shows that in the finite element model for CJ70 each leg is represented by a simplified beam. The main benefit for using simplified beam is that the simulation time is much quicker than for a detail FE-model. By using equivalent hydrodynamic and mass properties for the simplified beam and the original cantilever legs, the results become reliable and since the simulation time is much quicker the numerical accuracy of the simulation can be improved significantly. According to (Haver, 2012), simplified beam models can be used when they have been compared with the more detailed model and the results are in good agreement. It is important that the global result values for e.g. base shear, overturning moment and deck displacement are similar to the detailed model. The cons of using a simplified model is that the response simulations can be less detailed and doing an e.g. a pushover analysis would not be possible. Investigating the platforms response in a damaged condition would also require a more detailed finite element model.

The mass of the structure is modelled as 30 node masses, spread out along the structure. The buoyancy force should not be added as a separate command in USFOS, since the equivalent hydrodynamic diameter already corresponds to the submerged volume of the leg. The Master-Slave method is predefined for certain elements using the USFOS BLIND2P command. In short, Master-Slave method defines nodes such that the slaves depend linearly on the master nodes. Then the whole finite element solution for the structure can be described by the response in the master nodes and thus the required degrees of freedom can be reduced. For a more detailed description of the Master-Slave method see e.g. (Langen and Sigbjørnsson, 1979).

3.1 Spring Connections

As connections between the jack-up and the soil foundation, linear ground springs have been used. These are defined by the USFOS command SPRNG2GR and the material properties are described in SPRIDIAG command with the stiffness matrix shown in Table 3-1. The springs' translational and rotational stiffness have been calculated by DNV GL and is in accordance to DNV GLs recommended practices.

Table 3-1: Stiffness matrix for linear springs to ground for the CJ70 FEM model

	X	Y	Z
Translation [<i>N/m</i>]	2.43E+09	2.43E+09	1.40E+10
Rotation [<i>Nm/rad</i>]	8.00E+10	8.00E+10	8.00E+10

In the eigenvalue analysis (see Section 3.4) it has also been experimented by using both a pinned and a fixed connection instead.

3.2 Damping

Damping is the influence upon an oscillating system reducing the amplitude with time if there is no external force. For oscillating systems, the damping can be difficult to model, since the system has different factors affecting the damping. According to (Langen and Sigbjørnsson, 1979) simplified damping methods are shown to give satisfactory results for practical uses such as the damping of a platform. Two simplified methods for damping is Rayleigh Damping and Critical damping.

For *Rayleigh Damping* the damping matrix, \mathbf{C} is given as:

$$\mathbf{C} = \alpha_1 \mathbf{M} + \alpha_2 \mathbf{K} \quad (4)$$

Here it is assumed that the damping matrix is proportional to the mass – and stiffness matrices. Using *Rayleigh damping*, the damping ratio, λ_i , is satisfying the condition:

$$\lambda_i = \frac{1}{2} \left(\frac{\alpha_1}{\omega_i} + \alpha_2 \omega_i \right) \quad (5)$$

The constants α_1 and α_2 can be found if the damping ratio for two eigenfrequencies are known, and they are found as:

$$\alpha_1 = \frac{2\omega_1\omega_2}{\omega_2^2 - \omega_1^2} (\lambda_1\omega_2 - \lambda_2\omega_1) \quad (6)$$

$$\alpha_2 = \frac{2(\lambda_2\omega_2 - \lambda_1\omega_1)}{\omega_2^2 - \omega_1^2}$$

Another possibility is to use a percentage of critical damping. Critical damping is found as:

$$C_{cr} = \sqrt{2m k} \quad (7)$$

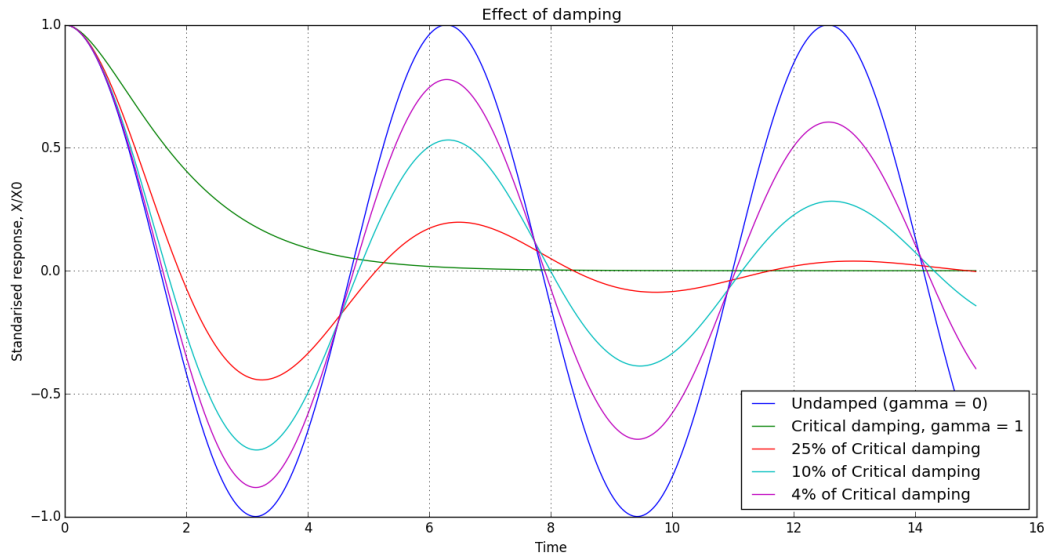


Figure 3-2: The effect of damping as a percentage of critical damping on a harmonic load. Load described by the function: $e^{-\gamma t} \cdot \cos(\omega_0 t - \alpha)$, where γ is the percentage of critical damping.

The damping comes from three sources, structural damping, soil damping and hydrodynamic damping. Structural (hysteric) damping is due to the material the jack-up is made of. Soil damping depends on the foundation and hydrodynamic (viscous) damping is due to interaction between the fluid and the structure. In *USFOS*, the relative velocity between the waves and the structure is used, which gives a viscous damping effect.

Damping is set according to DNV-GL standards and described in RP-C104 Self-elevating units (DNV, 2012). Recommended hydrodynamic damping is between 2-4% of critical damping, but since relative velocity is used in the *USFOS* simulations, this is already accounted for. The soil damping depends on spudcan and bottom conditions and has a recommended value between 0-2%. Structural damping is highly design related and generally around 1-3%. In general RP-C104 recommends a total damping of 6-9% for storm conditions and higher values requires further justifications. In a joint industry project (DNV, 1996) analyzing a jack-up, the structural damping is set to 2%. The report also uses a soil damping of 2% for linear springs due to hysteresis foundation damping.

Table 3-2: Damping ratios as percentage of critical damping

Structural Damping	2%
Soil Damping	2%
Hydrodynamic Damping	Relative Velocity in USFOS

This gives a total damping of 4% of critical plus the hydrodynamic damping which is accounted for in the Morrison equation by using relative velocity. The effect of using relative velocity is investigated in 5.7.3.

3.3 Leg Hydrodynamic properties

The hydrodynamic properties of the simplified beam has been calculated by DNV GL to give the CJ70-model equivalent values as a more detailed model using truss legs modelled by multiple beams. The hydrodynamic properties for the split tube chords have been calculated based on DNV-RP-C205, Sec 6.12.1 (DNV, 2010). For this model the equivalent drag coefficient is omnidirectional and based on an average for a 60 degree sector. The stiffness properties of the simplified beam model are based on DNV-RP-C104 Self-Elevating Units (DNV, 2012) section A1, table A-1 and case c. The hydrodynamic properties are based on the same DNV-RP-C104 from Section A6. The equivalent drag and inertia coefficients calculated by DNV GL and used in USFOS are listed in Table 3-3.

Table 3-3: Equivalent drag and inertia coefficients for the CJ70 FEM-model used in USFOS

Height Profile: z [m]	Equivalent Drag Coefficient: $C_D[-]$	Equivalent Inertia Coefficient $C_M[-]$
65	2.83	2.37
0.101	2.83	2.37
0.1	3.87	2.16
-17.4	3.87	2.16
-17.401	3.42	2.01
-111.9	3.42	2.01

3.4 Eigenvalue Analysis

For the general eigenvalue problem, the damping and excitation forces are set to 0. The general eigenvalue problem is then given by (Langen and Sigbjørnsson, 1979):

$$(K - \omega_n^2 M) \mathbf{r} = 0 \quad (8)$$

Finite Element Model for USFOS

Where ω_n is the eigenfrequency (natural frequency) and r are the eigenvectors. Here the mass term includes the added mass, which depends on both wave height and frequency for the time domain simulation. The natural period depends heavily on both the water depth and the sea bed conditions as it affects the stiffness matrix, K .

While the water depth has been kept constant at 110 meters, different sea bed conditions have been investigated. For good sea bed conditions and for a platform using bucket or piled footings the eigenperiod will be lower than a spud-can type or with soft sea bed conditions. A conservative approach would be to model the jack-up as pinned to the sea bed, while an optimistic would be a fixed connection.

A pinned connection means it can resist vertical and horizontal forces but not moment. The connection point is not allowed to translate, but can rotate freely. A fixed connection on the other hand, resists vertical and horizontal forces as well as a moment. They are also known as rigid connections due to their ability to restrain against both translation and rotation.

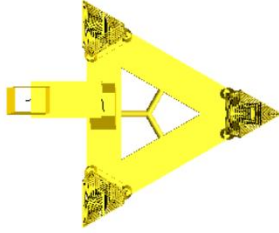

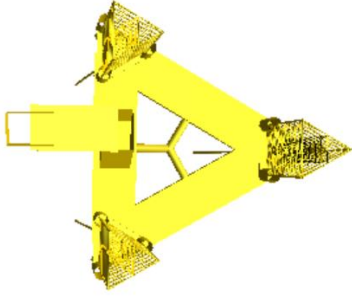

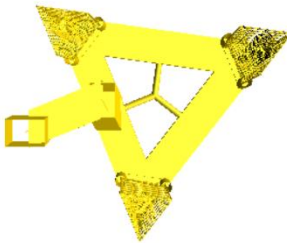

Both these connections have been investigated and also the spring connections for which DNV GL has calculated the stiffness matrix, (see Section 3.1). The resulting eigenvalue values have been calculated using USFOS for each of the connection types and are compared in Table 3-4.

Table 3-4: Comparison of eigenperiods using different sea bed connections

	Fixed	Springs	Pinned
1 st (bending along x)	5.59 s	8.02 s	11.05 s
2 nd (bending along y)	5.54 s	7.98 s	11.01 s
3 rd (torsional)	4.91 s	6.67 s	9.61 s

It was decided to continue using the spring connections defined by its stiffness matrix received from DNV GL These are the same as have been used to analyze the structure previously. The fixed and pinned connections gives an indication of the uncertainty in the eigenvalue calculations, where pinned is a conservative approach giving too large eigenvalues and fixed is the opposite giving too low eigenperiods. A visualization of the eigenmodes is shown in Table 3-5 and is from the USFOS graphical user interface.

Table 3-5: Visualization of the first eigenmodes with eigenvalues for CJ70 calculated using USFOS

Eigenmode and period	TOPVIEW	SIDEVIEW
		
Original model. No bending or torsion		
<p>1st : 8.03 s</p> <p>2nd : 7.98 s</p>		
Bending modes. The screen capture from USFOS shows the 1 st bending mode (along the x-axis). The 2 nd -mode(along the y-axis) gives bending perpendicular to the 1 st .		
<p>3rd : 6.67 s</p>		
1 st Torsional mode		

These eigenmodes are calculated using USFOS *eigenval* command with 40 eigenvectors and scaling the eigenvectors by a factor of 25 in the figure for visualization purposes. The 2nd bending

mode (along y-axis) is rotated 90 degrees compared to the 1st (along x-axis). The values are calculated with the gravitational forces, thus they differ slightly from the values DNV GL have calculated. By neglecting gravity in USFOS the values equal those received from DNV GL. The results are presented in Table 3-6. The method which gives the most correct answer depends on the modelling of the structure, but the difference is only about 5%.

Table 3-6: Comparison of eigenmodes for CJ70 using the two different methods

Eigenmode	USFOS (with gravity)	DNV GL/USFOS (no gravity)
1st (bending along x-axis)	8.03 s	7.63 s
2nd (bending along y-axis)	7.98 s	7.58s
3rd (torsion)	6.67	6.42 s

3.5 Finding the Worst Wave Heading

The drag coefficients of the model are calculated as omnidirectional and thus a directional analysis doesn't give a lot of information about the simplified beam model, but it is still important to do a quick analysis on which direction is to worst so that the extreme response is estimated conservatively. To do a quick directional analysis of the quasi-static response, equal Stokes 5th waves were stepped through the model for every 10th degree between 0 and 360.

The results are presented as the maximum response of each heading, divided by the mean of the maximum response for each of the 37 simulations. It can be seen that the variations in base shear are not very large, ± 10 percent. For overturning moment, the response is much larger for headings close to 180 degrees. This might be due to cancellations effects between the jack-up's legs. A degree of 180 (along the negative x-axis) is chosen as the worst direction for the platform. This is the heading that is used for the other analyses conducted in the rest of the thesis.

Finite Element Model for USFOS

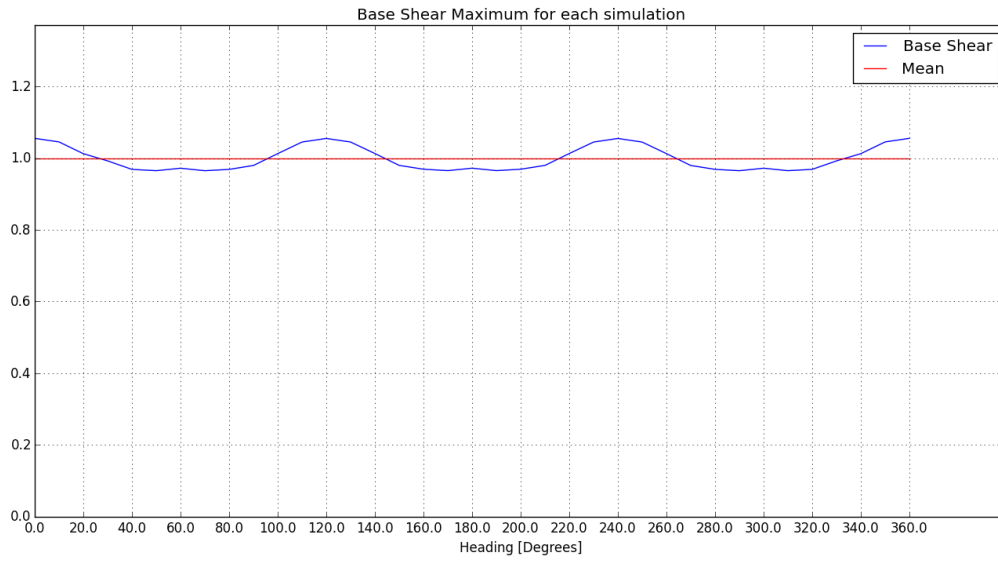


Figure 3-3: Base shear maximum for equal Stokes 5th waves with different wave headings, where the response is divided by the average of the whole sample for easier comparison.

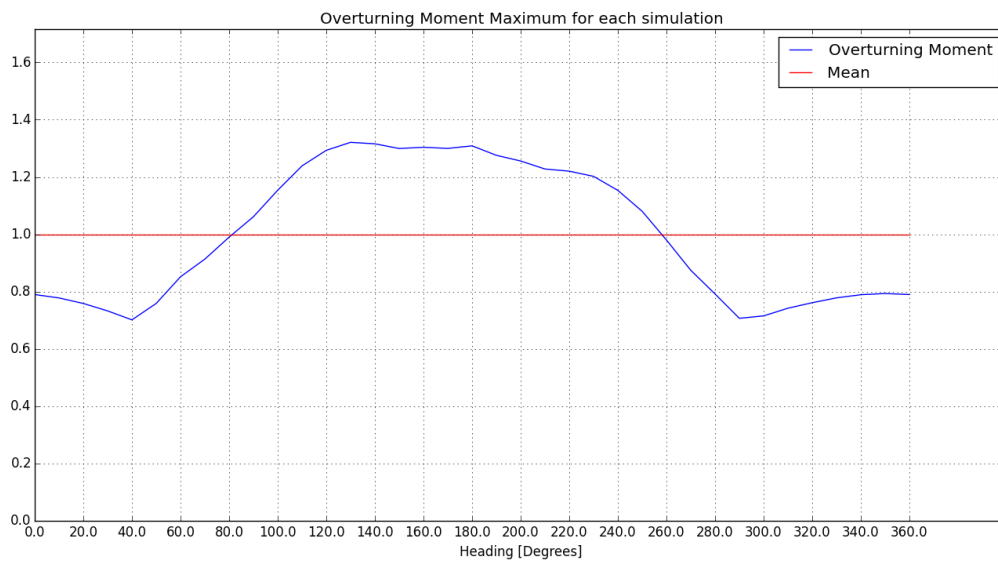


Figure 3-4: Overturning moment maximum for equal Stokes 5th waves with different wave headings, where the response is divided by the average of the whole sample for easier comparison.

3.6 Deck Displacement of node 209

To find the deck displacement for CJ70 the central node in the middle of the deck has been used. This is node 209 which has coordinates:

X:0.00
Y:0.00
Z:147.07

The deck displacement was then calculated using the nodal displacement in the negative x-direction. Since the waves were applied directly along the negative x-axis too, the displacements in y and z could be neglected.

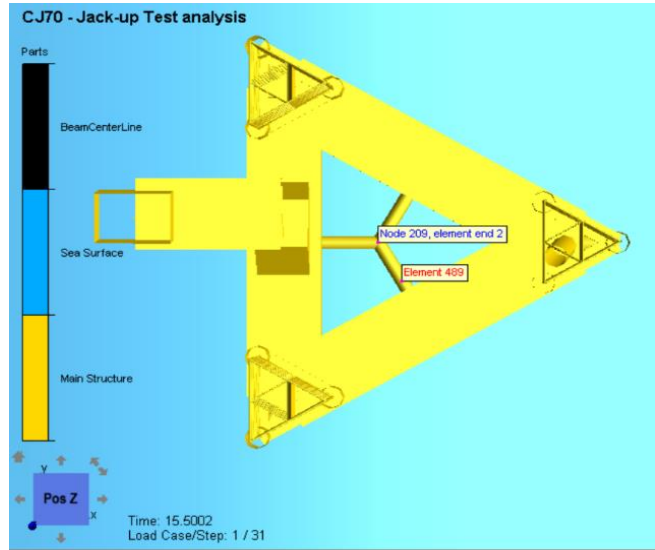


Figure 3-5: Platform Deck of CJ70, with the center (node 209) used for finding the deck displacement.

3.7 Summary

It has been concluded to continue the analysis focusing only on the Platform CJ70. The directional analysis showed that the base shear didn't depend much on the wave heading ($\pm 10\%$), but for overturning moment the difference was significantly larger and the largest response was found using heading of 180 degrees. This is therefore chosen as the wave direction that will be used for the rest of the USFOS simulations. The connections between the platform and the sea bed is modelled as springs, using the stiffness matrix calculated by DNV GL. The resulting highest eigenmode was then 8.03 and 7.98 seconds for bending and 6.67 for the torsion mode.

4 Metocean Report

Metocean is short for metrological and oceanographic. A typical metocean report contains all the relevant information about wind, waves and current with directions and temperatures for a specific site. In this thesis, the focus is on showing how to use a metocean report to find significant values for the extreme response in the structure. All parameters have units according to international SI standards.

The hindcast data used for this metocean report was gathered from a measurement point in the southern part of the North Sea, (see Section 2.1). This is the same area as the Ekofisk-field. The hindcast data dates back to the 1st of September 1957 and has continuously collected 166 053 sea states, each lasting 3 hours, until the 30th of June 2014. For each sea state the following data is measured: time (year, month, day, hour), wind speed, wind direction and significant wave height, spectral peak period and direction for total sea, wind sea and swell. In this report only the parameters describing the total sea (wind sea and swell combined) have been used. Directional differences have been neglected, so the results from the metocean report are omnidirectional. The data used was received on the file named ‘NS_south_WAM10_5631N_0341E.txt’. The layout of the all the data is shown in Table 4-1, with the relevant total sea Hs and Tp data highlighted in yellow.

Table 4-1: Hindcast data file, with the data used in the report highlighted in yellow

YEAR	WIND						TOTAL SEA					WIND SEA			SWELL		
	M	D	H	WSP	DIR		HS	TP	TM	DIRP	DIRM	HS	TP	DIRP	HS	TP	DIRP
1957	9	1	6	4.4	222		0.9	5.2	4.4	212	226	0.2	2.9	227	0.9	5.2	212
1957	9	1	9	4.9	214		0.8	5.2	4.4	212	218	0.3	3.2	212	0.8	5.2	212
1957	9	1	12	4.3	223		0.8	5.2	4.4	212	218	0.2	2.9	227	0.8	5.2	212
...
2014	6	30	15	8.8	323		1.6	6.9	4.9	347	339	1.3	6.3	332	1.1	7.6	2
2014	6	30	18	8.4	322		1.6	6.9	5	347	340	1.2	6.3	332	1.1	7.6	2

4.1 Scatter of Hs and Tp

The first step towards creating a metocean report was to make a scatter diagram of the distribution between significant wave height and spectral peak period for all the sea states. The data presented in this figure is the basis for all the results in the metocean report. Figure 4-1 shows a scatter of all sea states with Hs values plotted against Tp. The values for Tp appear to be grouped and not random as one would expect.

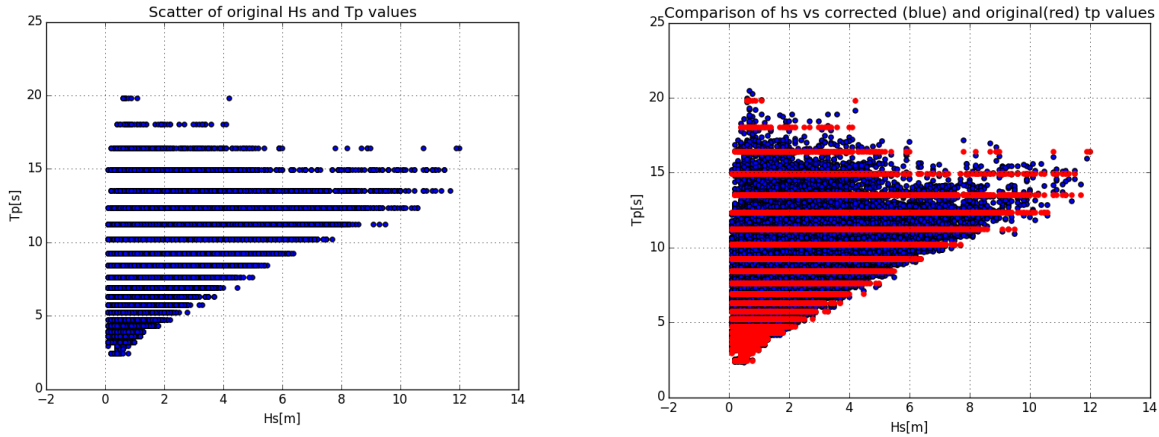


Figure 4-1: Left: Original Tp-Hs pairs for each sea state. Showing how logarithmic spacing causes Tp values to group. Right: Comparison of corrected (blue) and original (red) Tp-Hs pairs

The reason is that WAM10 was created in a time when storage space was critical and therefore used discrete logarithmic spacing to save disk space by only storing two digits worth of Tp data for each sea state. Tp values were stored as their logarithmic equivalent using one decimal place. This means that for example sea states with Tp between 17.28 and 19.1 would be stored as 2.9 since $\ln(17.28)=2.85$ and $\ln(19.1)=2.94$ which both round to 2.9 with one decimal place.

By running a python script that outputs each unique Tp value in the data set, the result is:

[2.4, 2.7, 2.9, 3.2, 3.6, 3.9, 4.3, 4.7, 5.2, 5.7, 6.3, 6.9, 7.6, 8.4, 9.2, 10.2, 11.2, 12.3, 13.5, 14.9 16.4, 18.0, 19.8]

This is only 23 different spectral peak periods, while doing the same for Hs gives 116 unique values between Hs=0.1m and Hs=12.0 m. Logarithmic spacing means that the difference between consecutive Tp values will increase logarithmically with increasing period. This means an inaccurate and unrealistic distribution of the largest Tp-values. The largest Tp values are also those which are associated with severe storms and are needed for extreme response estimation.

To correct for this unrealistic distribution, one can correct it by using a method recommended by Statoil in (Andersen, 2009). The following formulas are applied:

$$i = \text{ROUND}\left(1.0 + \frac{\ln\left(\frac{T_p^*}{3.244}\right)}{0.09525}\right) \quad (9)$$

$$T_{p_{correct}} = 3.244 \cdot \exp(0.09525 * (i - 0.5 - \text{RAND}))$$

Here *ROUND* is a function that rounds up/down to the closest integer with 0 decimal places. *RAND* generates a random number between 0 and 1. T_p^* is the original spectral peak period values found in the wam10 data.

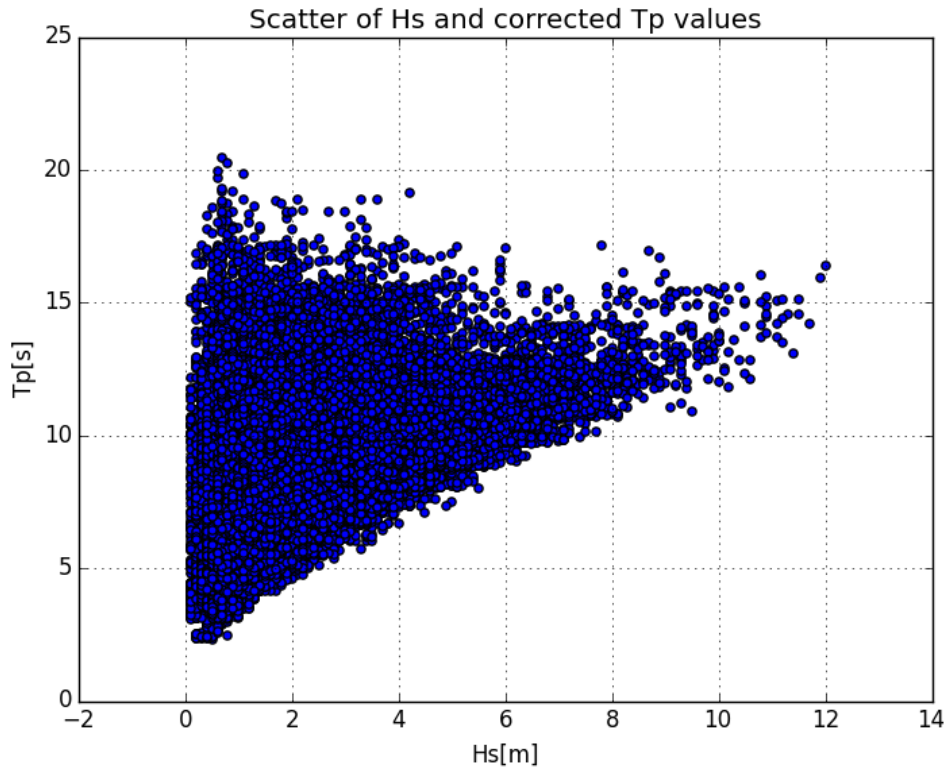


Figure 4-2: Final scatter showing Hs-Tp pairs using the corrected values for Tp

The final Tp and Hs values for each sea state is shown in Figure 4-2. These Hs-Tp pairs are the only input data used to create this metoccean report.

Based on the values displayed in Figure 4-2, a scatter diagram was also created. This was done by going through the data for each sea state and placing it in the correct column (tp) and row (hs). The

increments used was 1 meter and 1 second for h_s and t_p , respectively. The resulting scatter diagram is presented in Appendix 1, in the Appendix.

4.2 Marginal Distribution of Significant Wave Height

A probabilistic model for the significant wave height must be based on hindcast data for a specific location. Then it is important to choose a model that has a good fit to the data sample. From (Haver and Nyhus, 1986), a proposed hybrid model is shown to be good for sites in the North Sea. The distribution is also known as the lonowe model (Haver, 2013), which is short for L O g-N O rma L -W E ibull. The model consists of a log-normal distribution model for the lower values of h , until $h = \eta$ and a two parameter Weibull for $h > \eta$. The split at $h=\eta$ is done to accurately account for significant wave heights both in the lower (lognormal) and upper (Weibull) tail of the distribution.

Another possibility would have been to use a 3-parameter Weibull to describe the distribution of the significant wave heights. The mean, standard deviation and the skewness of the data sample would have to be equal to that of the Weibull distribution for the best fit. The lonowe model has been used in this thesis.

The lognormal distribution function

The lognormal probability density function is given as (Bury, 1975):

$$f_y(y) = \frac{1}{\sqrt{2\pi} \cdot \alpha \cdot y} \exp \left[-\frac{1}{2} \left(\frac{(\ln(y) - \theta)}{\alpha} \right)^2 \right], \quad y > 0 \quad (10)$$

Where the coefficients are:

α : Standard deviation of $\ln(y)$ for lognormal distribution

θ : Mean of $\ln(y)$ for lognormal distribution

The maximum likelihood estimators for θ and α^2 are given as: (Leira, 2014)

$$\hat{\theta} = \frac{1}{n} \sum_{i=1}^n \ln Y_i \quad (11)$$

$$\hat{\alpha}^2 = \frac{1}{n} \sum_{i=1}^n (\ln Y_i - \hat{\theta})^2$$

The Weibull distribution

The Weibull distribution is an 2- or 3-parameter empirical distribution with a lower limit of zero (Leira, 2014). The Weibull probability density function is (Bury, 1975):

$$f_x(x) = \frac{\beta}{\rho} \left(\frac{x}{\rho}\right)^{\beta-1} \cdot \exp\left[-\left(\frac{x}{\rho}\right)^\beta\right], \quad x \geq 0, \quad \beta > 0, \quad \rho > 0 \quad (12)$$

β : The shape parameter for the Weibull distribution

ρ : The scale parameter for the Weibull distribution.

The expected value and variance can be estimated by: (Leira, 2014)

$$E[X] = \rho \Gamma\left(1 + \frac{1}{\beta}\right) \quad (13)$$

$$\text{Var}[X] = \rho^2 \left\{ \Gamma\left(1 + \frac{2}{\beta}\right) - \Gamma^2\left(1 + \frac{1}{\beta}\right) \right\}$$

Γ – is the gamma function

A 3-parameters Weibull model can be obtained by introducing a location parameter, μ . This would be the equivalent of fitting to a variable $= Y - \mu$, instead of fitting to X such that the probability density function becomes:

$$f_Y(y) = \frac{\beta}{\rho} \left(\frac{y - \mu}{\rho}\right)^{\beta-1} \cdot \exp\left[-\left(\frac{y - \mu}{\rho}\right)^\beta\right] \quad (14)$$

The cumulative distribution function (CDF) for the 2-parameter Weibull distribution is: (Leira, 2014):

$$F_X(x) = 1 - \exp\left\{-\left(\frac{x}{\rho}\right)^\beta\right\}, \quad x \geq 0 \quad (15)$$

The Weibull parameters can also be found using a Weibull probability paper. The principle behind a probability paper is to alter the scaling of the axis so that the distribution function becomes linear. For a Weibull distribution this is done by rearranging and taking the natural logarithm twice.

$$\ln\left(-\ln(1 - F_x(x))\right) = \beta \ln x - \beta \ln \rho \quad (16)$$

The linear function then becomes:

$$z = \beta \cdot y + c \quad (17)$$

By assuming that: $\bar{F}(x_k) = \frac{k}{N+1}$, where x_k is the k 'th sample out of a total of N sorted values. The Weibull probability paper can now be plotted with the $z = \ln(-\ln(1 - F_x(x)))$ along the vertical axis and $y = \ln(x_k)$ along the horizontal. The distribution parameters can be found by applying the best fitted linear line to the resulting plot.

Lonowe distribution

By using the lognormal probability density function given in equation (10) and inserting H_s as the variable, the first part of the distribution is:

$$f_{H_s}(h_s) = \frac{1}{\sqrt{2\pi} \cdot \alpha \cdot h_s} \exp \left[-\frac{1}{2} \left(\frac{(\ln(h_s) - \theta)}{\alpha} \right)^2 \right]; \quad h_s \leq \eta \quad (18)$$

Correspondingly, with the Weibull probability density function from Eq. (12) :

$$f_{H_s}(h_s) = \frac{\beta}{\rho} \left(\frac{h_s}{\rho} \right)^{\beta-1} \cdot \exp \left[- \left(\frac{h_s}{\rho} \right)^\beta \right]; \quad h_s > \eta \quad (19)$$

Where the coefficients are:

α : Standard deviation of $\ln(h_s)$ for lognormal distribution

θ : Mean of $\ln(h_s)$ for lognormal distribution

β : The shape parameter for the Weibull distribution

ρ : The scale parameter for the Weibull distribution.

η : The cut-off value where the probabilistic models change.

The parameters of the Weibull-tail are estimated by requiring the model to be continuous at $h = \eta$ for both the probability density function $f_{H_s}(\eta)$ and the cumulative distribution function $F_{H_s}(\eta)$. Therefore this model should be considered a 3-parameter model (Haver and Nyhus, 1986).

To fit the model to the sample, a trick was to be implemented. First, 50 different values for the cut-off, η , was tested by using every 0.1 m between 0 m and up to 5 m. For each of these values of η the best fit for the Weibull parameters ρ and β was estimated using an iterative process. Also here

50 iterations was used to find the best values for ρ and β for each value of η . The values for β and ρ were found by iterating 50 times over Eq. (20).

$$\rho = \frac{\eta}{\left(-\ln\left(1 - F_{H_s(\log)}(\eta)\right)\right)^{\frac{1}{\beta}}} \quad (20)$$

$$\beta = \frac{f_{H_s(\log)}(\eta)}{\frac{1}{\rho} \cdot \left(\frac{\eta}{\rho}\right)^{\beta-1} \cdot \exp\left[-\left(\frac{\eta}{\rho}\right)^\beta\right]}$$

Then the best value for the cut-off η was then found by calculating the minimum mean square error (MMSE) between the proposed function and the sample for each value of η . The $\eta=H_s$ giving the lowest mean square error was selected and the corresponding ρ and β values were used. Remember that η was a parameter that was changing, for every execution of the for-loop in the python script, to find the optimal cut-off value for $h_s = \eta$. The increment used for η was 0.1m.

The cumulative probability of the sorted sample was estimated as:

$$F_X(x) = \frac{n_i}{N + 1} \quad (21)$$

The population can be compared to the distribution of H_s by paring the cumulative probability (along y-axis) with the sorted H_s -values from the sample (along x-axis). In Figure 4-3 the two separate distributions are shown together with the hindcast data. The yellow vertical line is the shift where the log-normal distribution is used until $h \leq \eta = 2.8$ and the Weibull distribution is used for wave heights above 2.8 meters. It is necessary to make sure that the function is continuous, so the pdf and cdf must be equal for both log-normal and Weibull at $h = \eta = 2.8$. The logarithm of 2.8=1.02, so that the cut-off point will appear at 1.02 in the graphs.

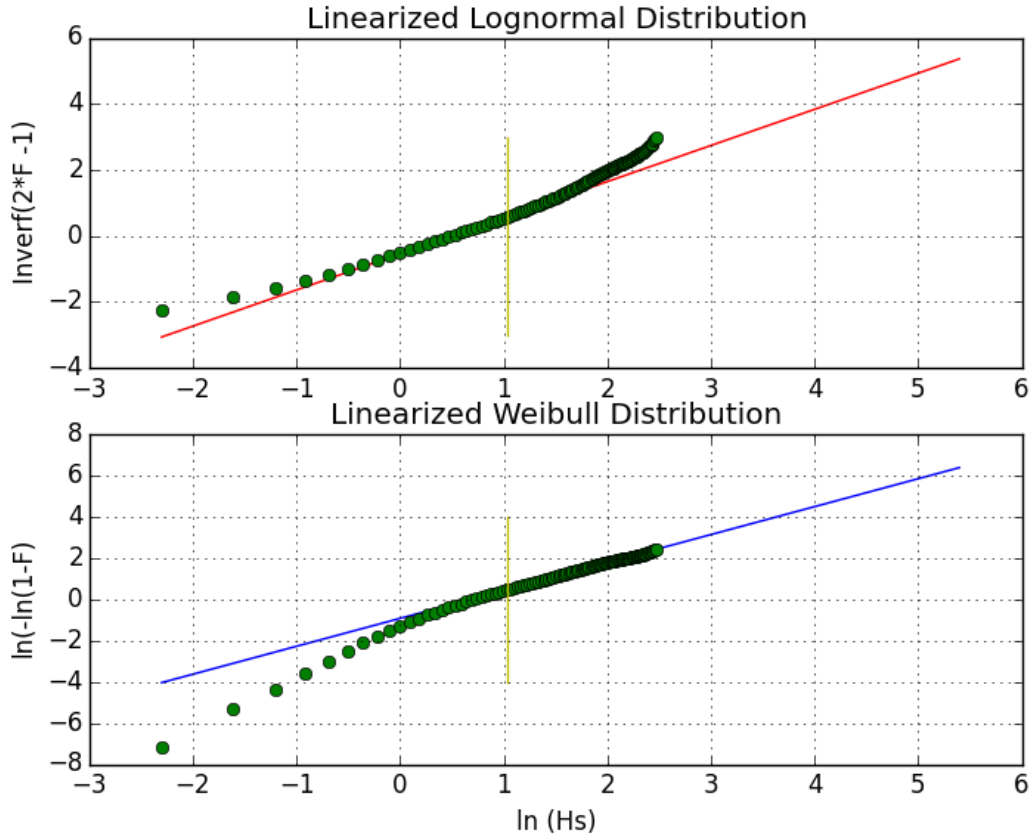


Figure 4-3: Hindcast data for H_s compared with the fitted Lognormal and 2-parameter Weibull distributions. The vertical yellow line is the final cut-off value for $h=\eta(=2.8)$ decided by using the least mean square error method. Both the Lognormal and the Weibull have been linearized in this representation using their respective functions.

The significant wave height for ALS and ULS is then estimated by rearranging the cumulative Weibull distribution with respect to H_s . It is important to remember that ALS and ULS give the annual probabilities of exceedance, so the probability of a single sea state exceeding q must be divided by the number of 3-hour sea states per year ($\frac{24}{8} \text{ hours} \cdot 365 \text{ days} =$), 2920. The estimates of H_s is then, by reorganizing the cumulative Weibull distribution:

$$H_{s_{ULS}} = \rho \cdot \left(-\ln \left(\frac{10^{-2}}{2920} \right)^{\frac{1}{\beta}} \right) \quad (22)$$

$$H_{S_{ALS}} = \rho \cdot \left(-\ln \left(\frac{10^{-4}}{2920} \right)^{\frac{1}{\beta}} \right)$$

The combined cumulative probability is plotted against H_s , with estimates for ULS and ALS, and shown in Figure 4-4. The resulting parameters for the log-normal and Weibull are presented in Table 4-2. Figure 4-5 shows the Weibull-linearized final distribution of H_s .

Table 4-2: Parameters for the lonowe hybrid distribution of H_s .

Log-Normal Distribution		Cut-off	Weibull Distribution	
θ (mean)	α (std. deviation)	η	β (Scale)	ρ (Shape)
0.4970	0.6463	2.8	1.3530	1.9921

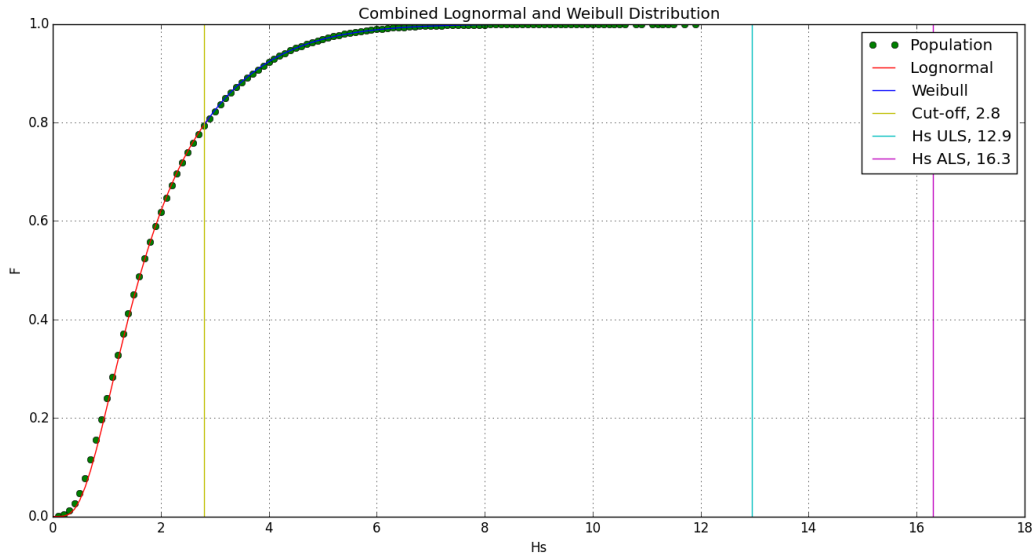


Figure 4-4: Final cumulative probability distribution for H_s . Distributed by using the Lonowe model. Estimates for ULS and ALS significant wave heights are included as vertical lines in the plot, at 12.9 m and 16.3 m respectively.

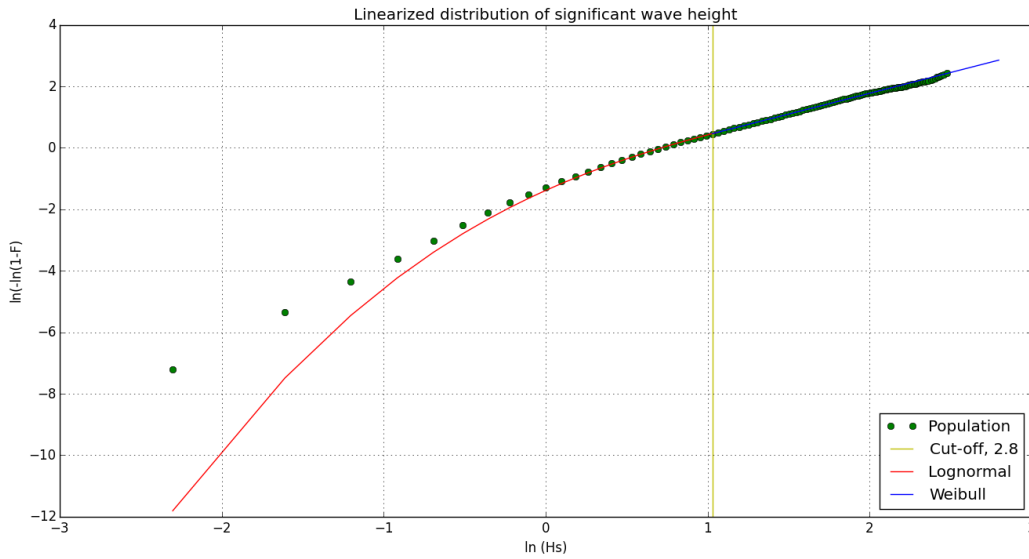


Figure 4-5: Weibull linearization of Figure 4-4. Showing the distribution of significant wave heights for the site.

The significant wave height defining the ULS is found to be 12.9 m and the ALS at 16.3 m.

Table 4-3: The significant wave height describing ULS and ALS

Hs ULS	Hs ALS
12.9 m	16.3

4.3 Conditional Distribution of Spectral Peak Period given Hs.

The conditional distribution of the spectral peak period, for a given value of significant wave height, is also of importance for the extreme response due to possible dynamic amplification. If the eigenperiod of the structure is close to the period of the waves, the response will be increased due to resonance. Also, different periods can cause cancelation effects on the jack-up’s legs or an increased response. (Haver, 2013) recommends using a log-normal model for the conditional distribution of T_p .

$$f_{T_p|H_s}(t|h_s) = \frac{1}{\sqrt{2\pi} \cdot \sigma(h_s) \cdot t_p} \exp \left[-\frac{1}{2} \left(\frac{(\ln(t_p) - \mu(h_s))}{\sigma(h_s)} \right)^2 \right] \quad (23)$$

Where:

$$\mu = E[\ln(T_p)]$$

$$\sigma^2 = Var [\ln (T_p)]$$

This means that the mean and variance in T_p must be found for each increment of H_s so that a function describing the change in mean and variance depending on H_s , is required. To estimate a good fit for the mean and the variance, the following functions have been shown to give good results (Haver, 2013):

$$\begin{aligned} \mu &= a_1 + a_2 \cdot h^{a_3} \\ \sigma^2 &= b_1 + b_2 \exp[-b_3 h] \end{aligned} \quad (24)$$

It is important to note that the variance cannot be negative, but in some cases b_1 can get a negative value. Then b_1 should be given a fixed, positive value (e.g. 0.002) and the best fit should be calculated again.

By using Eq (23) the distribution can be calculated. The mean and variance in T_p depends H_s and thus must be found for each increment of H_s , similarly to for the scatter diagram. The increment was set to 1 m, so 0-1 would be the first, and 12-13 the last group. The number of data points per group of H_s is then the same as the sum of each row in the scatter diagram, see Section 4.1. An increment of one meter was chosen to make sure there are many data points (accurate variance and mean) for each group of h_s . The last group, consisting only of two sea states above 12 meters, was not included in the sample since its variation is very inaccurate. It was experimented with adding it to the calculation of the mean and variance, but the fit was better using only the first 12 values. The mean and variance are assumed to be following equations in Eq. (24).

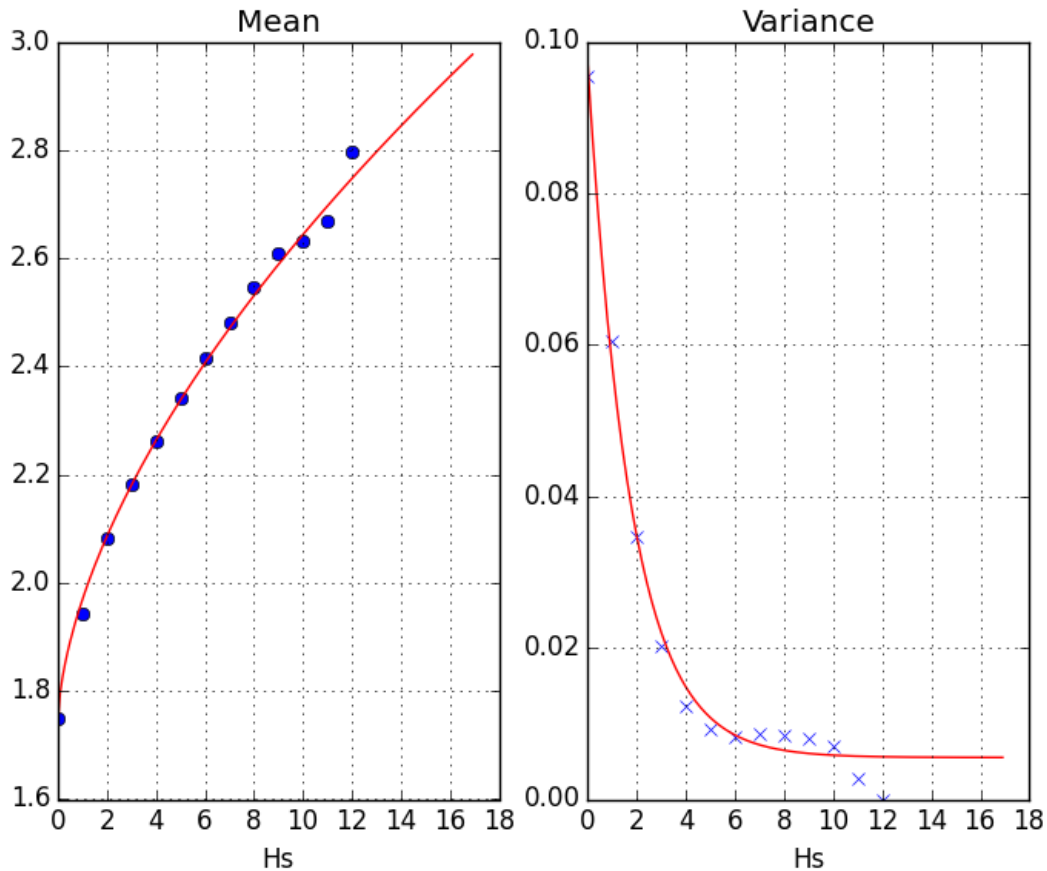


Figure 4-6: Plot of mean and variance of $\ln(T_p)$ for each group of H_s and the fitted function (red).

The 12 means and variances of $\ln(T_p)$ given H_s are plotted in Figure 4-6 with their respective fitted functions, according Eq. (24).

The best estimation for the a and b parameters were found using curve fitting. The curve fitting tool in the *Python* package *SciPy* has been used for this. It uses a nonlinear least square method to fit the data to the desired functions. As seen in Figure 4-6, it gives a reasonably good fit for the data. It is important to note that the variance cannot be negative, but in some cases $b1$ can get a negative value. Then $b1$ should be given a fixed, positive value and the best fit should be calculated again. In this data set this was not a problem, and a $b1$ value of 0.0055 was calculated by the optimizing tool. The resulting parameters are presented in Table 4-4.

Table 4-4: Parameters for mean and variance functions in the distribution of T_p given H_s

a_1	a_2	a_3	b_1	b_2	b_3
1.7392	0.2291	0.5965	0.0055	0.0913	0.5716

The final cumulative distribution function for T_p given H_s can now be calculated using Eq. (23). It is common to find the 90% confidence interval for ULS and ALS. This is done by calculating the upper 95% bound and the lower 5% bound. This is presented in Figure 4-7, together with the original data from the hindcast.

The extreme sea states can be used to estimate the extreme response of the structure. From the conditional distribution of T_p given H_s , the most extreme sea states for a return period of 100 and 10 000 years are found and presented in Table 4-5. These parameters can be used as input to describe the extreme sea states for the dynamic time domain simulations in USFOS.

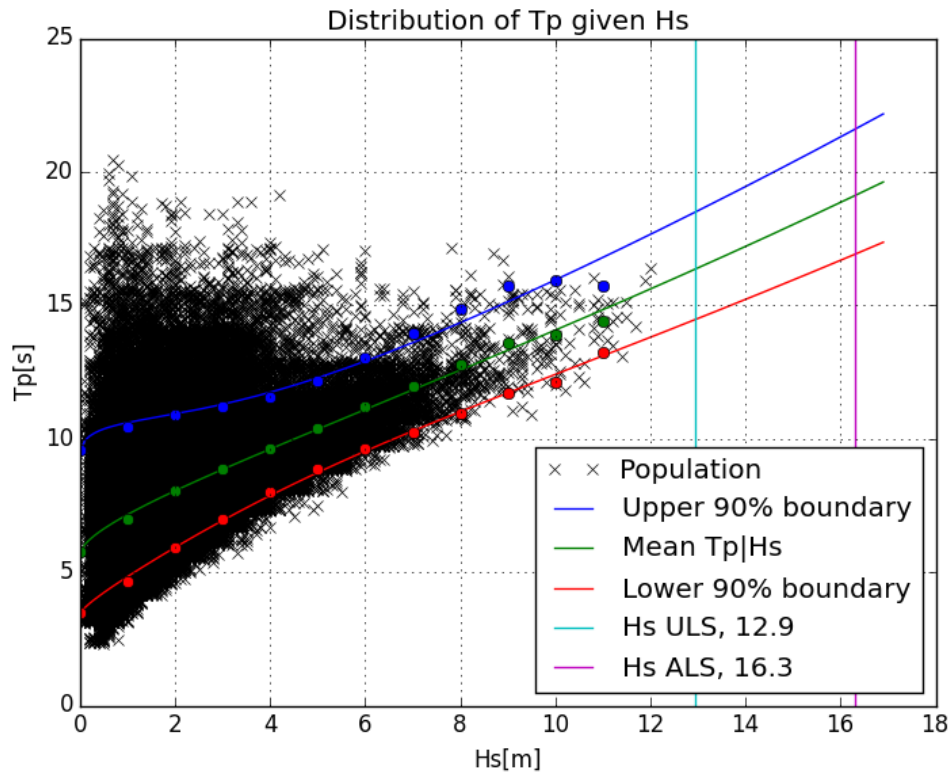


Figure 4-7: Cumulative distribution of T_p given H_s with a 90% confidence bound for the T_p interval, also showing the significant wave height for ALS and ULS. Original data set shown in black.

Table 4-5: Extreme sea states and their corresponding values for Hs and Tp

Return Period[years]	Hs[m]	Tp mean [s]	Tp lower 5%[s]	Tp upper 95% [s]
100 – ULS	12.9	16.4	14.5	18.5
10 000 - ALS	16.3	19.2	17.0	21.7

4.4 Distribution of Wave Heights

One way of estimating the extreme wave heights is to use the Forristall distribution of wave heights (Forristall, 1978). This method is also mentioned in (Haver, 2002). The Empirical Forristall wave height distribution is a Weibull type distribution that is dependent only on the significant wave heights of each sea state. The distribution and the parameters of the empirical model are given in (Forristall, 1978):

$$F_{H|(H_s, T_p)}(h|(h_s, t_p)) F_H(h|h_s) = 1 - \exp\left(-\left(\frac{h}{\alpha_H}\right)^{\beta_H}\right) \quad (25)$$

$$\alpha = 0.683 h_s$$

$$\beta = \ln(8.42) = 2.13$$

In (Haver, 2002), narrow banded variations of the Empirical Forristall model are listed and they include the Rayleigh Model and Næss Model, which both also depend on the wave period, but they are not considered in this report, see e.g (Næss, 1985)

In (Forristall, 1978) it is referred to (Jahns and Wheeler, 1973), which argues that as long as the number of waves are estimated on the basis of zero crossings, narrow spectrum statistics can be applied. Therefore the period used when calculating the number of maxima is the zero up-crossing period.

To find an estimate of the zero up-crossing period to use for the calculations (Haring et al., 1976) recommends using the zero up-crossing period as 80% of the spectral peak period. DNV GLs RP-C205 (DNV, 2010) has similar values, which are listed in equation (26). Since the platform is assumed located in the North Sea, the values from DNV RP C-205 have been used. They are based on the JONSWAP spectrum and using a peakedness parameter of $\gamma=3.3$. This is the same spectrum and peakedness as in Chapter 5.

This method neglects the variation in T_p for each sea state, but instead used the mean spectral period for the whole sample to calculate the zero up-crossing period, which can be estimated by: (DNV, 2010)

$$T_z = \frac{1}{1.2859} T_p = 0.7776 \cdot T_p \quad (26)$$

$$N = \frac{10800}{T_z}$$

Because of the hybrid distribution of H_s , the integral has to be divided in two parts: $h \leq \eta$ and $h > \eta$, using the log-normal and Weibull distributions respectively:

$$F_{H_{3h}}(h) = \int_0^\eta (F_{H|(H_s)})^N \cdot f_{H_s, \log-normal} dH_s + \int_\eta^\infty (F_{H|(H_s)})^N \cdot f_{H_s, Weibull} dH_s \quad (27)$$

In Python this is done by using 1000 iterations to go through every height from zero to 40 m and the built in Python integration functions from the SciPy package. Error estimates for the integrals are also found and seen to be in the order of 10^{-13} . The probability of a single 3-hour maximum to exceed the value for the limit states are: $10^{-2}/2920$ and $10^{-4}/2920$ for ULS and ALS respectively. 2920 is the number of 3-hour sea states per year. The results are presented in Figure 4-8.

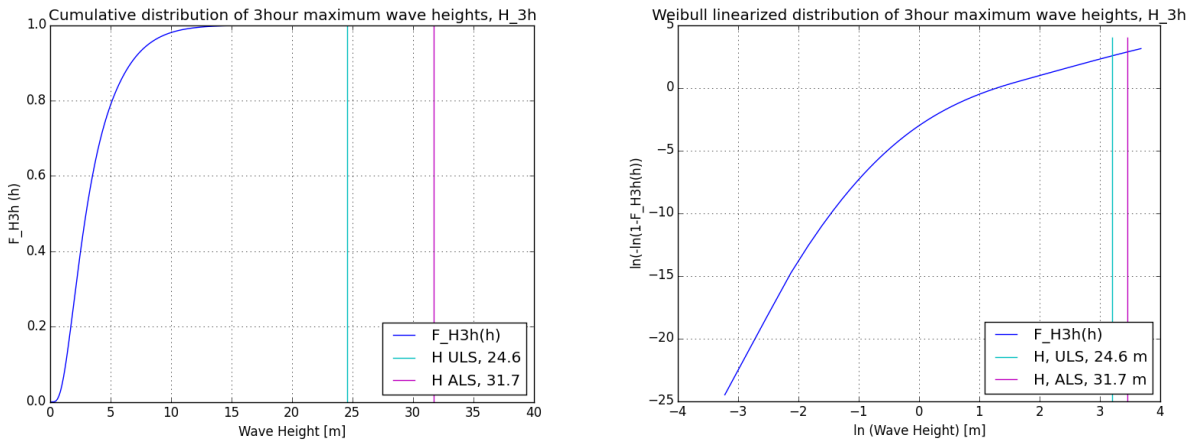


Figure 4-8: Cumulative Forristall distribution of the 3 hour maximum wave height, both regular and linearized with respect to the upper Weibull-part of the distribution.

According to N003 (NORSOK, 2007) the extreme wave height for the design wave method can be estimated as 1.9 times the significant wave height with a return period of 100 years (ULS). For a return period of 10 000 years (ALS), it is recommended to multiply with an additional 1.25 times

the $H_{\max 100 y}$. This can be a good comparison for the values obtained using Forristall Height distribution. The NORSOK estimates give:

$$\begin{aligned} H_{\max 100 y} &= H_{S ULS} \cdot 1.9 = 12.9 \cdot 1.9 = 24.51 \text{ m} \\ H_{\max 10\,000 y} &= H_{\max 100 y} \cdot 1.25 = 24.51 \cdot 1.25 = 30.64 \text{ m} \end{aligned}$$

While the results from the Forristall Height Distribution gives the following values:

$$\begin{aligned} H_{\max ULS} &= 24.6 \text{ m} \\ H_{\max ALS} &= 31.72 \text{ m} \end{aligned}$$

For ULS, defined by a 100 year return period, the difference between the two methods is only 0.37% in this case. For the 10 000-year return period for ALS, the difference is higher at 3.52%. The reason for this difference is that the Forristall Height distribution calculates the height for the specific site, while NORSOK is based on an estimate that is supposed to cover the whole Norwegian Continental Shelf. Using the Forristall Height distribution gives a difference between ULS and ALS at 28.9%, not 25% as recommended in NORSOK.

4.5 Distribution of Wave Crests

A Gaussian process cannot adequately describe the surface elevation of a wave due to the fact that real ocean waves observed in nature have higher crests and shallower troughs than given by the Rayleigh distribution. Therefore more advanced models have been created to improve the accuracy. The first was by Jahns and Wheeler more than forty years ago and introduced an empirical correction which can be further investigated in (Jahns and Wheeler, 1972). In this report the Forristall Crest Distribution (Forristall, 2000), has been used to estimate the maximum wave crests to be used for the design wave method. The Forristall crest distribution is a two-parameter Weibull based on second order wave theory. The short-term model for crest height is given by, (Forristall, 2000):

$$F_{C|H_s, T_1}(c|h, t_1, d) = 1 - \exp\left(-\left(\frac{c}{\alpha_F h}\right)^{\beta_F}\right) \quad (28)$$

where:

$$\begin{aligned} \alpha_F &= 0.3536 + 0.2892 s_1 + 0.1060 Ur \\ \beta_F &= 2.0 - 2.1597 s_1 + 0.0968 Ur^2 \end{aligned}$$

Here the sea is assumed to be long crested. The shape and scale parameters are found using two parameters, the steepness(s_1) and the Ursell Number (Ur) which are given by the following expressions:

$$s_1 = \frac{2 \pi h}{g t_1^2} \quad (29)$$

$$Ur = \frac{h}{k_1^2 d^3}$$

Where:

$$t_1 = \text{mean wave period[s]} = 1.0734 T_z = T_z \frac{1.0734}{1.2859} T_p = 0.8347 T_p; \text{ RP-C205(DNV, 2010)}$$

$$k_1 = \text{wave number corresponding to } t_1 = \left(\frac{2.0 \cdot \pi}{t_1} \right)^2 \cdot \frac{1}{g \cdot \tanh(k_1 \cdot d)}$$

d = depth [m]

g = gravitational constant [m/s²]

The distribution of wave crests have been calculated using the empirical Forristall Crest Distribution following equations (28) and (29). Since k_1 is dependent on the depth, 110 m have been used for these calculations. As a consequence of finite depth, the wave number must be found using an iterative process: (Faltinsen, 1993)

$$k = \frac{\left(\frac{2\pi}{t_1} \right)^2}{g \cdot \tanh(k \cdot d)} \quad (30)$$

The significant wave height found for ULS and ALS in Section 4.2 is used together with the average spectral peak period found I Section 4.3 to calculate the distribution parameters (presented in Table 4-6). The resulting distribution is shown in Figure 4-9.

Table 4-6: Parameters for the Forristall Crest Distribution

Parameter	Ultimate Limit State	Accidental Limit State
α	0.3686	0.3701
β	1.9038	1.9117
Steepness, s_1	0.0445	0.0409
Ursell number, Ur	0.0201	0.044

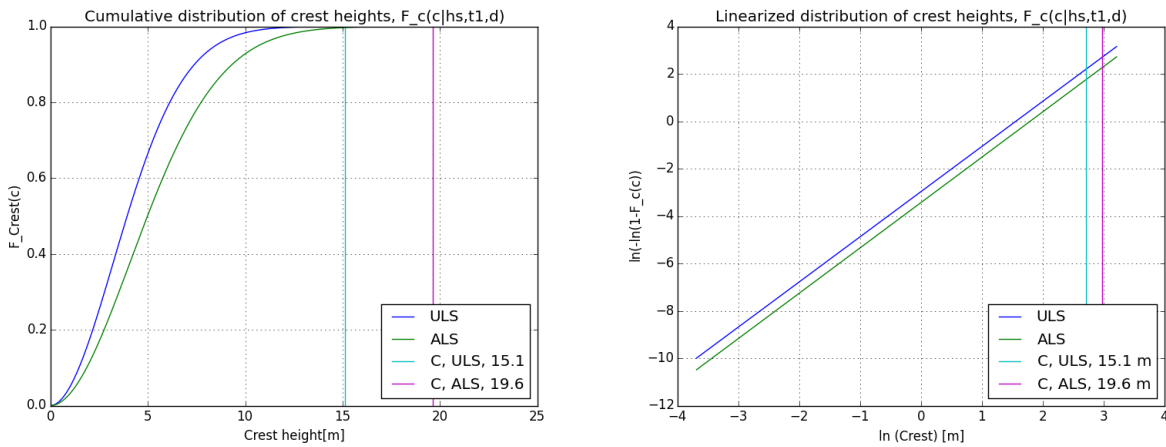


Figure 4-9: The Cumulative Forristall distribution of the 3-hour maximum Crest height both for regular and linearized Weibull distribution.

According to NORSOK a percentile of 90% or 95% should be used when finding the resulting crest. In this report 90% was used for ULS and 95% for ALS to ensure a good safety margin. This gives the results:

$$C_{ULS} = 15.125 \text{ m}$$

$$C_{ALS} = 19.625 \text{ m}$$

It is also possible to use the distribution of wave heights to estimate the wave crests. It consists of first finding the extreme wave height (Forristall, see Section 4.4) and use this to estimate the extreme wave crests by multiplying with a factor which is typically in the size of 58-62% (Haver, 2002).

Wave crest estimated from height: 14.76 m (ULS) and 19.03 m (ALS) using $C=0.6H$. These values are slightly lower than the values obtained by using the Forristall Crest distribution.

4.6 Environmental Contour Lines

The environmental contour line method can be used to select the worst sea states for a site by investigating their probability of exceedance. This method is described in (Haver, 2013) and (Haver and Winterstein, 2009). The principle is that probability of every sea state can be calculated based on its combination of T_p and H_s and thus a line connecting all sea states with an equal probability of exceedance can be found. This is method also known as the First Order Inverse Reliability Method (IFORM). The environmental contour line method assumes that short-term and long-term variation of the sea states can be decoupled. Then, it is possible to create a curve describing the long-term variations based on the values for H_s and T_p which has a given return period of X years.

The annual probability of exceedance, q , which corresponds to a probability of $\frac{1}{X}$ years, is represented by its radius in the Gaussian space, which can be is found by inverting the Gaussian distribution:

$$\Phi(r) = 1 - q/2920 \leftrightarrow r = -\Phi^{-1}(q/2920) \quad (31)$$

Here ϕ is the standard Gaussian distribution function. The Gaussian space u_1, u_2 , can be transformed into the H_s - T_p plane with the following Rosenblatt Transformations:

$$F_{H_s}(h) = \Phi(u_1) \quad (32)$$

$$F_{T_p|H_s}(h_s) = \Phi(u_2)$$

The environmental contour lines can now be calculated by using the distributions for H_s and T_p as found in Sections 4.2 and 4.3. The Rosenblatt transformations of a certain annual exceedance probability gives circles in the Gaussian space. This radius is calculated for the ultimate and accidental limit state, which have a return period of 100 and 10 000 years, respectively. The annual probability of exceedance, q , gives a radius of 4.498 and 5.395 for ULS and ALS. These circles in the Gaussian space u_1, u_2 , must now be transformed into the H_s - T_p plane with the Rosenblatt Transformations. Since the lonowe hybrid model has been used for the distribution of significant wave heights, it is important that the transformation is split in two parts:

For $h \leq \eta$, the Log-normal distribution is used:

$$\Phi\left(\frac{\ln h - \theta}{\alpha}\right) = \Phi(u_1) \quad (33)$$

The exponent of a normal distribution gives the log normal distribution, and thus:

$$h = \exp [\theta + \alpha \cdot u_1] \quad (34)$$

While, for $h > \eta$, the Weibull distribution gives the following result by rearranging with respect to h :

$$1 - \exp \left\{ - \left(\frac{h}{\rho} \right)^\beta \right\} = \Phi(u_1) \quad (35)$$

$$h = \rho [-\ln(1 - \Phi(u_1))]^{\frac{1}{\beta}} \quad (36)$$

For the conditional distribution of T_p given H_s , it is important to use the logarithm of T_p and remember that the logarithm of a lognormal variable is following the normal distribution:

$$F_{T_p|H_s}(t|h_s) = P(T_p \leq t | h_s) = \Phi(u_2) T_p \quad (37)$$

$$= P\left(\frac{\ln T_p - \mu_{\ln t_p}(h_s)}{\sigma_{\ln t_p}(h_s)} \leq \frac{\ln t - \mu_{\ln t_p}(h_s)}{\sigma_{\ln t_p}(h_s)} \right)$$

$$= \Phi\left(\frac{\ln t - \mu_{\ln t_p}(h_s)}{\sigma_{\ln t_p}(h_s)} \right) = \Phi(u_2)$$

$$u_2 = \frac{\ln t - \mu_{\ln t_p}(h_s)}{\sigma_{\ln t_p}(h_s)}$$

$$t = \exp [\mu_{\ln t_p}(h_s) + u_2 \sigma_{\ln t_p}(h_s)]$$

The q-probability contour lines then correspond to exceedance every 100 and 10 000 year. In the Gaussian space the contour lines will form in the shape of a circle, as seen in Figure 4-10. The radius for ULS is 4.5 and ALS is 5.4 in the Gaussian space. In the H_s - T_p plane the contour lines takes a different shape corresponding to the distribution of H_s and T_p given H_s . In Figure 4-10, the contour lines are plotted in the Gaussian plane and in H_s - T_p plane together with the population from the hindcast data. The contour lines seem to underestimate the variance of T_p for H_s values between 2-6, as two sea states are outside the limit for ALS and multiple outside ULS. Because of the low H_s for these sea states, this will not affect the extreme value calculations and the contour lines are kept as they are.

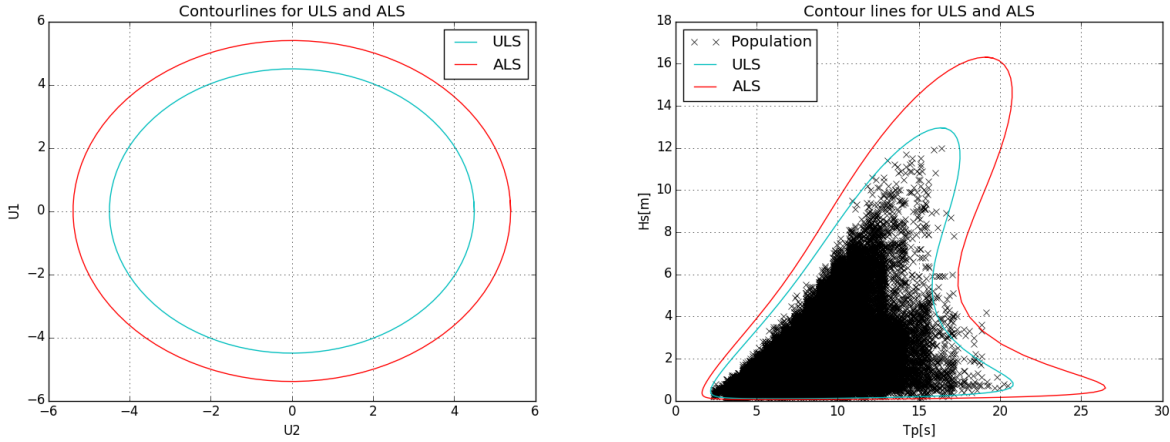


Figure 4-10: Environmental Contour lines in the Gaussian space (left) and in the Hs-Tp plane with sea state population (right)

4.7 Summary

An omnidirectional metocean report has been created for the Ekofisk-site based on 57-years of hindcast. The purpose behind this metocean report was to use it as input for estimating the extreme responses of a platform at Ekofisk. Therefore, the joint distribution of Hs and Tp, the Forristall distribution of wave heights and the Forristall crests distribution have been calculated and used to find the values that are exceeded with an annual of probability of 10^{-2} and 10^{-4} , corresponding to the ultimate and accidental limit states.

The joint distribution of significant wave heights and spectral peak period has been calculated and is displayed in Table 4-7. This Hs-Tp distribution can be multiplied with the distribution of the short-term response given Hs and Tp for an all-sea states long-term analysis of response. The methodology and result for this are presented in Section 5.4.

Both the Forristall Wave Height and the Forristall Crest distributions have been found and the largest heights are presented in Table 4-9 and crests in Table 4-10. These results can be used for the Design Wave Method when coupled with the correct period. This method and results are presented in section 5.1.

The environmental contour lines have been created for the Ekofisk based on the 100 and 10 000 return period and are shown in Figure 4-11. These can be to describe the response by the Environmental Contour Method, which is presented and conducted in Section 5.6.

Extreme Sea states from the joint distribution of Hs and Tp

Table 4-7: Parameters for the joint model of all-year, omnidirectional Hs and Tp

θ	α	η	β	ρ	a_1	a_2	a_3	b_1	b_2	b_3
0.4970	0.6463	2.8	1.3530	1.9921	1.7392	0.2291	0.5965	0.0055	0.0913	0.5716

Table 4-8: Extreme sea states and their corresponding values for Hs and Tp

Return Period[years]	Hs[m]	Tp mean [s]	Tp lower 5%[s]	Tp upper 95% [s]
100 – ULS	<i>12.9</i>	<i>16.4</i>	<i>14.5</i>	<i>18.5</i>
10 000 - ALS	<i>16.3</i>	<i>19.2</i>	<i>17.0</i>	<i>21.7</i>

The largest wave heights for ULS and ALS:

Table 4-9: Wave heights calculated from the Forristall wave height distribution and based on NORSOK recommendations

	Forristall Height	NORSOK
<i>3 hour max wave height ULS</i>	24.6 m	24.5 m
<i>3 Hour max wave height ALS</i>	31.7 m	30.6 m

The largest wave crests for ULS and ALS

Table 4-10: Wave crests calculated using Forristall crest distribution based on second order wave theory and calculated as a factor of wave height

	Forristall Crest	0.6 * Forristall Height
<i>3 hour max Crest ULS</i>	15.13 m	14.76 m
<i>3 Hour max Crest ALS</i>	19.63 m	19.03 m

Environmental Contour Lines Approach

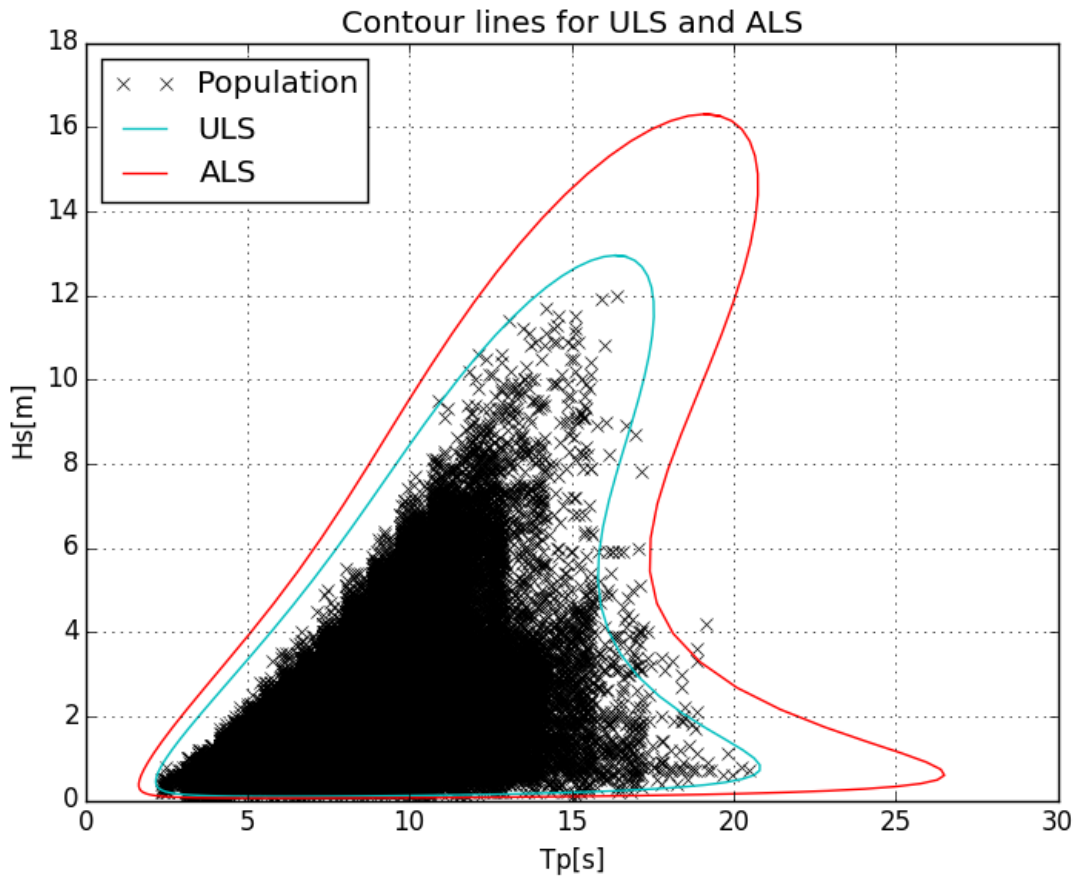


Figure 4-11: Final contour lines in the Hs-Tp plane for ULS(teal) and ALS (red) together with the original hindcast data (black)

5 Estimation of Extreme Response

There are various ways of estimating the extreme response of a structure and generally the main considerations are whether the analysis should be:

- Static or dynamic
- Linear or nonlinear
- Deterministic or stochastic

In general, the most consistent approach is the use a stochastic all sea states long-term approach. This method is described in detail and used for finding the dynamic extreme response in Section 5.4. A long-term analysis is based on being able to first describe the long-term environmental variation of the site (based on H_s and T_p) and on finding a distribution of the short-term response given the H_s and T_p of the sea state. This can be very time consuming and it can also be difficult to describe both the short-term response distribution and the long-term environmental variation accurately. The method is shown in Section 5.4, but using a limited amount of sea states and only finding the dynamic response due to time considerations.

Another, approximate method that has been shown to give good results (Haver and Winterstein, 2009) for complex extreme value problems is the Environmental Contour Method, described in Section 5.6. It is more of a stochastic short-term response analysis where the aim is to restrict the number of sea states that are investigated and rather focus on the most unfavorable sea state. Then a Gumbel-distribution is fitted to a sample of maximum values from 3-hour simulations for this sea state. An estimate of the response is then found by rearranging: (Haver and Winterstein, 2009)

$$F_{X_{3h}|H_s T_p}(x|h_q^*, t_q^*) = 1 - \alpha \quad (38)$$

Where h_q^* and t_q^* are the worst combination of H_s and T_p along the q -probability contour line. Usually all other sea state combinations are accounted for by using a rather high α -percentile. This is further described in 5.6.

The deterministic design wave method can be used to find a good and quick estimate of quasi-static response. This value is often compared to either the long-term analysis result or the environmental contour line result to find reasonable estimate of the α -percentile to use when calculating the EDAF.

The structure's response can found using the equation of equilibrium, as stated in Chapter 1. The total forces of the environmental load must equal the response of the platform:

Estimation of Extreme Response

$$M \ddot{x} + C \dot{x} + Kx = F(t) \quad (39)$$

This can be calculated quasi-statically when the response is so low that both the acceleration and velocity in the equation of motion can be neglected and assumed zero. The resulting equation of motion can then be assumed:

$$Kx = F(t) \quad (40)$$

The force is found from the Morrison equation when calculating the horizontal forces on slender offshore structures. It denotes the force per meter and can be written as: (Faltinsen, 1993)

$$dF = \rho\pi \frac{D^2}{4} C_M a_1 + \frac{\rho}{2} C_D |u|u \quad (41)$$

Where the positive force direction is in the wave propagation direction. C_M and C_D are the mass (inertia)- and drag coefficients, respectively.

For a jack-up type platform that consists of slender members, the force is going to be dominated by the drag term since the relation between $\frac{C_M \cdot d}{C_D \cdot H}$ is very low. The drag load depends on the velocity squared and for the extreme wave (high velocities in the crest) it is then safe to neglect the inertia term of the load. Thus from equation (41) the quasi-static drag force can now be estimated as the drag part of Morrison's equation:

$$F_D = \frac{1}{2} \rho D U^2 \quad (42)$$

In a quasi-static analysis the stiffness is assumed constant (not time dependent) making the quasi-static response:

$$x_{quasi-static}(t) = \frac{F(t)}{K} \quad (43)$$

The simplest way to estimate the extreme response of a structure is based on the Design Wave Method. Structures with low eigenperiods (less than 2 s (Haver, 2013)) can be considered to act quasi-statically and this method will then give good results.

5.1 Design Wave Method (Quasi-Static Response)

The Design Wave Method (Haver, 2013) is a quick and simple method for accurately estimating the quasi-static response in a structure. This is a deterministic method using a regular wave. It is effective for structures that have low eigenperiods and thus small dynamic effects. The method is based on the response being quasi-static and that the extreme load is found for the q-annual probability of exceedance largest wave. The most common wave profile to use is the Stokes 5th order and the advantage of the Stokes 5th order wave profile is that it describes the wave kinematics correctly up to the wave surface. Stokes waves are nonlinear periodic surface waves in an inviscid fluid with a constant depth and gives best results for deeper waters. The Stokes 5th order wave theory is presented in (Fenton, 1985) and the expression of the free surface profile is:

$$\begin{aligned} \kappa\eta(x) = kd &+ \epsilon \cos kx + \epsilon^2 B_{22} \cos(2kx) \\ &+ \epsilon^3 B_{31} (\cos kx - \cos 3kx) \\ &+ \epsilon^4 (B_{42} \cos 2kx + B_{44} \cos 4kx) \\ &+ \epsilon^5 (-(B_{53} + B_{55}) \cos kx \\ &+ B_{53} \cos 3kx + B_{55} \cos 5kx) + O(\epsilon^6) \end{aligned} \quad (44)$$

ϵ is the dimensionless wave amplitude: $\frac{\kappa H}{2}$, often known as wave steepness. This means the error due to neglected terms is of the sixth order. The values for the constants B_{ij} are implemented in USFOS and can also be found in Table 1 in (Fenton, 1985). The dimensionless coefficients are functions of kd , where k is the wave number and d is the depth. In Figure 5-1 the surface elevation of a Stokes 5th wave with wave height 20 meters and period 15 seconds is shown. The kinematics for the same wave are presented in Figure 5-2, as found in USFOS.

Estimation of Extreme Response

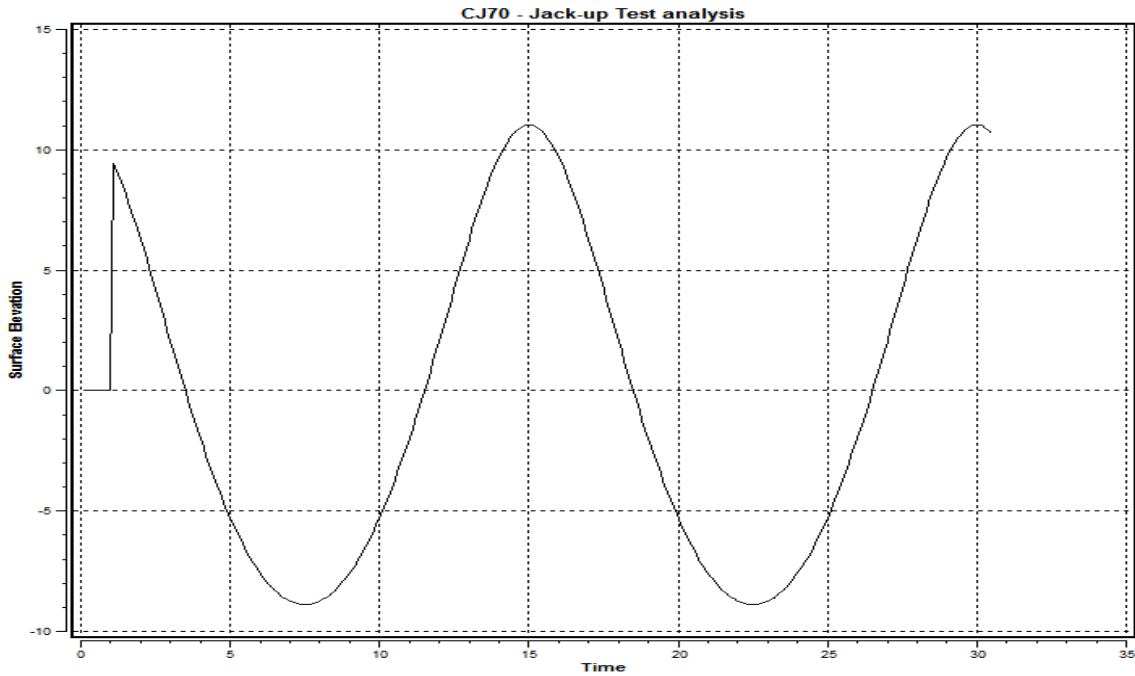


Figure 5-1: Surface elevation of Stokes 5th regular wave with height 20 m and period 15 seconds

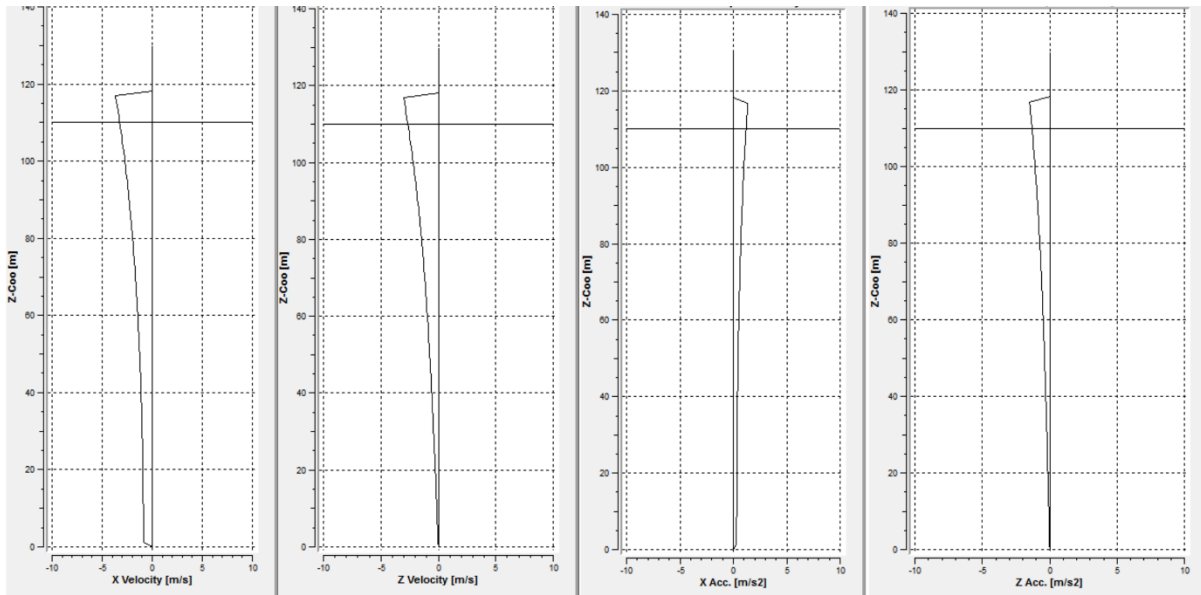


Figure 5-2: Wave kinematics of a 20 meter high, 15 second period Stokes 5th wave from USFOS. Collected 1.5 seconds before the crest when the wave was 10 meters high. Wave direction is 180 degrees (along the negative x-axis). From the left: Horizontal velocity, vertical velocity, horizontal acceleration and vertical acceleration.

Estimation of Extreme Response

The upcoming publication of NORSOK-N003 recommends that the input for the design wave should be the q-probability wave crest, C , and an associated mean wave period, T (see Scope by Professor Sverre Haver). Previously, the wave height was used but since real ocean waves have higher crests than troughs, using the crest-height gives more accurate results. This can be found from e.g. the Forristall Crest distribution (see Section 4.5). The corresponding period to be used is then the mean wave period (see Section 4.3). The alternative would be to use the q-probability wave height (e.g. from the Forristall Height Distribution, Section 4.4) and the least favorable wave period within the 90% band.

In this thesis the omnidirectional wave heights and periods have been used, and thus the wave direction should be set as the least favorable for the structure (as found in Section 3.5). It is common to fit the Stokes profile to the 100-year crest height when using the Design Wave method, so that the q-probability of annual exceedance would be 10^{-2} , which is the probability for ULS.

To find the response from the Stokes 5th order wave, a quasi-static solution of the equation of motion is solved as the wave passes through the structure, and the maximum value of the response (e.g. base shear, deck displacement or overturning moment) is the resulting design wave response.

The design wave method should in principle only be used for statically behaving structures such with low eigenperiods so that the dynamics can be neglected. For structures significantly influenced by dynamics, such as jack-ups, an irregular sea long-term analysis should be used, but the design wave method is a quick way to verify the results of the static time domain simulation.

Based on the metocean results from Chapter 4, the Stokes 5th profile has been created using both Forristall wave height (Section 4.4) and Forristall wave crest (Section 4.5). When defining the Stokes wave based on the q-probability largest crest height, the conditional mean wave period is used, which is found from the metocean results and presented together with the resulting responses in Table 5-1.

Since the Stokes 5th wave in USFOS is defined by its total wave height, not the crest height, the input used in the head-file was 26.65 m (ULS) and 33.55 (ALS) resulting in the correct crest heights from (Section 4.5), which are 15.1m and 19.6 m respectively. Table 5-1 shows the resulting responses for both ULS and ALS.

Estimation of Extreme Response

Table 5-1: Resulting responses calculated with Design Wave Method using Stokes 5th wave based on crest height from Forristall Crest distribution and the mean spectral peak period.

	<i>Crest [m]</i>	<i>Period [s]</i>	<i>Deck Displacement [m]</i>	<i>Base Shear [N]</i>	<i>Overturning Moment [Nm]</i>
ULS	15.1	16.4	0.27	1.00E+07	1.43E+09
ALS	19.6	19.2	0.52	1.98E+07	2.26E+09

When using the Forristall wave height corresponding to the q-annual probability of exceedance, as found in (Section 4.4), the worst period within the 90-percent confidence band must be found. It is sufficient to test for the lowest, highest and middle period of the band and find the period corresponding to the highest response. These periods are shown in Table 5-2 for both ULS and ALS together with the resulting responses. The largest quasi-static response was found for the upper band of the period for both ULS and ALS.

Table 5-2: Resulting responses calculated with Design Wave Method using Stokes 5th wave based on wave height from Forristall Wave Height distribution and 90% confidence band of periods.

Profile decided by Wave Height		<i>Deck Displacement [m]</i>	<i>Base Shear [N]</i>	<i>Overturning Moment [Nm]</i>
ULS: Wave height 24.6 m				
<i>T [s]</i>	14.5	0.18	0.72E+07	1.21E+09
<i>T [s]</i>	16.4	0.23	0.83E+07	1.27E+09
<i>T [s]</i>	18.5	0.26	0.96E+07	1.33E+09
ALS: Wave height 31.7 m				
<i>T [s]</i>	17	0.42	1.53E+07	1.93E+09
<i>T [s]</i>	19.2	0.46	1.75E+07	2.03E+09
<i>T [s]</i>	21.7	0.47	1.96E+07	2.14E+09

The new (crest) and old (wave height) methods of the design wave approach can be compared by investigating the results in Table 5-1 and Table 5-2. For ULS, the response based on the largest crest are between 7-10% larger than for the response based on wave height. For ALS, the difference is between 3-13% depending on the response. Using the crest height gives the largest values in every case. A comparison of the two methods is presented in Table 5-3.

Table 5-3: Comparison of the two methods for estimating the design wave response. The result is presented as the factor, by which crest-method is larger than the height-method.

Crest/Height	<i>Deck Displacement</i>	<i>Base Shear</i>	<i>Overturning Moment</i>
ULS	1.082	1.069	1.096
ALS	1.133	1.032	1.075

The resulting response from the crest-method (presented in Table 5-1) are the ones that will be used when finding the EDAF and comparing with the static results from the contour line method.

5.2 The Principles of Time Domain Simulations

A stochastic approach will yield a more consistent estimation of the response than using a deterministic design wave approach and when also introducing the system's stiffness and damping, the correct dynamic response can be calculated. The first step towards solutions in the time domain for any structure is solving the equation of motion due to environmental loading at time t , which can be described as:

$$m \ddot{x}(t) + c(x, \dot{x})\dot{x}(t) + k(x, \dot{x}) x(t) = Q(t) \quad (45)$$

Where:

- x is the motion of the structure, whether it is translation or rotation.
- m is the mass of the system (mass and added mass)
- $c(x, \dot{x})$ is the damping of the system
- $k(x, \dot{x})$ is the stiffness of the system
- $Q(t)$ is the external loading on the system in the direction of the selected degree of freedom
- \dot{x} and \ddot{x} are the first and second time derivatives of x , respectively.

In this equation the left hand side describe the mechanical characteristics (response) while the right side describe the loading. The matrix form of equation (45) can be described as:

$$M \ddot{x} + C\dot{x} + Kx = Q(t) \quad (46)$$

A time domain solution is in principle a step by step solution of this equation. This can be solved by numerically integrating the equation of motion. Assuming $x(t_i)$, $\dot{x}_i(t_i)$, $\ddot{x}_i(t_i)$ and $q_{i+1} = q(t_{i+1})$ is known then displacement (x_{i+1}) at time $t = t_{i+1}$ can be found. The dynamic equation of motion for time $t = t_{i+1}$ is then given as:

$$m \ddot{x}_{i+1} + c \dot{x}_{i+1} + kx_{i+1} = q_{i+1} \quad (47)$$

Then the response values for $t = t_i$ is used as the initial conditions to solve the response for $t = t_{i+1}$. There are various methods for solving the equation of motion in the time domain, but one of the most commonly used is one of the variations of the Newmark β -method (Langen and Sigbjørnsson, 1979)

Basic Steps of Time domain Analysis

For a time domain simulation to have a good accuracy it is important that the time step (Δt) between $t = t_i$ and $t = t_{i+1}$ is adequately small. Then the steps of a time domain analysis for an offshore structure, e.g. a jack-up, could be the following (Haver, 2013):

1. Use a possible sea state from the area to simulate the surface elevation for a duration of time (usually three hours for a sea state). In this report the sea elevation is calculated based on the JONSWAP spectrum with input values for H_s , T_p and $\gamma = 3.3$.
2. Calculate the kinematics in the fluid due to the load on the exposed jack-up structure from the sea level and to the exact surface.
3. Calculate the loads on the submerged part of the jack-up structure at each time step during the time period in which the surface elevation covers the members.
4. Solve the equation of motion using the loads found in 2 and 3. If the motions in the jack-up are small, the mechanical part of the equation of motion can be linearized and calculated as quasi-static. For large motions the damping and stiffness coefficients need to be calculated again for every time step. The result is the response which can be e.g. base shear or the overturning moment. For most practical application a linear mechanical system is applied, but not for the extreme response in jack-ups.

5.3 Uncertainties in Time Domain Simulations

5.3.1 Air Gap Analysis

One important assumption that can have a huge impact on the extreme response is that there is no wave-on deck impact. The air gap is the distance between the free water surface and deck of the platform. The instantaneous air gap can be found as

$$a(x, y, t) = a_0 + z(x, y, t) - \eta(x, y, t) \quad (48)$$

Where a_0 is the still water air gap. For a fixed structure such as a jack-up the translation in heave, z , can be neglected. A negative air gap means that the wave crests can impact the deck of the platform and then large slamming loads must be accounted for. The no wave-on deck impact assumption is valid if there still is air gap for ALS surface elevation. The largest possible surface elevation is for the ALS(10 000 year return period) crest which is almost 20 meters at the Ekofisk site. The storm-surge and tide should also be added to this calculation, but was not part of the metocean data. The platform has an air gap of about 32 meters between the deck and the still water. This means there is no risk of wave-on deck impact and this is a safe assumption

5.3.2 Stokes 5th vs Static Time Domain Simulation

A good way to check the results of a static time domain simulation is to compare the results with those of a regular (Stokes 5th) wave with the same parameters describing the wave.

This is a verification study to see how well the response from the short-term static time domain analysis compare with the response acquired using a Stokes 5th wave with equal parameters. By investigating the surface elevation in the short-term time domain analysis, certain waves were selected for comparison with Stokes 5th using the same wave crest and wave period. The period T is chosen as the time between two subsequent troughs. The most correct results comes from defining the Stokes 5th wave to have the same crest height as the wave in the static long-term simulation. For the Stokes 5th wave, the drag coefficient is lower than for the long-term simulation since the time domain analysis uses this higher drag coefficient to compensate for higher order wave effects that are not included in linear wave theory (see Subsections 5.3.3 and 5.7.4). Another possibility would be to fit the Stokes 5th wave to have an equal wave height as the time domain simulation. Both methods have been investigated and the plots of surface elevation, deck displacement, base shear and overturning moment is presented in

Three large waves were selected from the static time domain simulation and their responses were compared to those of a Stokes 5th wave. The waves were selected because they were large and had a distinct shape:

Estimation of Extreme Response

1st: The first wave has a crest of 14.9 meters and a period of 18.5 seconds. The total wave height is 23.6, so this is a typical asymmetric wave with a much larger crest than trough.

2nd: The second wave has the same crest height (11.5meters) and wave height (21.0 meters) as the Stokes wave and is thus the perfect example for comparing the results. The period is 15.6 seconds.

3rd: This third wave has a deeper trough than the crest is high and is therefore very different to the Stokes 5th wave. The crest is 13.3 meters and the wave height 28.8 meters.

The irregular wave from the static time domain simulation shows a good comparison with the Stokes 5th of equal crests height for all three waves, but the values are generally around 10-15 %. Fitting with equal wave height can give very large inaccuracies for the response, especially if the trough is larger than the crest, as for the 3rd wave. The best method is to use the same crest height for the comparison. The main reason is that the largest response generally comes from the crest and that the depth of the trough doesn't affect the extreme response in the same way. This is because of the wave kinematics and the horizontal velocity is always larger in the crest than in the trough.

Stokes 5th wave consistently gives 10-20% larger responses (depending on the type) due to higher order effects that is not included in the linear wave theory of the static time domain simulation. This is further discussed in Subsection 5.3.3 and also investigated in more detail in the sensitivity study of Subsection 5.7.4.

From the overturning moment plots it is possible to spot some inaccuracies or errors when the response nears a zero-value. For both the 1st and the 2nd wave there is a jump which doesn't fit well with the other responses. This will be discussed further in Section 5.3.3.

One would expect that the 2nd wave and the Stokes 5th would get responses that look more alike since the waves have almost exactly the same shape. One possible explanation to this is that since the 2nd wave is irregular and the plot in the table shows the just the elevation at one point against time, this might not actually be the real shape of the wave. The plot shows the height in the z plane versus time, but for an irregular wave that is not the same as seeing the wave in the x and z plane. This means that the wave not necessarily looks exactly like the Stokes 5th wave when it passes by another point on the platform. These surface elevations are extracted at the center of the jack-up, but the response is felt in the three legs which are spaces 70 meters apart. This should be investigated further and that can be done by using USFOS to extract the surface elevation of the irregular wave at multiple points along the platform. This will give the wavelength and the wave height and this should be used to be compared to Stokes 5th for a more accurate result.

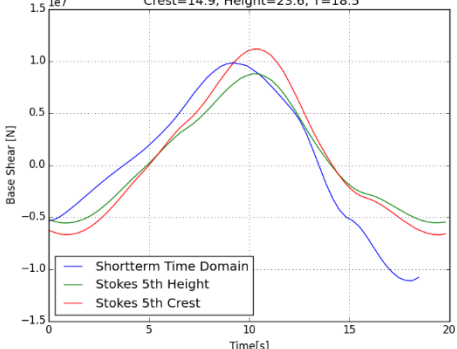
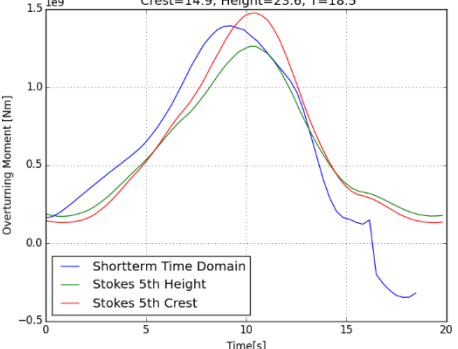
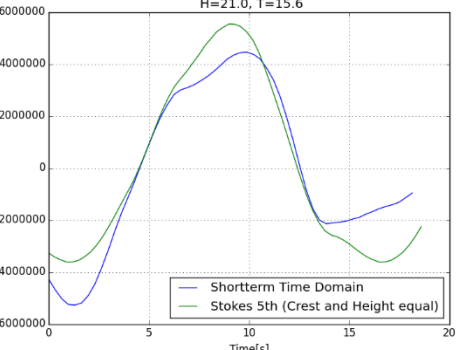
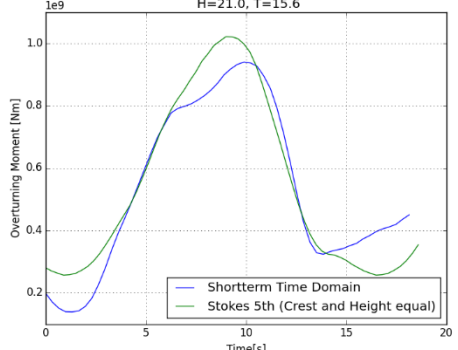
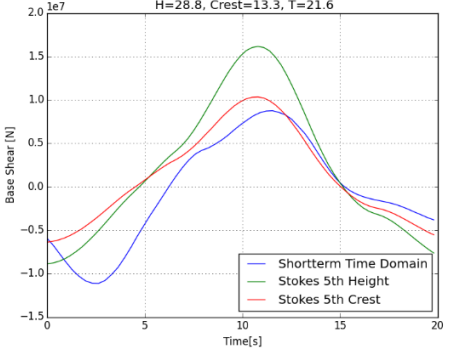
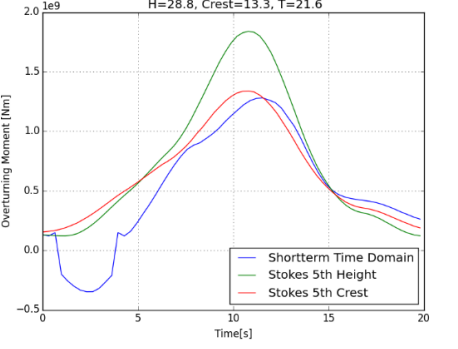
Estimation of Extreme Response

Table 5-4: Summary of all three different waves picked from the short-term time domain (blue) simulation and compared against Stokes 5th with both equal height (green) and equal crest (red) for surface elevation, deck displacement, base shear and overturning moment.

Comparison#	Surface Elevation [m]	Deck Displacement [m]
<p>1) Crest: 14.9m (red), Height: 23.6m (green). Period 18.5s</p>		
<p>2) Crest: 11.5m (green), Height: 21.0m (green). Period 15.6 s</p>		
<p>3) Crest: 13.3m (red) Height: 28.8m (green). Period 21.6 s</p>		

Estimation of Extreme Response

Table 5-5: Summary of all three different waves picked from the short-term time domain (blue) simulation and compared against Stokes 5th with both equal height (green) and equal crest (red) for surface elevation, deck displacement, base shear and overturning moment.

Base Shear [N]	Overturning Moment [Nm]	Comparison#
<p>Regular wave (Stokes 5th) vs static time domain for: Crest=14.9, Height=23.6, T=18.5</p>  <p>— Shortterm Time Domain — Stokes 5th Height — Stokes 5th Crest</p>	<p>Regular wave (Stokes 5th) vs static time domain for: Crest=14.9, Height=23.6, T=18.5</p>  <p>— Shortterm Time Domain — Stokes 5th Height — Stokes 5th Crest</p>	<p>1)</p> <p>Crest:14.9m (red) Height:23.6m (green) Period 18.5s</p>
<p>Regular wave (Stokes 5th) vs static time domain for: H=21.0, T=15.6</p>  <p>— Shortterm Time Domain — Stokes 5th (Crest and Height equal)</p>	<p>Regular wave (Stokes 5th) vs static time domain for: H=21.0, T=15.6</p>  <p>— Shortterm Time Domain — Stokes 5th (Crest and Height equal)</p>	<p>2)</p> <p>Crest:11.5m (green), Height:21.0m (green). Period 15.6 s</p>
<p>Regular wave (Stokes 5th) vs static time domain for: H=28.8, Crest=13.3, T=21.6</p>  <p>— Shortterm Time Domain — Stokes 5th Height — Stokes 5th Crest</p>	<p>Regular wave (Stokes 5th) vs static time domain for: H=28.8, Crest=13.3, T=21.6</p>  <p>— Shortterm Time Domain — Stokes 5th Height — Stokes 5th Crest</p>	<p>3)</p> <p>Crest:13.3m (red) Height:28.8m (green). Period 21.6 s</p>

5.3.3 Error in Reaction Overturning Moment in USFOS.

From the 1st and 3rd waves in Table 5-4, it is quite obvious that there are some problems with the calculation of the reaction overturning moment (OTM). This could be a numerical error, but it would be strange that only the overturning moment gets these abrupt changes, when the response calculations are smooth for both deck displacement and base shear. By looking at the 2nd wave it is also strange that the overturning moment doesn't become negative at any point, while both the other responses do.

Sometimes there are some problems when calculating the overturning moment due to the finite element modelling. The reason can be some either loosely modelled or strictly locked nodes that misbehave, but by investigating the structure in Xact (USFOS GUI) it was not possible to find any.

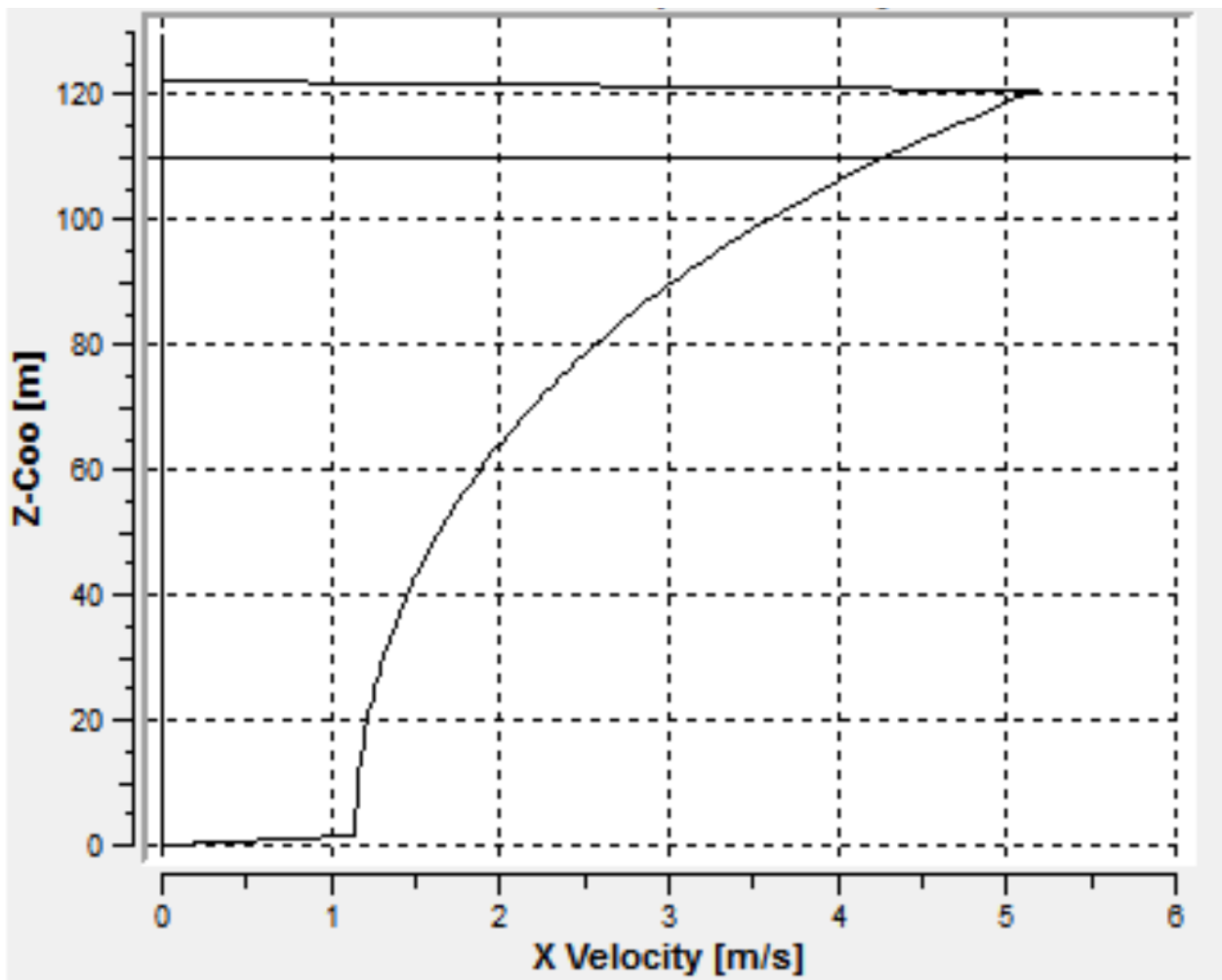


Figure 5-3: Stoke 5th horizontal velocity underneath the crest of a 20 meter high Stokes 5th wave.

A very rough and shallow estimate of the overturning moment would be to multiply the base shear reaction with the height of the platform. The depth is 110 meters and assuming this as the point of

Estimation of Extreme Response

attack will probably overestimate the momentum. By investigating Figure 5-3 and knowing that the force depends on the velocity squared, this should be an overestimation.

Table 5-6: Comparison of overturning moment from USFOS with rough overestimation based on the base shear

Wave	Base Shear · 110m	Overturning Moment	Difference	%
1 st	1.10E+09	1.40E+09	3.00E+08	27.27%
2 nd	4.95E+08	9.50E+08	4.55E+08	91.92%
3 rd	9.46E+08	1.30E+09	3.54E+08	37.42%

Figure 5-4 shows how the momentum and base shear changes with time. The momentum oscillates around a value of around 5E+08 which doesn't make much sense for a platform only subjected to wave loads. There is no current and for linear wave theory, the wave load should oscillate around a value close to zero, as seen for base shear.

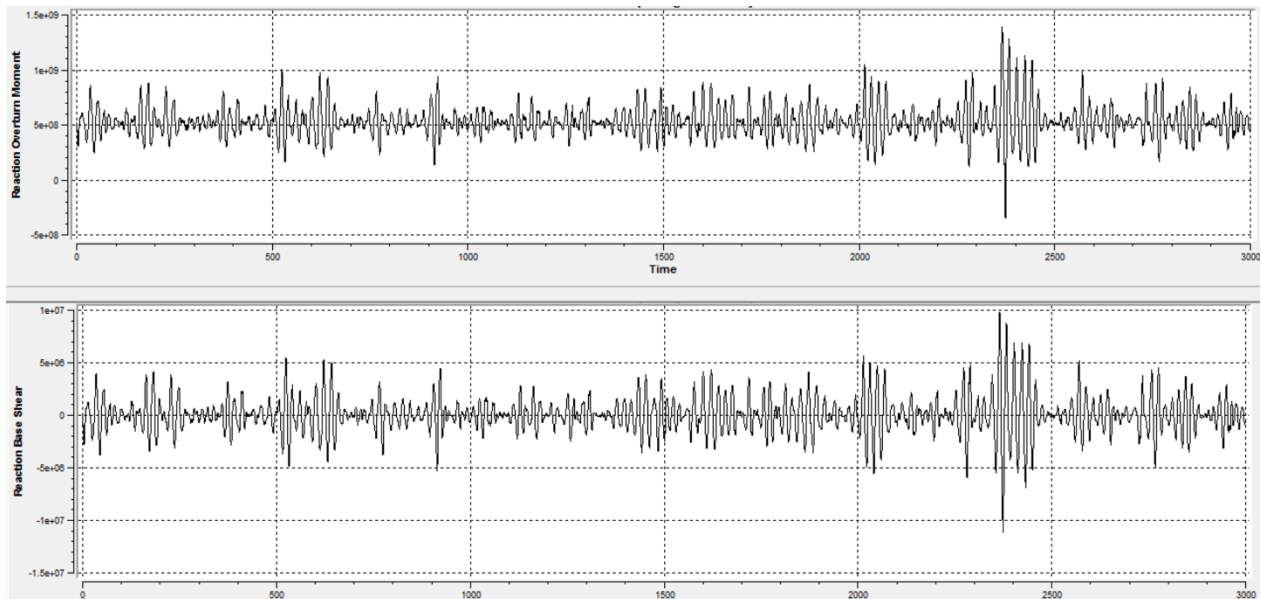


Figure 5-4: The reaction base shear and reaction overturning moment for USFOS. The moment has a non-zero mean value around which it oscillates

It looks like the value of the static overturning moment has a constant error of about 5.2E8. For all the analyses conducted in this thesis, the overturning moment results seem to follow the same trends as base shear and deck displacement so it's not necessarily 100% wrong. Maybe the

“constant” value could have been subtracted for the sample and the results would be accurate, but this would require further analysis.

Based on these graphs and arguments it is recommended not to trust the resulting response from the overturning moment calculations and rather focus on base shear and deck displacement.

5.3.4 Surface Elevation and Wave Kinematics

There are different ways and methods do describe the sea surface elevation and it is common to simplify by using first order (linear) waves. When simplifying, higher order effects get neglected on the behalf of quicker simulations. For the extreme response estimation this is a problem for two reasons. 1) since nonlinear effects are the reason the crests are higher than the troughs are deep (Marthinsen and Winterstein, 1992). This is because of the skewness and the irregularity of higher order waves. (Stansberg, 1998) refers to (Longuet-Higgins, 1963) discoveries where it was shown that the skewness always is positive for infinite water depths. 2) The nonlinear velocity dependence of the drag force require more accurate kinematics for correct results.

There are deterministic methods that account for the skewness, but not the irregularity, such as using Stokes 5th regular waves. USFOS’ built-in module uses linear wave theory and extrapolates the wave kinematics to the instantaneous sea surface (see Wheeler stretching), but improved accuracy could be achieved by using second order wave theory for the surface elevation and use (linear) Wheeler stretching for the kinematics. The most correct solution would be to completely base wave kinematics on second order theory. For extreme crests a certain contribution from third and higher effects should also be expected, but the second-order contribution is the most important and also the first step towards a more correct surface realization than the linear description (Stansberg, 1998).

Airy Wave Theory

Linear wave theory is often referred to as Airy Wave Theory since George Airy was the first to postulate it in 1841. It describes the propagation of linear gravity waves under certain conditions. The depth must be equal for the whole layer and the fluid must be homogenous, inviscid, irrotational and incompressible. It is based on the potential flow approach, where the motion of the waves can be described by its velocity potential, ϕ , and the flow velocity \mathbf{V} is represented by:(Faltinsen, 1993)

$$\mathbf{V} = \nabla\phi = \frac{\partial\phi}{\partial x}\mathbf{i} + \frac{\partial\phi}{\partial y}\mathbf{j} + \frac{\partial\phi}{\partial z}\mathbf{k} \quad (49)$$

For an irrotational ($\nabla \times \mathbf{V} = 0$), inviscid and incompressible ($\nabla \cdot \mathbf{V} = 0$) fluid it follows that the velocity potential has to satisfy the Laplace equation:

$$\frac{\partial^2 \phi}{\partial x^2} + \frac{\partial^2 \phi}{\partial y^2} + \frac{\partial^2 \phi}{\partial z^2} = 0 \quad (50)$$

When applying the boundary conditions (bottom, dynamic free surface, kinematic and combined free surface) to (50) the physical problem can be described mathematically.

Statistics of Linear Waves

Statistical models can be used to describe the random nature of the ocean surface at a certain location. For simplicity, one directional waves in a two dimensional space are assumed. Then the surface elevation can then be described by:

$$\zeta(x, t) = \sum_{n=1}^N \zeta_{An} \cos(\omega_n t - k_n x + \epsilon_n) \quad (51)$$

Where the frequency $\omega_n^2 = g \cdot k_n$ for deep water waves. g is the gravitational constant, k is the wave number and ϵ_n is the phase of wave component n . ϵ_n is a stochastic variable that is statistically independent and identically distributed between 0 and 2π . The following assumptions are used for the wave process:

- Stationary: Within a short time period, known as a sea state (usually between 20 minutes and 3 hours for ocean waves depending on location) the mean and the variance is constant.
- Gaussian distribution. The surface elevation follows a normal distribution with zero mean and variance σ^2 .
- Ergodic. One single time series can represent the whole process, and the mean and variance is found by time averaging the time sample.

For the stationary Gaussian process, the surface elevation simplifies to:

$$\zeta(t) = \sum_{n=1}^N \zeta_{An} \cos(\omega_n t + \epsilon_n) \quad (52)$$

Estimation of Extreme Response

The energy (kinetic + potential) in a wave can be described by its amplitude and wavelength. For linear waves, the total energy per unit is given by(Myrhaug, 2007):

$$E_n = \frac{1}{2} \rho g \zeta_{An}^2 \quad (53)$$

ρ is the density of sea water $\left[\frac{kg}{m^3}\right]$

g is the gravitaional constant $\left[\frac{m}{s^2}\right]$

The total energy in a sea state can then be described by the sum of the N harmonic components, found by combining (52) and (53) :

$$\frac{E}{\rho g} = \sum_{n=1}^N \frac{1}{2} \zeta_{An}^2 (\omega_n) \quad (54)$$

Where $\zeta_{An}^2(\omega_n)$ is the amplitude for the linear wave component with frequency, ω_n . It can be interesting to find the energy at different frequencies since an offshore structures responses are largely impacted by the load frequency if it has a high eigenperiod. By introducing the wave energy spectrum for $\zeta(t), S(\omega)$, so that the area within a small frequency interval, $\Delta\omega$, equals the total energy of all the components within this area:

$$\frac{1}{2} \zeta_{An}^2 = S(\omega_n) \Delta\omega \quad (55)$$

The total energy is found by combining equations (54) and (55):

$$\frac{E}{\rho g} = \sum_{n=1}^N \frac{1}{2} \zeta_{An}^2 = \sum_{n=1}^N S(\omega_n) \Delta\omega \quad (56)$$

By imagining that $N \rightarrow \infty$ so that $\Delta\omega \rightarrow 0$, the total energy becomes:

$$\frac{E}{\rho g} = \frac{1}{2} \zeta_A^2 = \int_0^{\infty} S(\omega) d\omega \quad (57)$$

The surface elevation can be found from the spectrum as:

$$\zeta_{An} = \sqrt{2S(\omega_n)\Delta\omega} \quad (58)$$

This spectrum will now contain all necessary information of the statistical properties of $\zeta(t)$ (such as μ, σ or *kurtosis*) since the moments of the spectrum can be used to establish information of the surface realization. The n'th moment is found as:

$$m_n = \int_0^{\infty} \omega^n \cdot S(\omega) d\omega \quad (59)$$

The variance is now found as:

$$m_0 = \sigma^2 = \int_0^{\infty} S(\omega) d\omega \quad (60)$$

Other important values that can be established are, from (Myrhaug, 2007) and (Myrhaug, 2005)

$$H_S = 4 \sqrt{m_0}, \text{ estimate for significant wave height} \quad (61)$$

$$\omega_{01} = \frac{m_1}{m_0}, \text{ mean frequency of the spectrum}$$

$$T_{m01} = \frac{2\pi}{\omega_{m01}}, \text{ mean period of the spectrum}$$

$$\omega_{m02} = \sqrt{\frac{m_2}{m_0}}, \text{ the mean zero up-crossing frequency of the spectrum.}$$

$$T_{m02} = \frac{2\pi}{\omega_{m02}}, \text{ mean zero up-crossing period of spectrum. Used to calculate the number of global maxima}$$

$$T_{m24} = 2\pi \cdot \sqrt{\frac{m_2}{m_4}}, \text{ mean period between local maxima.}$$

The relation between T_{m02} and T_{m24} describes how narrow banded the process is and a value of 1 means the process is completely narrow banded.

Wheeler stretching

Linear (Airy) wave theory only describes the kinematics up to the mean water surface. Wheeler stretching is also known as stretched Airy theory, and is the most commonly used method to estimate kinematics at the sea surface. It is based on linear theory. By Wheeler stretching the kinematics at the mean water level are applied to the free water surface and the velocity and acceleration profiles down to the sea bottom are stretched accordingly, see Figure 5-6. This is achieved by substituting the original z value with a stretched value, z_s using the following formula: (DNV, 2013)

$$z = \frac{z_s - \zeta}{1 + \left(\frac{\zeta}{d}\right)}; -d < z < 0; -d < z_s < \eta \quad (62)$$

Where d is the water depth and ζ is the wave elevation. A figurative sketch depicting Wheeler stretching is shown in Figure 5-6a.

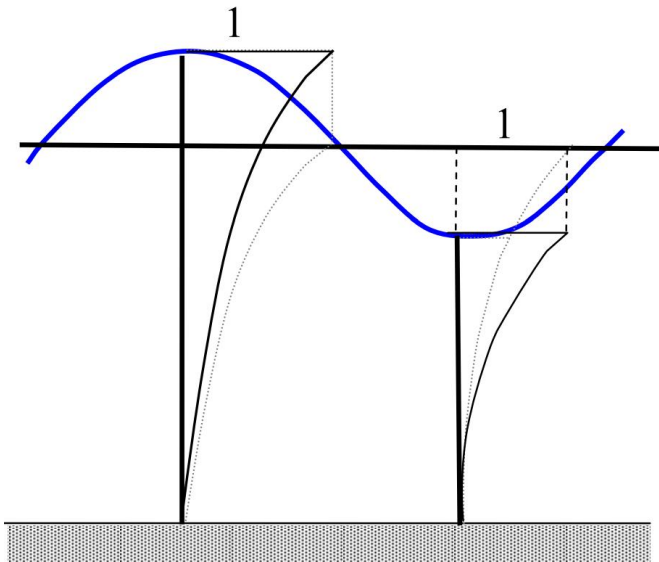


Figure 5-6a: Graphical illustration of Wheeler Stretching, figure from the USFOS theory-manual, (SINTEF, 2010).

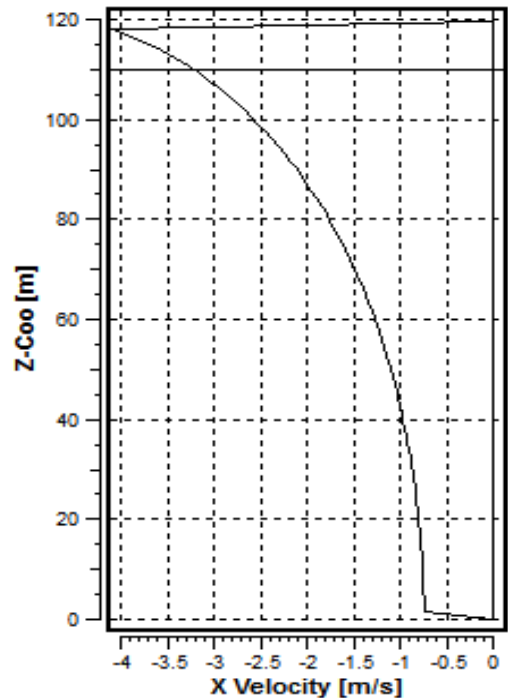


Figure 5-6b: Horizontal velocity for linear wave theory with Wheeler stretching as found in USFOS for wave with a crest of 11.5 meters. The direction is the negative x -direction.

Wheeler stretching is necessary since the Airy Wave theory (linear) only describe the wave kinematics up to $z=0$. Wheeler stretching has shown to be very accurate when it comes to calculating the velocity at the free surface, but unfortunately underestimates the velocity profile underneath the surface. (DNV, 2013) This is a well-known weakness and makes Wheeler stretching less than ideal for accurate calculation of loads on drag dominated structures such as a jack-up. The actual wave kinematics found in USFOS is presented in Figure 5-6.

Increased Drag Coefficient

Wheeler stretching is implemented to account for the kinematics at the real sea surface (not $z=0$), but underestimates the crests velocities because of the positive skewness of higher order waves, compared to linear waves, the crests should be higher than the troughs are deep (Marthinsen and Winterstein, 1992). NORSOK in N-003 (NORSOK, 2007) recommends to increase the drag coefficient for surface piercing framed structures consisting of tubular slender members (such as jack-ups) when calculating extreme hydrodynamic loads based on Morison’s equation. The drag coefficient for time domain simulations should be increased as displayed in Table 5-7 if the sea is modeled as a Gaussian process.

Table 5-7: Drag coefficient to be used for simulations according to NORSOK 003.

	Design Wave (Stokes 5 th order)		Time domain analysis(Gaussian)	
	C _D	C _M	C _D	C _M
Above water surface	0.65	1.6	1.15	1.6
Below water surface	1.05	1.2	1.15	1.2

The hydrodynamic coefficients are calibrated to give a reasonable quasi-static load level. This increase is only for extreme response estimation, while for fatigue assessments the increased extreme crest will not have any impact and generally would be unnecessary.

Second order wave theory

The second order perturbation for unidirectional waves in deep water can be expressed as: (Sharma and Dean, 1981)

First order surface elevation:

$$\zeta^{(1)} = \sum_{n=1}^N a_n \cos(\phi_n) \tag{63}$$

Second order surface elevation:

$$\begin{aligned} \zeta^{(2)} = & \sum_{n=1}^N \frac{1}{2} a_n^2 k_n \cos(2 \phi_n) \\ + & \sum_{n=1}^{N-1} \sum_{m=n+1}^N \frac{1}{2} a_n a_m ((k_n + k_m) \cos(\phi_n + \phi_m) - (k_m - k_n) \cos(\phi_m - \phi_n)) \end{aligned} \quad (64)$$

First order velocity potential:

$$\phi^{(1)} = \sum_{n=1}^N \frac{a_n \omega_n}{k_n} \cos(\phi_n) e^{k_n z} \quad (65)$$

Second order velocity potential:

$$\phi^{(2)} = - \sum_{n=1}^{N-1} \sum_{m=n+1}^N a_n a_m \omega_m \sin(\phi_m - \phi_n) e^{(k_m - k_n) z} \quad (66)$$

With $\omega_n^2 = g k_n$, $\phi_n = k_n x - \omega_n t + \epsilon_n$ and $k_m > k_n$

Here $\zeta^{(1)}$ and $\zeta^{(2)}$ denotes the first and second order component of the wave elevation and $\phi^{(1)}$ and $\phi^{(2)}$ the first and second order components of the velocity potential.

The total surface elevation is now found as:

$$\zeta(t) = \zeta^{(1)}(t) + \zeta^{(2)}(t) \quad (67)$$

In Figure 5-7, the difference between linear and second order waves is shown by showing each of the components of the second order wave realization, linear + sum-frequency + difference frequency. The figure shows that the difference-frequency is slowly varying and only by \pm one meter, while the sum-frequency is more locally important and contributes several meters to the maxima.

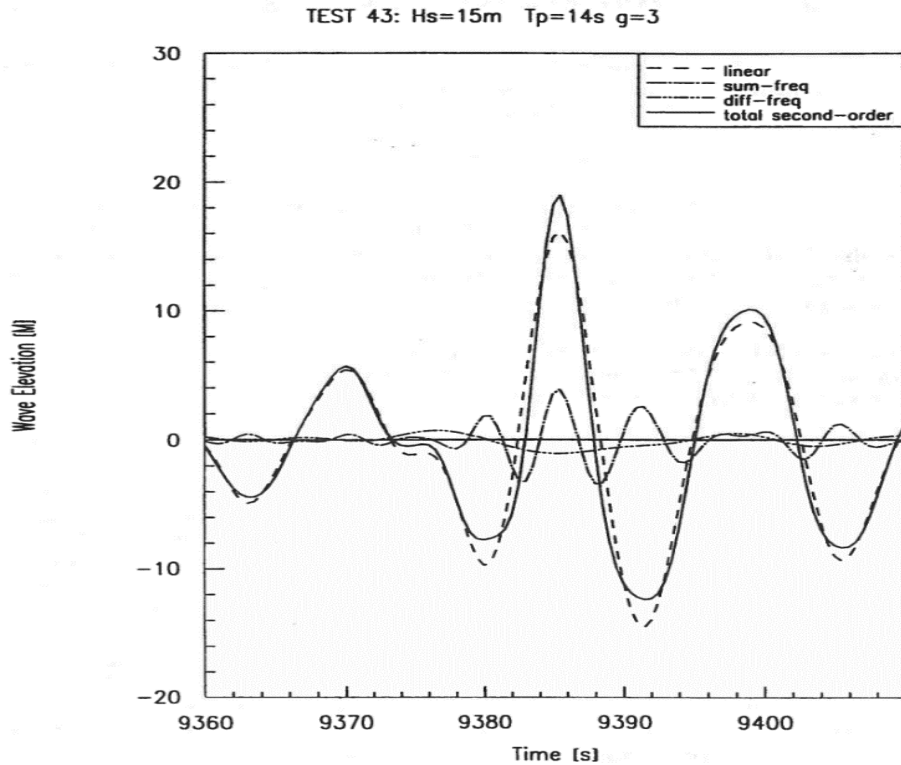


Figure 5-7: Detailed composition of extreme waves, showing each of the contributions from linear, sum-frequency and difference frequency. Figure from (Stansberg, 1998)

Linear waves have a crest height of $C = \frac{1}{2}H$ but by implementing the second order terms, (Stansberg, 1998), finds this factor to be between 0.55-0.60 due to asymmetry. Second-order waves also showed to have a 30% larger scatter in their extreme values than linear waves and the 100-year sea state had a 15% larger crest than the Rayleigh estimate (Stansberg, 1998). From Figure 5-7 its clear that the extreme response is strongly affected by the second order component as it increase the largest waves and increases the horizontal velocity at the crest. Especially for jack-ups (drag dominated) this effect is larger because of the nonlinear dependency on the relative velocity between the structure and the wave particles.

Figure 5-8, shows measured horizontal velocities underneath a large crest and a comparison between second-order and linear theory. The second-order theory is based on Johannssen (see (Johannessen, 2008)), which calculates the velocity directly at the instantaneous free surface. It clearly shows an improvement compared to linear theory.

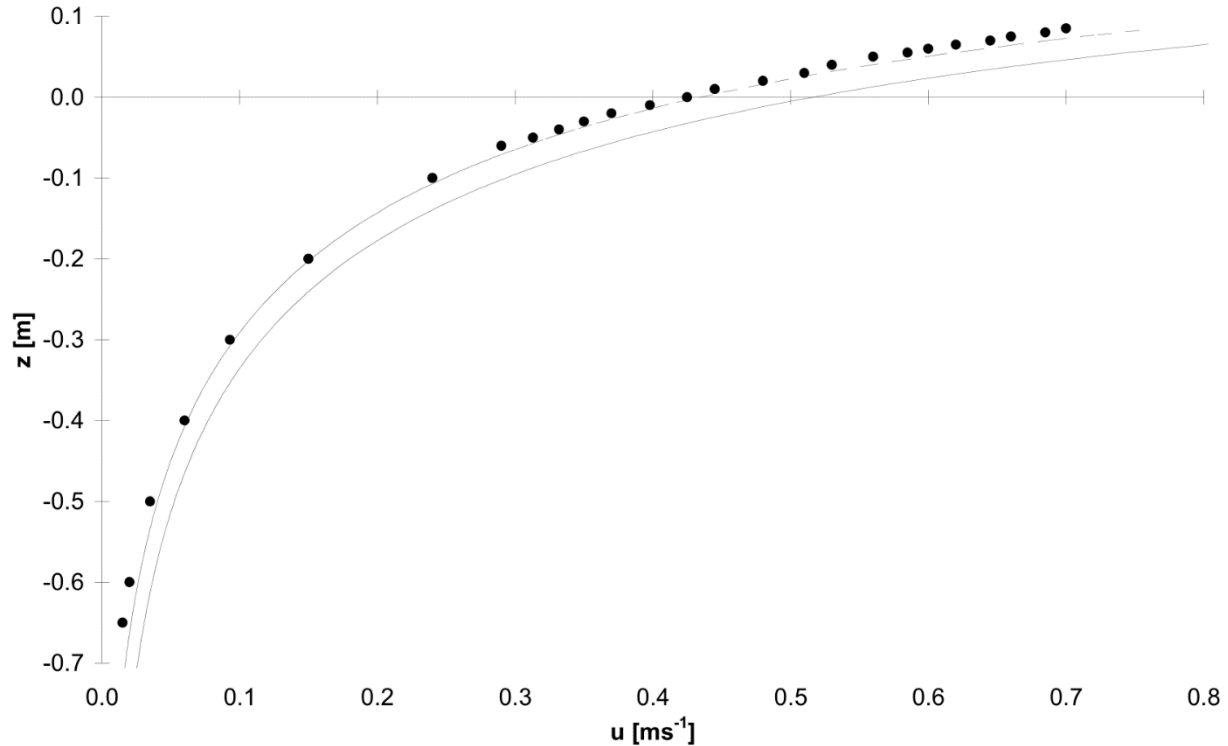


Figure 5-8: Horizontal velocity underneath a large crest. Measurements (dots), linear based on free waves only (solid line) and second order (dotted line). Figure from (Johannessen, 2008)

The conclusion from (DNV, 2013) is that the second-order theory is robust with respect to modelling irregular wave, but currently this is not a requirement and there is no recommended method on how to implement a second order process to create the sea realization in N-003. There is however, a requirement that the drag coefficient is increased according to Table 5-7 for time-domain simulations.

5.3.5 USFOS Uncertainties

All computational software used to calculate and estimate real world phenomena such as the response of a structure in waves needs to do certain assumptions and simplifications. Doing dynamic time domain analyses is time consuming and requires the equation of motion and the damping and stiffness matrices to be solved for every time step. There are certain methods to reduce the simulation time and some of these might result in inaccurate results if no used properly. These methods are presented and discussed in the following paragraphs.

Spool-to-Peak-Wave

Spool-to-Peak-Wave (SpoolWave) is a command in USFOS that finds the n -th largest wave in a simulation. The sea surface realization is calculated before the responses so that USFOS can find the n ($=5$ was used in this thesis) largest wave elevations and the time they occur. Then the response is only calculated for these 5 waves instead of running the whole 3 hour (10800) second long simulation. An illustratory drawing from the USFOS manual is shown in Figure 5-9.

200 seconds of dynamic analysis with a time step of 0.25 seconds before the wave hits. The responses are calculated for the five largest orders by running USFOS five times where ORDER is replaced with 1,2,3,4 and 5. The SpoolWav-command in USFOS is implemented to make the simulations go faster but it must be implemented with caution as to not disrupt the accuracy of the results. For this to be true it must be confirmed that all dynamics effects are accounted for during 200 seconds of analysis and that the largest response will not come from a wave that is smaller than the sixth largest.

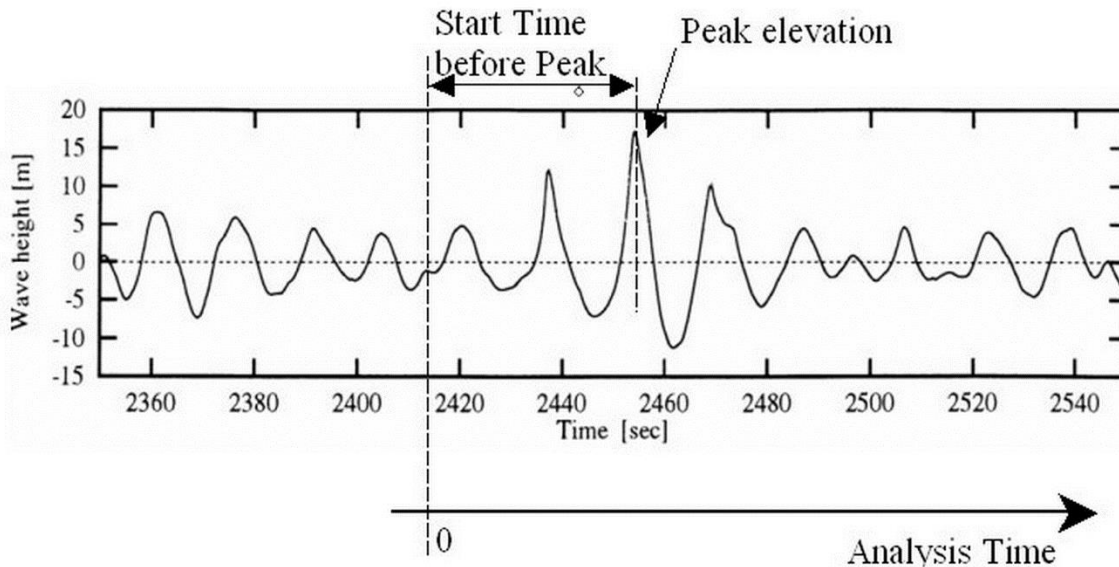


Figure 5-9: USFOS spool to peak wave command. Figure from (SINTEF, 2010)

For a structure where the response could be calculated as quasi-static it would be sufficient to find just the largest wave and limited time before peak. Since the jack-up has such a low stiffness and thus high eigenperiod, dynamics must be accounted for. Therefore 200 seconds before the peak has been simulated so that the structure will experience all the dynamic effects of the wave train.

According to the Master Thesis of Bækkelal (Bækkelal, 2014), it was shown that a drag dominated structure with eigenperiod of 9 seconds had a fully developed sea realization with all the dynamics effects after 150 seconds. The longer the eigenperiod, the more time was needed. Since the jack-up has a lower eigenperiod and was simulated for 200 seconds it is reasonable to assume this will not affect the results.

The five largest waves were simulated for each seed. In USFOS this is defined by the order command, so 1st order is the largest crest and 5th order is the 5th largest crest. For each seed the python program records which order had the largest maximum for each response. 60 dynamic long-term simulations with different seeds of a sea state with Hs 12.9 m and period 16.0 seconds has been investigated. The number of maximum from each order, depending on the response, is presented in a Table 5-8.

Table 5-8: Distribution table of which of the largest wave crest (descending order) gave the maximum response for each seed. In total 60 seeds for dynamic analysis using Hs 12.9 and Tp 16.0

Order	Percentage	Deck Displacement	Base Shear	Overturning Moment
<i>1st</i>	53.89%	33	35	29
<i>2nd</i>	15.56%	8	10	10
<i>3rd</i>	12.22%	8	7	7
<i>4th</i>	13.33%	7	6	11
<i>5th</i>	5.00%	4	2	3

The results show that as much as 5% of the extreme responses come from the fifth largest crest, but there is no way of telling how many of the maxima would have come from even higher orders. This indicates that some of the extreme values might have been missed and that either more waves the full 3-hour simulation should be used. The recommended action would be to simulate a large number of full 3-hour sea realizations and see how many of the extreme responses come from even higher order waves and then conclude on the number of wave orders that is required. If the required order is very high, the time saved by using spool-wave command might not be worthwhile.

JONSWAPUSFOS allows for various wave spectra, but a good spectrum for describing the short-term variability in the North Sea is the JONSWAP spectrum. Joint North Sea Wave Project (JONSWAP) is based on measurements from shallow waters in the North Sea between 1968 and 1969 and was presented in (Hasselmann et al., 1973) It is basically a more peaked version of the Pierson-Moskowitz (PM) spectrum, see (Pierson and Moskowitz, 1964) for further information.

JONSWAP is a 5-parameter spectrum and is defined by (Hasselmann et al., 1973):

$$S(\omega) = \alpha \frac{g^2}{\omega^5} \exp \left[-\frac{5}{4} \left(\frac{\omega_p}{\omega} \right)^4 \right] \gamma^{\exp \left[-\frac{1}{2} \left(\frac{\omega - \omega_p}{\sigma \omega_p} \right)^2 \right]} \quad (68)$$

For practical purposes, JONSWAP is usually simplified and approximated to be a three parameter spectrum that is only dependent on H_s , T_p and the peakedness factor, γ , which is suggested as 3.3 (Hasselmann et al., 1973). For practical applications such as USFOS the resulting spectrum is then (SINTEF, 2010):

$$S(\omega) = \frac{5}{32\pi} H_s^2 T_p \left(\frac{\omega_p}{\omega} \right)^5 \exp \left[-\frac{5}{4} \left(\frac{\omega_p}{\omega} \right)^4 \right] [1 - 0.287 \ln(\gamma)] \cdot \gamma^{e^{\left(\frac{\left(\frac{\omega}{\omega_p} - 1 \right)^2}{2\sigma^2} \right)}} \quad (69)$$

This single peaked spectrum now has a peak that is a factor of γ higher than for the PM-spectrum. σ is usually set 0.07 for frequencies below the peak and 0.09 above. The spectrum describes the local wind generated seas, but does not account for swell sea. Swell sea is due to waves generated far from the location and thus is not directly affected by the wind at the site. Swell seas usually have longer wavelengths, and thus periods, and result in a second peak in the lower part of the wave spectrum. To properly account for swell seas, a double peaked spectrum should be used, see e.g. (Torsethaugen and Haver, 2004) for further information. The JONSWAP spectrum is expected to be a reasonable model for $3.6 < \frac{T_p}{\sqrt{H_s}} < 5$, (DNV, 2010)

In this thesis a peakedness factor, $\gamma = 3.3$ has been used.

In USFOS the wave spectrum is defined with these lines:

```
'WAVEDATA Loadcase Type Hs Tp Direct Seed Surflev Depth N_ini
WAVEDATA 2 SPECT HS TP 180 SEED 110. 110. 0
'
nFreq Type T_Min T_Max iGrid Gamma
300 JONSWAP 3.0 25.0 3 3.3
```

The value for H_s and T_p is set according to the sea state and the value of seed is changed for every run so that the generated wave data will be random and different for each seed. A JONSWAP spectrum is generated with 300 different frequencies. iGrid 3 means that the equal area method is

used (see Equal Areas Projection of Harmonic Components) for distributing the frequencies. The frequency range is set between 3.0 s and 25.0 seconds for the time domain simulations.

Equal Area Projection of Harmonic Components

For USFOS it is possible to choose between two methods for realizing the sea surface; either the constant frequency span method (Fast Fourier Transform) or the equal area projection method (EAP). The Fast Fourier Transform (FFT) method uses an even frequency span, that means:

$$\Delta\omega = \frac{\omega_{\max} - \omega_{\min}}{N_{\text{components}}} = \text{constant} \quad (70)$$

The method is sketched in the left part of Figure 5-10. The problem with this method is that it will repeat itself very quickly for a broad band process, unless the number of components is very large. Using many components require a lot of computational power (or time) since the number of frequencies have to be solved at each time step. The surface realization will repeat itself after:

$$T = \frac{2\pi}{\Delta\omega} = \frac{2\pi N}{\omega_{\max} - \omega_{\min}} \quad (71)$$

Which for a simulation of 3 hours, 10800 seconds and with wave periods of [3s, 25s], means that almost 3300 different frequencies are needed. One way to make a realistic surface realization for three hours without using 3300 different frequency components is to use the Equal Area Projected method. The EAP method spaces frequency components so that the spectral area is equal for each frequency. The EAP method results in many frequencies and a low $\Delta\omega$ around the spectral peak, but fewer frequencies and larger $\Delta\omega$ in the edges of the spectrum. This can be a problem when the eigenvalue of the structure lies in the beginning or the end of the spectrum, but for the jack-up the eigenvalue (8.0s) is well within the denser part of the spectrum. Figure 5-10 depicts the two methods next to each other and shows how the equal area as calculated.

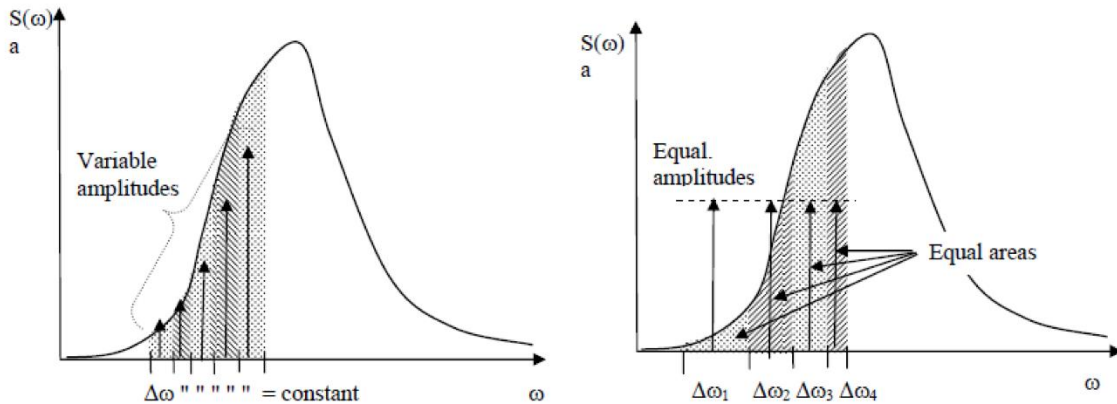


Figure 5-10: Illustrative figure explaining the difference between Fast Fourier Transform and Equal Area Projection of frequencies in the spectrum, taken from (SINTEF, 2010)

The main argument for using the EAP method is that the energy rich parts of the spectrum are the most important for the irregular sea realization and thus the frequencies should be concentrated in this area. Since the eigenperiod of the jack-up is as high as 8 seconds this is inside the energy rich area and the dynamic effects will be accounted for. For other structures with a lower eigenperiod, it could be a problem that there aren't enough frequencies around the eigenperiod, so the dynamic effects get underestimated.

300 frequencies have been used and according to talks with Professor Jørgen Amdahl this should be more than sufficient.

5.4 Accounting for Dynamic Effects

For drag dominated structures such as a jack-ups, dynamic effects are important and must be accounted when calculating the extreme response. Once the natural period of the structure increases past 2 seconds the mass and damping terms should no longer be neglected (NORSOK, 2007). This means that the whole equation of motion, Eq.(45), must be solved for every time step. It is now important to find the eigenvalues of the system (see Section 3.4)

5.4.1 Dynamic Amplification Factor

It is possible to account for some of the dynamics by including a dynamic amplification factor (DAF) which can be found from a simplified one degree of freedom system with the same mass

and stiffness matrixes as the platform. This is effective when the dynamic amplification is low, preferably below 1.1

The simplified dynamic amplification factor can be estimated from: (DNV, 2012)

$$DAF = \frac{1}{\sqrt{\left[1 - \left(\frac{T_0}{T}\right)^2\right]^2 + \left(\frac{2\xi T_0}{T}\right)^2}} \quad (72)$$

Where

$T_0 = \text{Natural period}$

$T = \text{Period of load (wave period)}$

$\xi = \text{Damping ratio}$

The quasi-static response (e.g. from Design Wave Method) is then multiplied with the DAF to get a more accurate result for the dynamic response of the structure. This simplified DAF is applied for ULS and ALS estimations, but not for FLS (fatigue limit state).

5.4.2 Equivalent Dynamic Amplification Factor

If the DAF is larger than 1.1 the *equivalent dynamic amplification factor (EDAF)* must be found. EDAF is the factor that is used to multiply the q-annual probability of exceedance quasi-static response in order to obtain a reasonable estimate of the q-probability dynamic response.

$$EDAF = \frac{X_{dyn,q}}{X_{sta,q}} \quad (73)$$

There are multiple methods of estimating the dynamic and static responses such as long-term analysis (described in Section 5.5) and the Environmental Contour Method (described in Section 5.6). By using one of these methods to find the extreme response, the EDAF is calculated by using the worst q-probability dynamic load and the worst q-probability static load.

The focus of the thesis has been on finding a good estimate for the EDAF based on the Contour Line Method. The dynamic effects are much larger for sea states with periods that are closer the structure's eigenvalue, so the largest dynamic and static responses must not necessarily come from the same sea state. The value of the EDAF depends on which q-probability is used to find the extreme response.

5.4.3 Equivalent Acceleration Field

Even though the EDAF is the focus of this study, in the industry it is common practice to use an equivalent acceleration field to account for the dynamics. The EDAF is not applied directly, but is rather implemented as an equivalent acceleration field along the structure. The dominating inertia forces has its origin from the acceleration of the total mass. The dynamic response is calculated based on a static analysis using extra acceleration field to increase the response by the same amount as the EDAF. The purpose of the EDAF is to account for the difference between the load and response and thus:

$$x_{dyn} = x_{sta} \cdot EDAF \rightarrow F_{dyn} \approx F_{sta} \cdot EDAF = M \cdot (a_{wave} + a_{field}) \quad (74)$$

The acceleration field must be calculated so that the new static load (after implementing the acceleration field) is equal to the estimated dynamic load (the static multiplied with the EDAF)

$$F_{dyn} \approx EDAF \cdot F_{sta} \quad (75)$$

$$F_{sta} \cdot EDAF = M (a_{wave} + a_{field})$$

$$M \cdot a_{field} = F_{sta} \cdot EDAF - F_{sta} = F_{sta}(EDA F - 1)$$

$$a_{field} = \frac{(EDA F - 1) \cdot F_{static}}{M}$$

There are more advanced methods to calculate the acceleration field along the structure and it does not have to be constant, but can be used to account for momentum as well by using a linear acceleration field.

5.5 Long-Term Analysis

Doing an all sea states long-term analysis of nonlinear extreme response for a jack-up is the most comprehensive, but also the most accurate method to estimate the response if done correctly. The principle behind the method is to go through every possible sea state and multiply its probability of occurrence with the distribution of the maximum response for that same sea state.

The long-term environmental variability follows a log-normal probability density function and was calculated in the metocean report and can be used directly based on those parameters. The distribution of the largest response, dependent on H_s and T_p , on the other hand is not possible to know without doing stochastic time domain simulations of every single sea state using multiple seeds. Then the Gumbel parameters, α and β must be calculated for each and every sea state. Doing

this is simply not feasible for every possible sea state, so instead, a trick is implemented. First the Gumbel-parameters for certain selected sea states in different positions along the Hs-Tp plane must be calculated. Then it is possible to use interpolation to estimate the values of the Gumbel parameters for other sea states based on the ones that have already been calculated. The Gumbel distribution of the extreme response will now have parameters that are dependent on the significant wave height and spectral peak period of the sea state, $\alpha(hs, tp)$ and $\beta(hs, tp)$. The more sea states that are selected and the more seeds that are simulated for each of the selected sea state increases the accuracy of the method.

Conducting a complete long-term analysis that can correctly account for all probable sea states during a time span of e.g. 10 000 years is a time consuming affair and for accurate results for the 3-hour max response multiple simulations must be conducted for various sea states with different Hs and Tp values. The method used in (Baarholm et al., 2010) initially uses about 70 different sea states to cover a wide variety of Hs-Tp pairs and to cover all possible sea states within the 10^{-4} (10 000 year) q-probability contour. Then an additional 15 sea states are selected in the Hs-Tp area where the largest contributions to F_{x3h} were found to come from. Each of these selected sea states need to be simulated with various different seeds for the results to be trustworthy. The number of different seeds should be at least 20 (See Section 5.7.1) and then the extreme response can be estimated using the Gumbel-distribution at a certain alpha-percentile.

To do a full long-term analysis would not have been possible due to time considerations and a simplified approach showing the method has been conducted instead. Only 18 sea states were selected and each sea state has been simulated using 20 different seeds in USFOS. All the simulations have been with dynamics in USFOS. There was only time to do a long-term dynamic analysis but the steps to do a static one would be exactly the same. Also, a complete long-term analysis would follow these same steps, but with additional sea states for more accurate response results.

One of the assumptions for long-term analysis of maximum response is statistical independence. This means it is assumed that all individual global maxima are statistically independent which overestimates the extreme values by a few percent (Leira, 2014). This is due to two different contributions. The first is that the correlation is not taken into account for adjacent maxima within a stationary sea state, this only has a minor effect. The second contribution comes from the fact that two real adjacent sea states have a strong correlation, but when assumed statistically independent it's equally likely that a storm is followed by a calm sea state or a rough one. This means that statistical independence is a slightly conservative assumption.

5.5.1 Selecting Sea States for Extreme Response Simulations

The sea states were selected with a requirement that they were located outside the contour lines for the 10 000 year return sea states. This is so that interpolation can give values for every sea state within the chosen boundaries. The exact Hs-Tp values that were used, have been presented in Table 5-9, together with the sea state number. Groups of three sea states, with the same Hs but different Tp values, were selected to be able to estimate the extreme response for all possible combinations of Hs and Tp.

Table 5-9: Numbered Sea States used for the long-term analysis and their corresponding Hs and Tp parameters.

Sea State #	Hs[m]	Tp[s]		
1:3	2	2	10	25
4:6	6	6	12	18
7:9	10	9	15	20
10:12	13	12	17	21
13:15	15	14	19	22
15:18	17	16	20	23

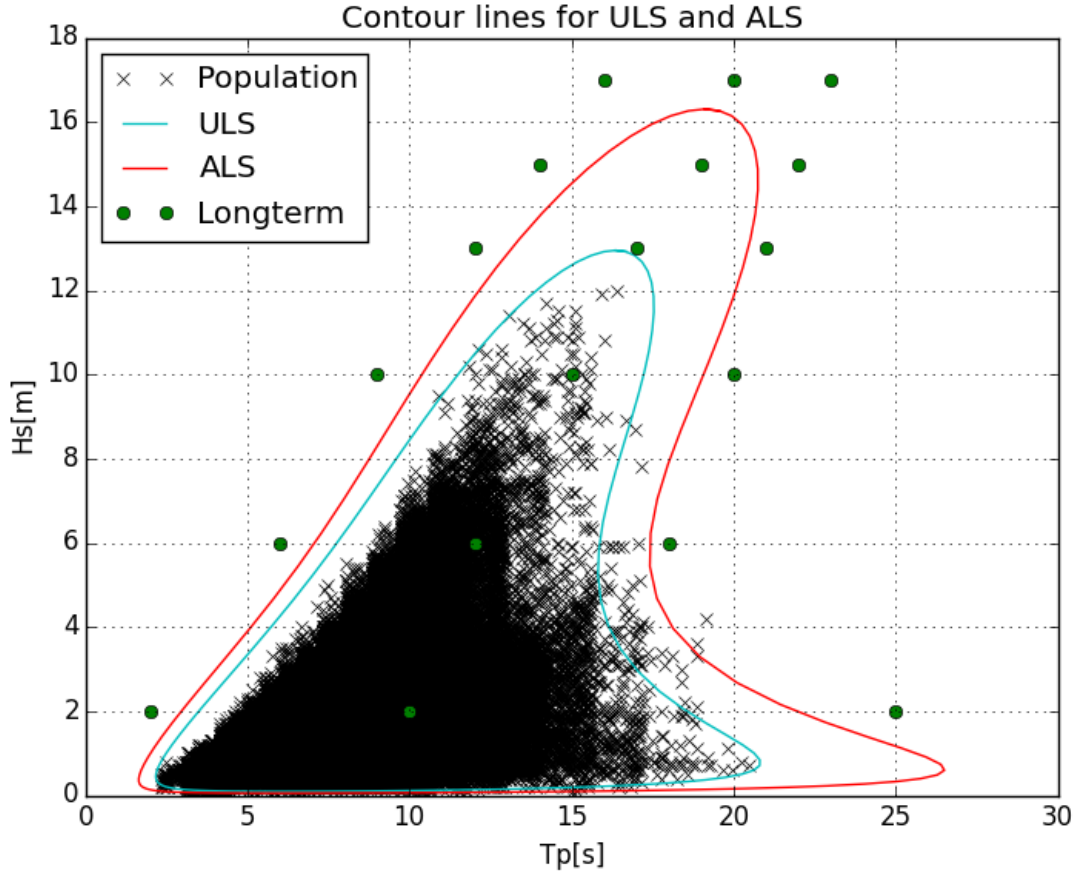


Figure 5-11: The selected sea states (green) for the long-term analysis of response, together with the contour lines for ULS (teal) and ALS (red) in the T_p - H_s plane.

5.5.2 Extreme Response Distribution

For each sea state, the maximum response, Y_i was extracted from each simulation and collected in a sample: $Y_{maxima} = Y_1, Y, \dots, Y_{20}$ and the mean and standard deviation, μ and σ of the sample was calculated. The distribution of $F_{X_{3h}|H_s T_p}$ can be estimated using the Gumbel distribution (Haver, 2013). The Gumbel parameters for each of the 18 selected sea states, $\alpha_1, \alpha_2 \dots \alpha_{18}$ and $\beta_1, \beta_2, \dots, \beta_{18}$ were calculated from the standardized Gumbel method based on using the method of moments, which according (Bury, 1975) can be found as:

$$\alpha = \mu - 0.5772 \cdot \beta \quad (76)$$

$$\beta = \sigma \frac{\sqrt{6}}{\pi} \approx \sigma \cdot 0.7797$$

From the distribution of $F_{X_{3h}|H_s T_p}$ in Eq.(77), it is seen that the Gumbel distributions parameters are conditionally dependent on the H_s and T_p of the sea state:

$$F_{X_{3h}|H_s T_p}(x|h_s, t_p) = \exp \left\{ - \exp \left[- \frac{(x - \alpha(h_s, t_p))}{\beta(h_s, t_p)} \right] \right\} \quad (77)$$

Since only 18 different sea states have been simulated for the long-term analysis, it is important to find a way to approximate values for $\alpha(h_s, t_p)$ and $\beta(h_s, t_p)$. To find these Gumbel parameters, the radial basis function was used(Orr, 1996). In python the radial basis function is built in the SciPy(Scientific Python)-package. This is a multiquadratic interpolation function for n-dimensions that is radially symmetric around selected points, and the radial basis function can then be found as the sum of:(Orr, 1996):

$$f(x) = \sum_{j=1}^m w_j h_j(x) \quad (78)$$

Where w is a weighting function, and the basis is function for a multi-quadratic solution at point x is given by:

$$h(x) = \sqrt{\left(\frac{r}{\epsilon}\right)^2 + 1} \quad (79)$$

r is the radius, and ϵ is an estimate of the distance between the nodes and for the first guess this was set to 5. Then the program automatically selects the best value for ϵ . This function is used to approximate the Gumbel parameters of α and β for all values of H_s and T_p based on the α and β results obtained from the 18 selected sea states in the long-term simulations. In Python, the value for $\alpha(h_s, t_p)$ and $\beta(h_s, t_p)$ was generated for 1000 h_s values evenly spaced between 0.0m and 18.0 m and also 1000 t_p values between 0.0 s and 30.0 s. This gives a total of 1 000 000 different α and β values.

The resulting interpolation function for the Base Shear response is shown as a color plot for $\alpha(location)$ in Figure 5-12 and $\beta(scale)$ in Figure 5-13, together with the selected long-term simulation sea states (dots) and the contour lines for ULS (teal) and ALS (red) for the Base Shear. Similar plots for Deck Displacement and Overturning Moment are in the appendix A.3

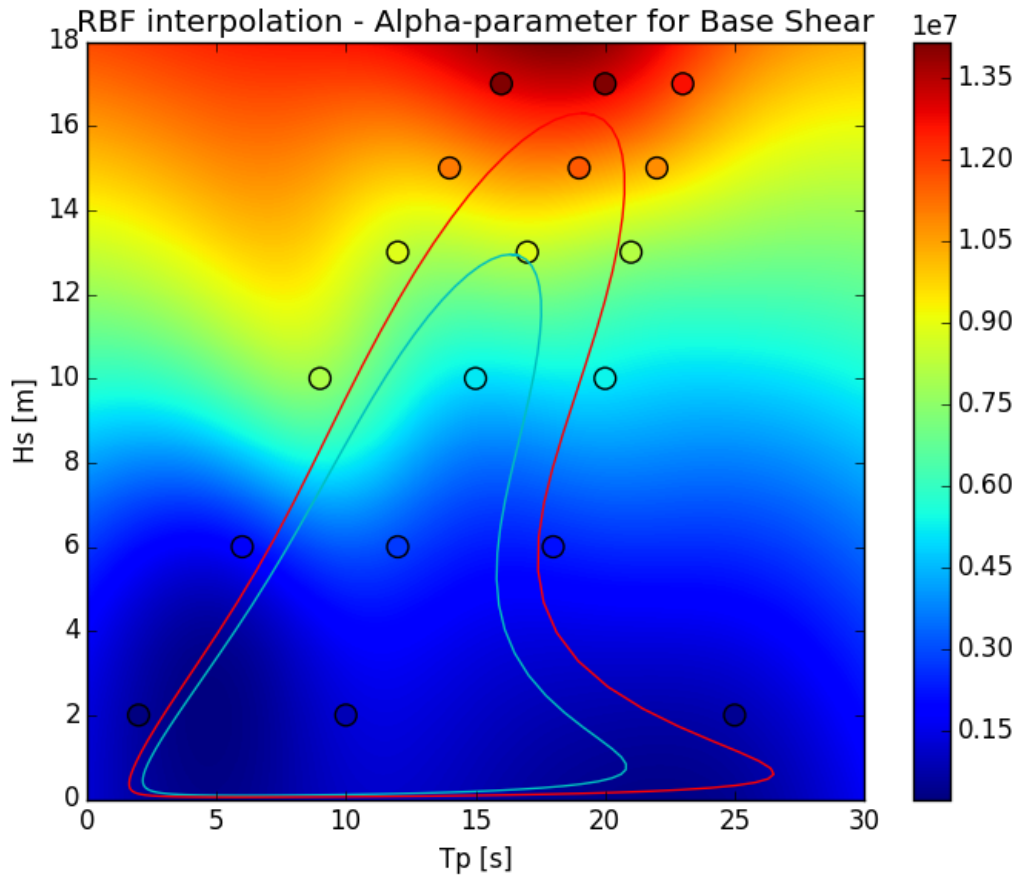


Figure 5-12: The location parameter, $\alpha(h_s, t_p)$, for the Gumbel distribution of extreme response for every value of H_s and T_p for Base Shear [N]. Created by interpolation, using the radial basis function with 18 selected sea states (circles) as input. Teal and Red contour lines are for ULS and ALS, respectively.

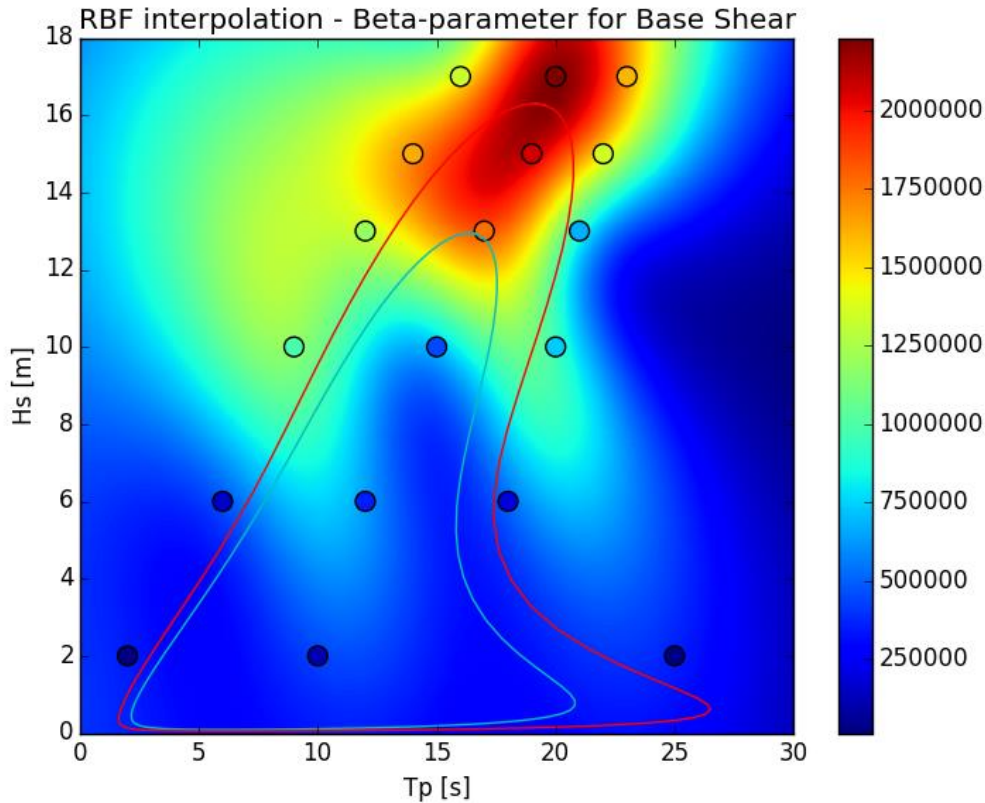


Figure 5-13: The scale parameter, $\beta(h_s, t_p)$, for the Gumbel distribution of extreme response for every value of H_s and T_p for Base Shear [N]. Created by interpolation, using the radial basis function with 18 selected sea states (circles) as input. Teal and Red contour lines are for ULS and ALS, respectively.

All these calculations are done in the *longtermSpline.py* script and results are written to an npz-file which can be read by *python* and loaded into other programs. The interpolated function seems to give accurate results for the sea states along the top, while the lower H_s -values are not that accurate. Only the high H_s sea states contribute to the extreme response so this doesn't affect the ULS or ALS responses. If additional sea states were to be simulated in USFOS the focus should be on adding more the between the top of the ULS and ALS contour lines.

5.5.3 Maximum Response

The total distribution of the largest 3-hour maximum can now be found by setting x_q equal to the value that is exceeded once every year with a probability q , then the cumulative distribution function must be:

Estimation of Extreme Response

$$F_{x_{3h}}(x_q) = \iint_{h_s t_p} F_{X_{3h}|H_s T_p}(x_q|h, t) f_{H_s T_p}(h_s, t_p) dt_p dh_s \quad (80)$$

With $x_q = x_{0.01}$ for ALS and $x = x_{0.0001}$ for ULS.

The probability of exceedance is found from:

$$Q_{X_{3h}}(x_q) = 1 - F_{x_{3h}}(x_q) = \frac{q}{\eta_T} = \frac{q}{2920} \quad (81)$$

Since η_T is the number of 3-hour sea states per year. This gives a probability of exceedance for a single sea state equal to:

$$ULS: Q_{X_{3h}}(x_{0.01}) = 3.42465753425e - 06$$

$$ALS: Q_{X_{3h}}(x_{0.0001}) = 3.42465753425e - 08$$

For the results to be accurate, since the probabilities are so low ($O(10^{-6})$ and $O(10^{-8})$), it is extremely important that:

$$\iint_{h_s t_p} f_{H_s T_p}(h_s, t_p) dt_p dh_s = 1.0000000000 \quad (82)$$

Is equal to 1 and correct to an order of $O(10^{-8})$. When using a numerical integration with limited computational power, this can be acquired by introducing a factor enforcing this number. For numerical iteration using 1000 steps for each h_s and t_p , this factor was calculated to be: 0.99999968331.

The long-term variation of the ocean environment can be described by the joint probability density function for H_s and T_p :

$$f_{H_s T_p}(h_s, t_p) = factor \cdot f_{T_p|H_s}(t_p|h_s) \cdot f_{H_s}(h_s) \quad (83)$$

Where $f_{H_s}(h_s)$ is calculated as in the metocean report (Section 4.2) and $f_{T_p|H_s}(t|h_s)$ from Section 4.3.

Estimation of Extreme Response

The distribution function of the largest response in any 3-hour sea state can be found from (Baarholm et al., 2010) and is now given as:

$$Q_{X_{3h}}(x) = 1 - F_{x_{3h}}(x) = \int_{H_s} \int_{T_p} (1 - F_{X_{3h}|H_s T_p}(x|h_s, t_p)) \cdot f_{H_s T_p}(h_s, t_p) dh_s dt_p \quad (84)$$

The response, x , corresponding to this probability will be the governing response for the long-term analysis, and is presented in Table 5-9.

Table 5-10: Results from the Long-term dynamic analysis of the CJ70-platform for both ULS and ALS

Responses from Dynamic Long-term Analysis				
<i>Limit State</i>	<i>Return Period</i>	<i>Deck Displacement</i>	<i>Base Shear</i>	<i>Overturning moment</i>
	<i>[years]</i>	<i>[m]</i>	<i>[N]</i>	<i>[Nm]</i>
<i>ULS</i>	100	0.43	10.8E+06	1.92E+09
<i>ALS</i>	10 000	0.69	19.2E+06	2.69E+09

5.5.4 Relative Contribution to Extreme Response for each Sea State

By calculating the probability of the response, x , exceeding x_q for each combination of (Hs,Tp), the result will give a map showing the relative contribution to the extreme response of certain sea states in the long-term analysis.

$$Q_{X|(H_s, T_p)}(x > x_q) = \left(1 - F_{X_{3h}|H_s T_p}(x|h_s, t_p)\right) \cdot f_{H_s T_p}(h_s, t_p) dh_s dt_p \quad (85)$$

This was calculated in python using 1000 values for both Hs and Tp, making it one million different sea states in total, and then plotted as a color map to show where the largest contributions come from. The results depend on the q-annual probability of exceedance so the $x_q = x_{0.01}$ for ULS will have a different pattern than $x_q = x_{0.0001}$ for ALS. There are also differences between the resulting patterns depending of the response, therefore this has been done for both deck displacement and base shear.

The figures (Figure 5-14: Figure 5-15) show that deck displacement is more dependent on the dynamics than base shear, and can exceed the ULS state for sea states with lower hs values, since

Estimation of Extreme Response

the t_p values are closer to the eigenperiod. For ALS only sea states near the top of the contour make contributions. This shows which sea states need the most attention when doing a long-term analysis. Therefore a high concentration of sea states around these areas should be selected for response simulations for an accurate long-term analysis.

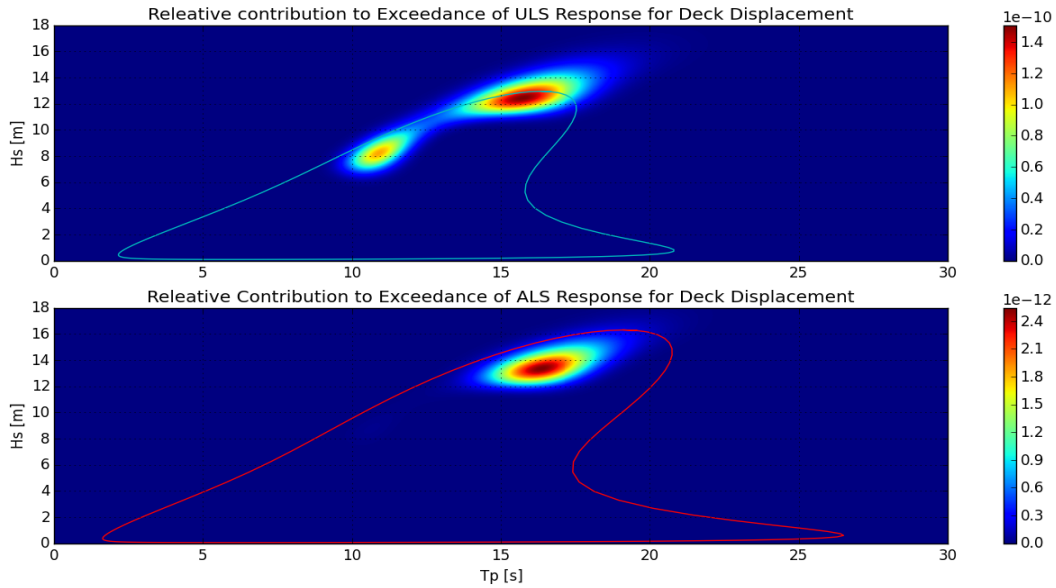


Figure 5-14: Relative contribution to the probability of the response exceeding the limit states for Deck Displacement given the sea states parameters of H_s and T_p . Shown together with the respective environmental contours for ULS (upper) and ALS(lower)

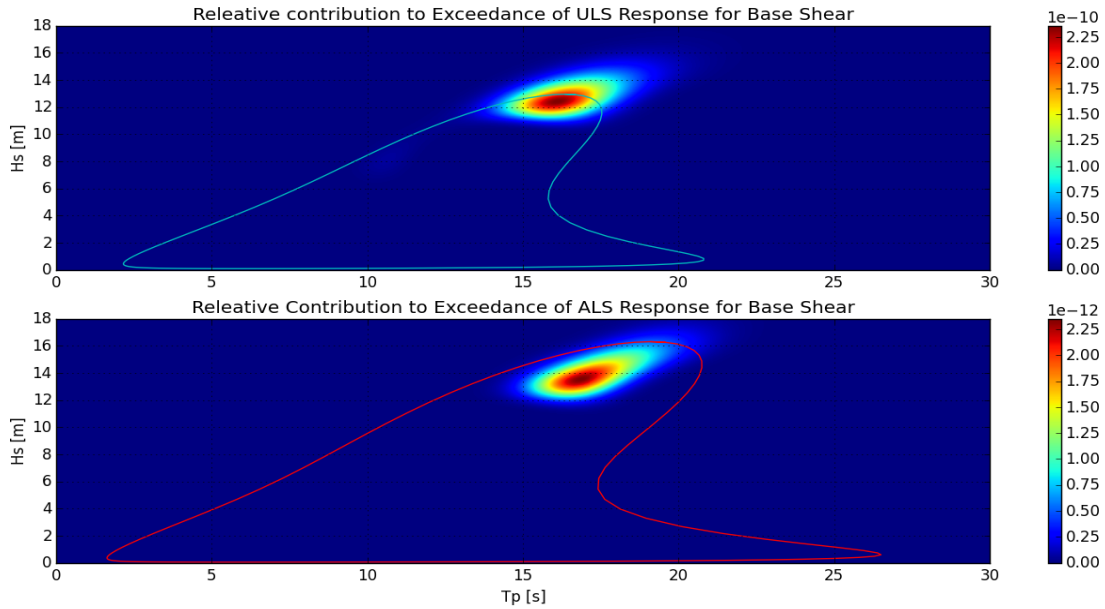


Figure 5-15: Relative contribution to the probability of the response exceeding the limit states for Base Shear given the sea states parameters of H_s and T_p . Shown together with the respective environmental contours for ULS (upper) and ALS(lower)

5.6 Environmental Contour Method

This is a method to estimate the extreme response based on only considering a few sea states along the environmental contours with an annual probability of exceedance, q . These environmental contour lines in the H_s - T_p plane have been calculated in Section 4.6. They will be used to make an accurate and practical estimation of the extreme response for the structure by just simulating the worst sea state for static and dynamic response. This is an alternative method to find the response maximum without having to do a long-term analysis. The method assumes that the environmental (metocean) and response analysis can be decoupled which is very convenient for nonlinear problems such as for a jack-up. The principle is to first find the worst sea state (with regard to response) along the contour line for both the static and the dynamic analysis. Then run multiple simulations of the response using this sea state and generate a Gumbel extreme response distribution based on the maximum from each seed. It is important to select a good level for the cumulative probability, α , such that the response x_α represents the response level of q adequately. The α -percentile can be found as:

$$P(x_{3h} > x_\alpha) = 1 - \alpha \quad (86)$$

So an α -percentile of 0.90 means that 1 in 10 times the response will be larger than the estimated q -probability of exceedance, which in this thesis is defined by the ultimate and accidental limit states.

Steps of the Environmental Contour Method for Maximum Response Estimation

After creating the environmental contours (as shown in Section 4.6), the following methodology is applied when finding design criteria by the environmental contour method for quasi-static and dynamic response: (Haver, 2012)

1. First the design wave method (see Subsection 5.3.5) is used find the static response of the structure. The static q-probability is preferably described by the q-probability crest height and the corresponding conditional mean wave period.
2. This step is to identify the most critical sea states along the q-probability contour line and find out which is the worst for the current response. For structures with large eigenperiods it cannot be assumed that the largest quasi-static and dynamic response occurs for the same sea state. Therefore, a screening study with x-different seeds for multiple (five or more) sea states along the q-probability contour is conducted. This is done for both for static and dynamic analysis. The sea states should be selected as those close to the highest significant wave and have a higher focus on the lower part of spectral peak periods(closer to the eigenperiod). A suggestion would be to use the sea state along the q-probability contour with the highest Hs, one with a slightly higher Tp and three with lower Tp values. All sea states should be chosen close to the highest Hs (top of the contour), as the response is largely dependent on wave height. A sea state with a spectral peak period equal to, and equal to two times the eigenperiod should also be inspected. The characteristic response for each sea state can then be calculated with the following equation: (Haver, 2012)

$$x_{3h} = E[X_{3h}] + 1.3 \cdot STD[X_{3h}] \quad (87)$$

Where X_{3h} , is a sample containing the maximum response of each seed and x_{3h} is the characteristic response of the sea state.

3. The sea state with the highest value for x_{3h_s} is chosen as the worst static sea state X_s . The number of seeds per sea state, M, using the same value for Hs and Tp, should be at least 20, but higher is more accurate. The 3-hour maximum quasi-static load from each of the M samples should be pooled into an extreme value sample $\{x_{s,3h,1}, x_{s,3h,2}, \dots, x_{s,3h,M}\}$ and fitted to a Gumbel distribution. The q-probability value of X_s , $x_{s,q}$ is now estimated by the value corresponding to the cumulative probability of α (α -quartile). One possibility is to use $\alpha = 0.9$ for $q = 10^{-2}$, and $\alpha = 0.95$ for $q = 10^{-4}$, but the preferred method is to find the α -percentile corresponding to the response from the Design Wave Method (5.3.5).

4. In principle, step nr 3) is repeated using dynamic analysis. The worst sea state, X_d , is the sea state with the largest dynamic characteristic response, x_{3hd} . A Gumbel distribution is fitted to a sample of M - 3-hour extreme values for dynamic load. The q-probability dynamic load, $x_{d,q}$, is estimated at the α -quartile found in 3)
5. Now the equivalent dynamic amplification factor (EDAF) can be estimated from the static and dynamic response values at the α -percentile using equation:

$$EDAF_q = \frac{x_{d,q}}{x_{s,q}} \quad (88)$$

The EDAF (equivalent dynamic amplification factor) can now be used as a factor to find the dynamic loading based on the quasi-static loading. The EDAF is typically calculated from a simplified finite element model, and then applied to more complex models for use in quasi-static analyses as an equivalent acceleration field. The environmental contour method is an approximate method and the effect of all non-considered sea states is accounted for by choosing a rather high α -quartile.

5.6.1 Calculating the Most Unfavourable Sea State

Selecting the most unfavorable sea state could be done from model-test, but this isn't available for the model. The second best option is to do stochastic nonlinear finite element simulations. To find out which sea states are the worst for both dynamic and static simulations, a screening study has been conducted. Five sea states were selected along the both 10^{-2} and 10^{-4} annual probability of exceedance contours as found in Section 4.6. The selection process included picking one at the eigenperiod, one at two times the eigenperiod and the others close to the top of the contour, where the significant wave height is the highest. The first five sea states for ULS and ALS are presented in Table 5-11. Each of the sea states were simulated for 3-hours in USFOS, using 10 different seeds.

Table 5-11: The five selected sea states along the contour lines for ULS and ALS

	ULS		ALS	
#	Tp [s]	Hs [m]	Tp [s]	Hs [m]
1	8.0 (eigenperiod)	6.3	8.0 (eigenperiod)	7.1
2	14.0	12.0	16.0 (2x eigenperiod)	15.2
3	15.0	12.6	17.5	16.0
4	16.0 (2x eigenperiod)	12.9	19.0	16.3
5	17.0	12.8	20.0	16.1

Estimation of Extreme Response

The base shear, overturning moment and deck displacement were recorded as the responses. There have been some problems with the overturning moment calculations in USFOS (Section 5.3.3) therefore the main focus has been put on the base shear and deck displacement responses.

Using the Spool Wave command in USFOS, the 5 largest surface elevations were simulated both dynamically and statically for each sea state and using 10 seeds. The 10 seeds have been the same for all sea states that were investigated since it can be assumed this will give a more systematic analysis than using 10 random seeds for each of the sea states. Five different sea states along the contour line, represented by pairs of T_p and H_s , were used. It was found that for both ALS and ULS the worst sea state was close to the top, so an extra 6th sea state was simulated using the same 10 seeds to ensure that an even higher period wouldn't increase the statistic nor dynamic response. The chosen sea states are marked in Figure 5-16 with a star, and the two 6th sea states have a slightly darker color than the initial five. By looking at the results (See subsection 5.7.1) it was decided to do an additional 10 simulations of each sea state, so the total number of seeds was 20.

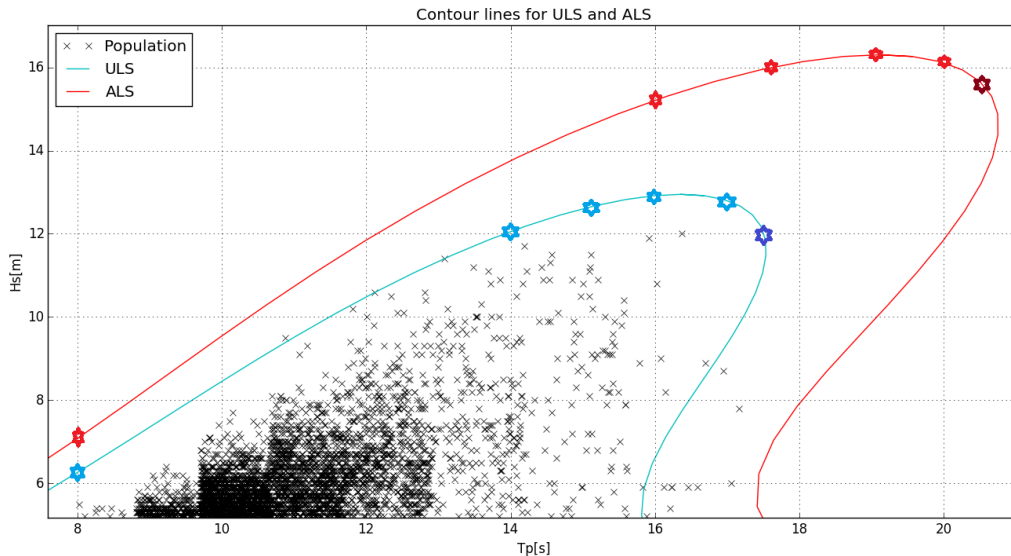


Figure 5-16: Zoomed in version of the contour lines showing the five initial sea states and the 6th, additional, sea state (slightly darker) for ULS and ALS. The first sea state is placed at the eigenperiod, which is 8 seconds.

The characteristic response for each of the 20 sea states was calculated using Eq. (87), which defines characteristic response as $x_{3h} = E[X_{3h}] + 1.3 \cdot STD[X_{3h}]$. In Table 5-12 the responses for ULS is shown, while ALS is presented in Table 5-13.

Estimation of Extreme Response

Table 5-12: Characteristic response for ULS for each sea state, based on 20 seeds using the 5 largest wave elevations. The largest responses are displayed in bold.

CHARACTERISTIC RESPONSE - ULTIMATE LIMIT STATE											
Sea State			Deck Displacement [m]			Base Shear [N]			Overturning Moment [Nm]		
No#	Hs[m]	Tp[s]	Dynamic	Static	Factor	Dynamic	Static	Factor	Dynamic	Static	Factor
1	6.3	8.0	0.38	0.07	5.54	7.76E+06	1.94E+06	4.00	1.81E+09	7.07E+08	2.56
2	12.0	14.0	0.39	0.20	1.98	9.47E+06	6.27E+06	1.51	1.77E+09	1.12E+09	1.58
3	12.6	15.0	0.37	0.22	1.65	9.63E+06	7.06E+06	1.36	1.68E+09	1.23E+09	1.37
4	12.9	16.0	0.45	0.24	1.86	1.15E+07	7.72E+06	1.49	1.89E+09	1.29E+09	1.47
5	12.8	17.0	0.40	0.27	1.51	1.12E+07	8.75E+06	1.28	1.83E+09	1.37E+09	1.34
6	12.0	17.5	0.34	0.21	1.65	9.51E+06	6.90E+06	1.38	1.62E+09	1.17E+09	1.39

Table 5-13: Characteristic response for ALS for each sea state, based on 20 seeds using the 5 largest wave elevations. The largest responses are displayed in bold.

CHARACTERISTIC RESPONSE - ACCIDENTAL DAMAGE LIMIT STATE											
Sea State			Deck Displacement [m]			Base Shear [N]			Overturning Moment [Nm]		
No#	Hs[m]	Tp[s]	Dynamic	Static	Factor	Dynamic	Static	Factor	Dynamic	Static	Factor
1	7.1	8.0	0.44	0.08	5.25	9.07E+06	2.38E+06	3.81	2.03E+09	7.54E+08	2.70
2	15.2	16.0	0.61	0.35	1.76	1.55E+07	1.08E+07	1.43	2.38E+09	1.62E+09	1.47
3	16.0	17.5	0.59	0.38	1.55	1.64E+07	1.23E+07	1.34	2.46E+09	1.72E+09	1.43
4	16.3	19.0	0.61	0.47	1.30	1.88E+07	1.65E+07	1.14	2.57E+09	2.04E+09	1.26
5	16.1	20.0	0.58	0.44	1.33	1.76E+07	1.52E+07	1.16	2.45E+09	1.92E+09	1.28
6	15.7	20.5	0.53	0.43	1.24	1.65E+07	1.49E+07	1.10	2.30E+09	1.89E+09	1.22

It can be seen that the sea state close to the eigenperiod (8.0 seconds) has a very large (>5) amplification factor between dynamic and static results, which is to be expected since dynamics play a large part here. For ULS all the largest dynamic responses are found in the fourth sea state, while all the largest static responses are for the fifth sea state. This means that 30 additional USFOS simulations with new seeds were to be conducted for dynamic response for sea state #4 and for static response of sea state #5.

For ALS the fourth sea state gives the largest responses for both static and dynamic analysis, but for deck displacement the response is equally large for sea state two. Therefore 30 additional dynamic and static simulations using new seeds will be run for sea state #4, and also 30 additional dynamic responses for sea state #2 to compare which has the highest values.

By running an additional 30 seeds for dynamic analysis of sea state #2 and sea state #4 and analyzing the largest maximum, the average, the standard deviation and the characteristic response, the results in Table 5-14 are acquired.

Table 5-14: Comparison of 30 new seeds for the two sea states that showed the same dynamic response for deck displacement in the screening study

Sea State	Largest Maximum	Average	Std. dev.	Char. Resp.
#2	0.646 m	0.481 m	0.090	0.599 m
#4	0.722 m	0.482 m	0.095	0.605 m
<i>Change:</i>	11.64%	0.10 %	5.33%	1.12 %

This shows that the response for sea state #4 is larger for all four parameters with the 30 new seeds, even though the differences are small. The largest maximum is 12% larger and since the extreme response is what this report is estimating, it is decided use the fourth sea state for the dynamic response found using environmental contour method. This sea state also gave the largest responses for both base shear and overturning moment.

5.6.2 Distribution of Maximum Response

The four critical sea states have been selected and their defining parameters are listed in Table 5-15. Each of these sea states were then simulated 30 times in USFOS with new seeds.

Table 5-15: Summary of parameters of the worst sea states for Environmental Contour Method

<i>Limit State:</i>	ULS			ALS		
<i>Analysis Type</i>	#	<i>Hs[m]</i>	<i>Tp[s]</i>	#	<i>Hs[m]</i>	<i>Tp[s]</i>
Static	5	12.8	17	4	16.3	19.0
Dynamic	4	12.9	16.0	4	16.3	19.0

The distribution of the largest of N-maxima, Y_m , follows the Gumbel distribution for growing values of N. The Gumbel distribution is given as: (Bury, 1975)

$$F_{Y_m}(y) = \exp\left(-\exp\left(-\frac{y-\alpha}{\beta}\right)\right) \quad (89)$$

where:

β is the scale parameter

α is the location parameter

For the sample, N is 30 and the α and β -parameters can be estimated based on the method of moments by using the same formulas as in Eq. (76) in Section 5.4 about the long-term analysis of response. Once these parameters are found, the Gumbel-distribution can be generated for both the

static and dynamic analysis. The Gumbel distribution can be linearized by rearranging Eq. (89), which gives the following equation:

$$z = -\ln(-\ln(F_{Y_m})) \quad (90)$$

The cumulative probability of the sorted sample, with N maximum values, was estimated as in Eq. (21) in the metocean report, based on its order:

$$P(y < y_i) = \frac{i}{N + 1} \quad (91)$$

One important parameter when calculating the EDAF from the Gumbel distribution of static and dynamic response, is the α –percentile. This is usually selected as the probability where the static contour line response is equal to the quasi-static response from the Design Wave Method. Another possibility is to compare with the results of the long-term analysis. Since the long-term-analysis only was conducted for the dynamic response, the α -percentile is also selected as the probability where the maximum response from the long-term dynamic analysis equals the Gumbel distribution of the dynamic response. The third option for estimating the EDAF, if neither the Design Wave Method nor a long-term analysis has been conducted, is to set the α -percentile 0.90.

5.6.3 Results

The Gumbel distribution for static and dynamic analysis, showing the α -percentile from both the Design Wave Method and the Long-term analysis have been plotted for the following:

Estimation of Extreme Response

ULS, $q = 10^{-2}$, return period 100 years

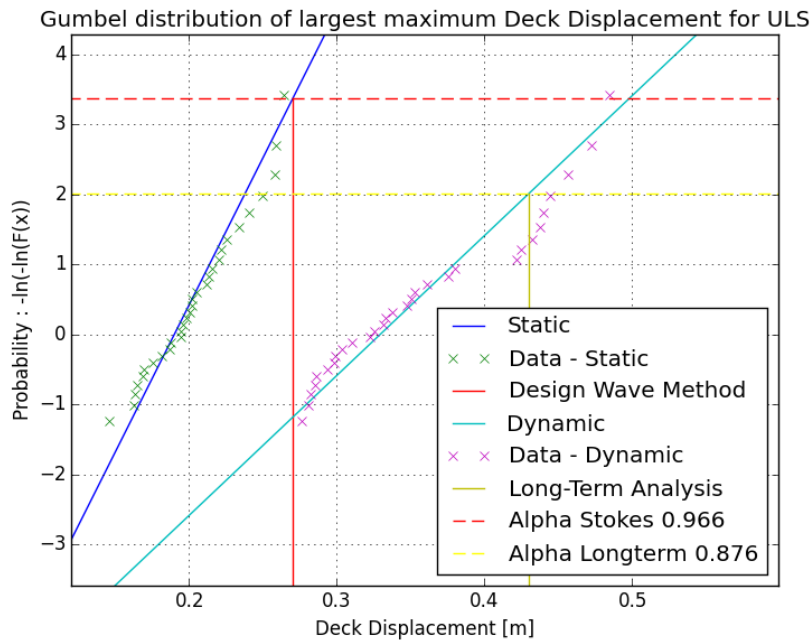


Figure 5-17: Extreme distribution of deck displacement for ULS from Environmental Contour

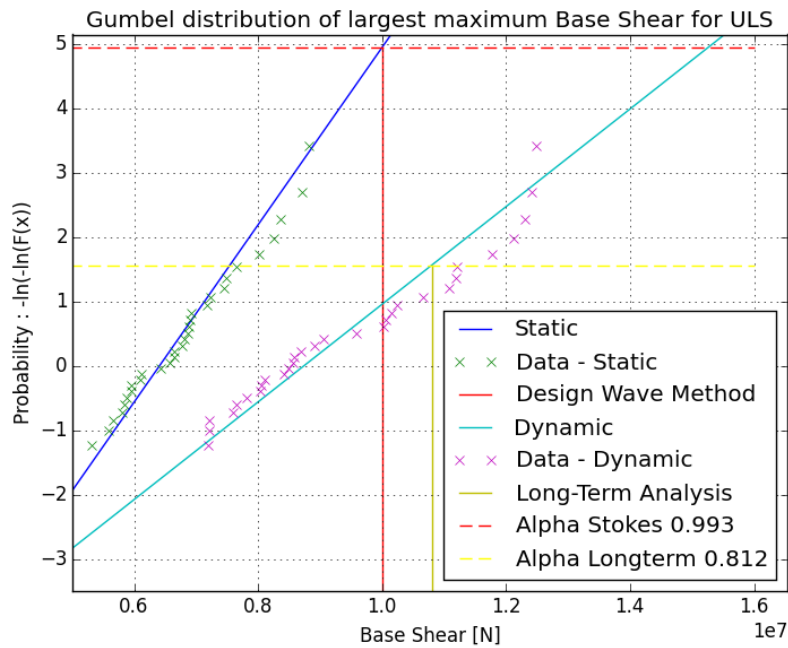


Figure 5-18: Extreme distribution of Base Shear for ULS from Environmental Contour

Estimation of Extreme Response

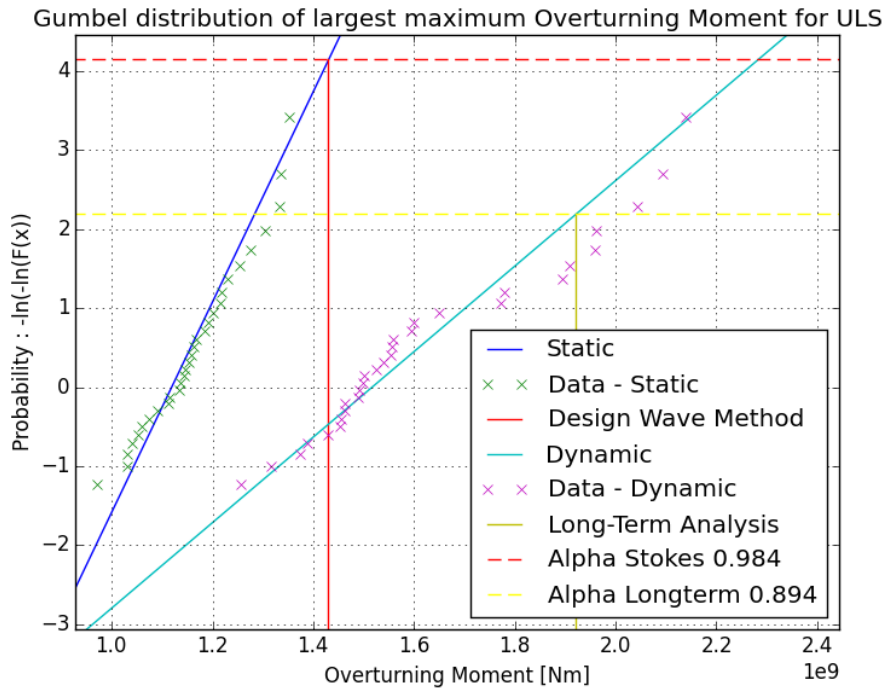


Figure 5-19: Extreme distribution of Overturning Moment for ULS from Environmental Contour

ALS, $q=10^{-4}$, return period 10 000 years.

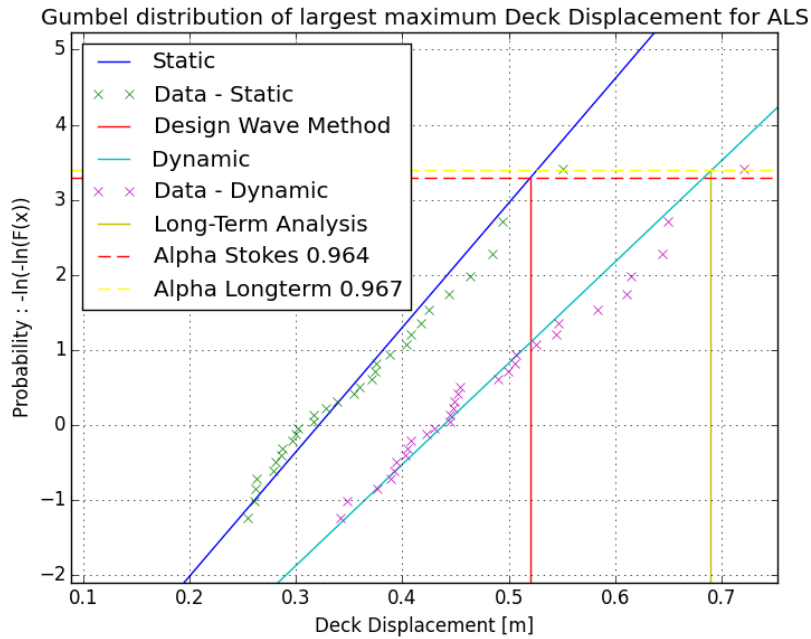


Figure 5-20: Extreme distribution of Deck Displacement for ALS from Environmental Contour

Estimation of Extreme Response

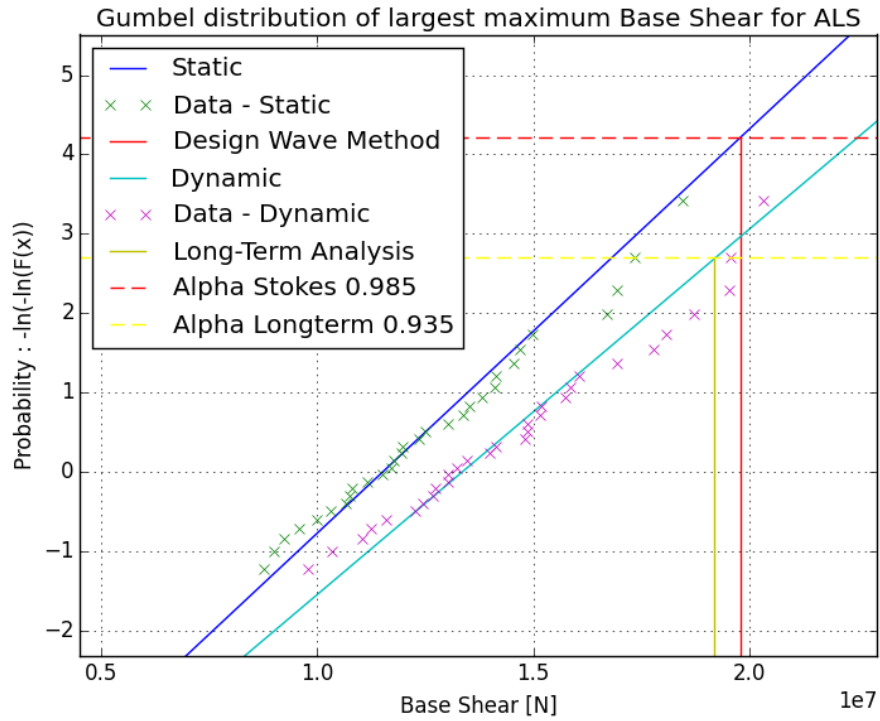


Figure 5-21: Extreme distribution of Base Shear for ALS from Environmental Contour

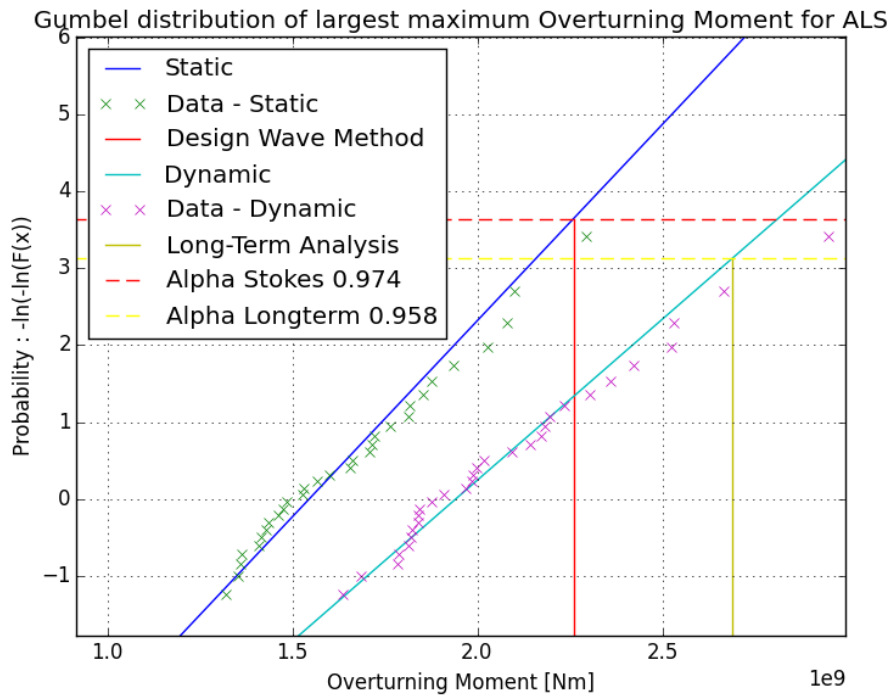


Figure 5-22: Extreme distribution of Overturning Moment for ALS from Environmental Contour

Table 5-16: Resulting equivalent dynamic amplification factors found using the Environmental Contour Method for ULS and ALS. The alpha-percentile has been found from three different methods, the quasi-static Design-Wave, dynamic long-term analysis and the old procedure of using an α -percentile of 90.

Alpha-percentile found from comparison with:		ULTIMATE LIMIT STATE			ACCIDENTAL LIMIT STATE		
		DD	BS	OTM	DD	BS	OTM
Design Wave	Alpha	0.966	0.993	0.984	0.964	0.986	0.974
(Quasi-static)	EDAF	1.85	1.53	1.60	1.32	1.14	1.25
Long-term	Alpha	0.88	0.81	0.89	0.97	0.93	0.96
(Dynamic)	EDAF	1.80	1.43	1.49	1.31	1.14	1.24
90-percentile	Alpha	0.90	0.90	0.90	0.90	0.90	0.90
(Static)	EDAF	1.81	1.46	1.50	1.33	1.15	1.25

Table 5-16 shows that the equivalent dynamic amplification factor depends more on which response and limit state is used than on the α -percentile. For the ultimate limit state the dynamic effect is stronger than for ALS. This is since the wave period is short and closer to the eigenperiod for ULS. Deck displacement has the highest EDAF and has a dynamic increase of response at 80-85%. For base shear the EDAF is lower, but the increase is still more than significant and between 43-53%. For the reasons discussed in Section 5.3, the Overturning Moment shouldn't be completely trusted, but the EDAF is in between that of the deck displacement and base shear, which is what was to expect from previous similar analyses. For ALS the EDAF is lower, but the dynamic effect is still significant and using a regular DAF would not be adequate for any of the responses. The reason the EDAF is much lower is since the spectral peak period is higher for ALS and thus the wave loads interact with the eigenperiods in a different way than for ULS.

The EDAF is highest based on the α -percentile from the Design Wave Method. This α -percentile is very high, around 0.96-0.99, depending on the response, for both limit states. The reason is that the results from the Design Wave method use fifth order kinematics while the time domain simulations are of a linear nature. This is further discussed in Subsection 5.7.4.

5.7 Sensitivity Studies

5.7.1 Number of Seeds in Sea State Selection

For the environmental contour method it is important to find the correct most unfavorable sea state. This is a quick sensitivity study to see how many seeds are needed. First 10 different seeds were simulated for each of the 6 sea states. Then 10 new and different seeds were simulated and the worst sea states picked for each response. Finally the two sets of 10 seeds were combined to the final set of 20 different seeds. All the 20 seeds were used when selecting the most unfavorable sea

Estimation of Extreme Response

state in Section 5.6. Assuming that the 20 seeds gives the correct answer of which sea state is the most unfavorable for each response, it is possible to investigate the error of just using 10. The comparison between the 1st 10 seeds, the 2nd 10 seeds and the combined 20 seeds are presented in Table 5-17 and Table 5-18. The results are quite clear and show that using only 10 seeds would not have been sufficient. Five of the sea states could have been chosen erroneously by using only 10 seeds. This shows that further analysis, perhaps by increasing with another set of 20 seeds should be conducted to test the validity of the combined 20 seed set. The fact that all the responses have the same sea state as the most unfavorable given the same type of analysis (static/dynamic) and same limit state(ULS / ALS) makes sense since a structure’s responses are strongly correlated.

Table 5-17: Comparison of which sea state is selected as the most unfavorable for the Ultimate Limit State using 2 sets of 10 different seeds and also the combined (which is assumed correct) 20 seeds. Bold numbers signify an error.

<i>ULS - Selecting the most unfavorable Sea State for contour line method</i>	STATIC			DYNAMIC		
	<i>1st</i>	<i>2nd</i>	<i>Combined</i>	<i>1st</i>	<i>2nd</i>	<i>Combined</i>
	<i>10seeds</i>	<i>10seeds</i>	<i>20 seeds</i>	<i>10seeds</i>	<i>10seeds</i>	<i>20 seeds</i>
Deck Displacement	4	5	5	4	4	4
Base Shear	5	5	5	4	5	4
Overturning Moment	4	5	5	4	4	4

Table 5-18: Comparison of which sea state is selected as the most unfavorable for the Accidental Damage Limit State using 2 sets of 10 different seeds and also the combined (which is assumed correct) 20 seeds. Bold numbers signify an error.

<i>ALS - Selecting the most unfavorable Sea State for contour line method</i>	STATIC			DYNAMIC		
	<i>1st</i>	<i>2nd</i>	<i>Combined</i>	<i>1st</i>	<i>2nd</i>	<i>Combined</i>
	<i>10seeds</i>	<i>10seeds</i>	<i>20 seeds</i>	<i>10seeds</i>	<i>10seeds</i>	<i>20 seeds</i>
Deck Displacement	4	4	4	2	4	4
Base Shear	4	4	4	4	4	4
Overturning Moment	4	4	4	5	4	4

5.7.2 Number of Seeds in Most Unfavorable Sea State

The purpose of this sensitivity study is to investigate the validity of the Gumbel extreme response distribution, using 30 seeds (as done in 5.6). The results are for the ultimate limit state using the

worst sea state for the dynamic analysis. This is sea state#4 and it has an Hs of 12.9 and Tp 16.0. The purpose was to simulate another 30 seeds and see what effect this had on the Gumbel distribution. The result for base shear is presented in Figure 5-23 and for base shear and overturning moment is in Appendix A.5

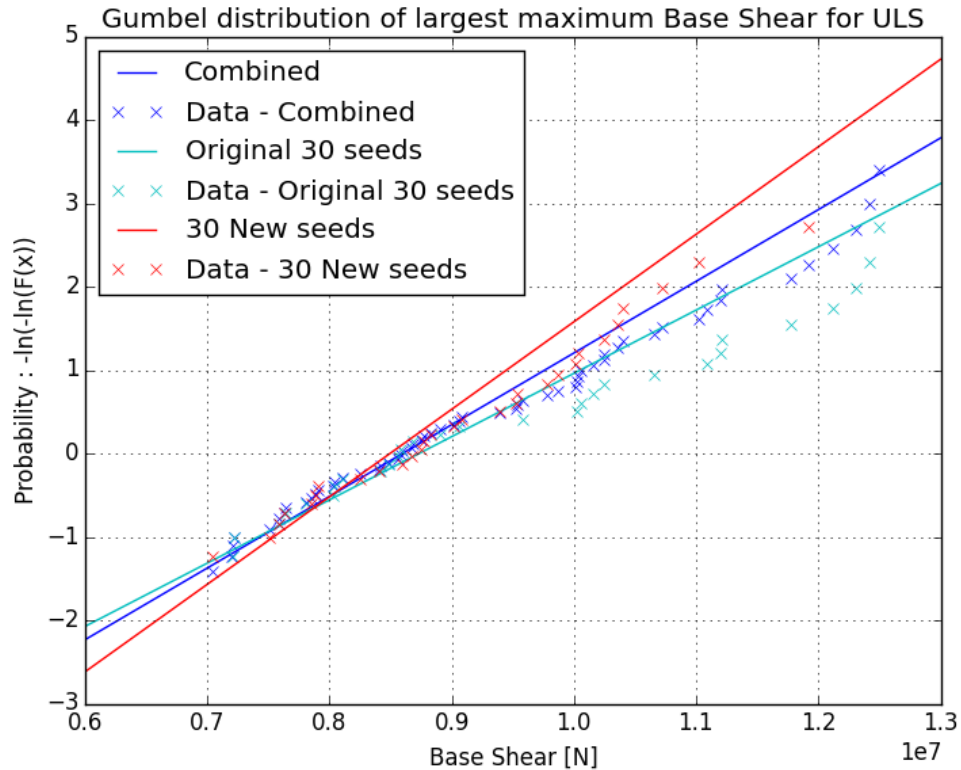


Figure 5-23: Comparison of resulting Gumbel extreme base shear distribution for the worst sea state for ULS using the original 30 seeds (teal), 30 new seeds (red) and the two samples combined into of containing 60 seeds (blue).

The characteristic response of each sea state is given by: $x_{3h} = E[X_{3h}] + 1.3 \cdot STD[X_{3h}]$. Where X_{3h} , is the sample containing the maximum response of each seed for the sea state. The two 30-seed can now be compared with respect to the difference between dynamic and static response and also what impact this has on the dynamic amplification factor.

Table 5-19: Comparison of the characteristic response for the two different samples of the largest maximum from 30 seeds

	DYNAMIC			STATIC			Dynamic Amplification Factor		
	DD	BS	OTM	DD	BS	OTM	DD	BS	OTM
Original	0.44	1.17E+07	1.93E+09	0.25	8.09E+06	1.31E+09	1.76	1.45	1.47
New	0.40	1.06E+07	1.76E+09	0.23	7.48E+06	1.25E+09	1.73	1.42	1.41
Difference	10.48%	9.95%	10.02%	9.01%	8.21%	5.43%	1.35%	1.60%	4.36%

Table 5-19 shows that even though the difference in response between the new 30 seeds and the original 30 seeds are about 10%, the dynamic amplification factor is still the very similar. This shows the robustness of the method and that the EDAF is not that sensitive to aleatoric (statistical) errors. The EDAF can now be used to calculate the dynamic response based on a larger sample of static analysis with a lower aleatoric error. If the EDAF is too low or too high this would lead to an epistemic error.

5.7.3 Relative Velocity

The hydrodynamic damping of the structure has been accounted for by the use of relative velocity in USFOS. This results in a viscous damping that can have a large impact on the total extreme response since the drag term of the Morison equation depends on the velocity squared. Two of the selected sea states from the Environmental Contour Method, one for ULS and one for ALS, have been simulated again in USFOS using the same 30 seeds. The same seeds have been used so that all the conditions are the exactly equal and using relative velocity or not is the only difference. The characteristic response is calculated as earlier in the report, (see Section 5.6). The results show that the viscous damping from relative velocity play a large part when calculating the extreme response. The difference is significant for all the responses and lie in the area around 14-22% larger when relative velocity is not accounted for. The difference is slightly higher for ALS than ULS. This makes sense since the waves are larger for ALS and the response depends on the velocity squared. The large impact of using relative velocity together with the total 4% structural and soil damping might be too much and should be investigated further.

Table 5-20: Comparison of the characteristic response when using relative velocity to account for viscous damping and without. For ULS, sea state #4 and for ALS sea state #2 from the Environmental Conter Method has been used. The same 30 seeds were used for all simulations.

Characteristic Response	ULTIMATE LIMIT STATE			ACCIDENTAL LIMIT STATE		
	DD[m]	BS[N]	OTM[Nm]	DD[m]	BS[N]	OTM[Nm]
With Relative Velocity	0.44	1.17E+07	1.93E+09	0.60	1.59E+07	2.44E+09
Without Relative Velocity	0.53	1.33E+07	2.21E+09	0.73	1.83E+07	2.88E+09
Difference	19.2%	13.7%	14.5%	22.0%	15.1%	18.0%

5.7.4 Increased Drag Coefficient to Account for Higher Order Effects

Simplified beam models, such as the finite element model of CJ70, are used to reduce the computation time of time domain simulations. When using the Design Wave Method based on a deterministic Stokes 5th wave all the wave kinematics are correct up to the sea surface and an accurate quasi-static response is acquired. For time domain simulations in USFOS linear wave theory in combination with Wheeler stretching is used to calculate the wave kinematics. This is not sufficient to account for the higher crests and higher horizontal velocities in higher order waves, so N003 (NORSOK, 2007), recommends increasing the drag coefficient for time domain simulations as shown in Table 5-7 and in Subsection 5.3.3 CJ70 is modelled as a beam but has equivalent hydrodynamic properties made for time domain analyses. To properly compare the static time domain response with Stokes 5th, the drag coefficient must be reduced the Design Wave Method. This is done by reverting the increased drag coefficient as shown in N-003. It was decided to reduce the values using the same factor as recommended in NORSOK N-003. Table 5-21 shows the drag coefficient for both time domain and Stoke 5th regular wave analysis.

Table 5-21: Drag coefficient of the original model used in time domain simulation with linear wave theory and the altered drag coefficient for Stokes 5th regular wave.

	Height profile, z [m]	C _D (Time Domain)	C _D (Stokes 5 th)
Dry	65	2.83	1.60
Dry	0.101	2.83	1.60
Dry	0.1	3.87	2.18
Wet	-17.4	3.87	3.53
Wet	-40.1	3.42	3.12
Wet	-111.9	3.42	3.12

By finding the extreme quasi-static response from the Design Wave Method (see Section 5.1) using both the time-domain drag coefficient and the Stokes 5th coefficient, it is possible to find the impact of the increased drag coefficient. Table 5-22 shows the results of the comparison, and the response is about 20- 25% larger using the time-domain drag coefficients. The results are similar for both ALS and ULS.

Estimation of Extreme Response

Table 5-22: Resulting Stokes 5th response for original time domain drag coefficients and reduced values:

Drag Coefficient	Limit State	DD[m]	BS[N]	OTM[Nm]
<i>Original</i>	<i>ULS</i>	0.36	1.29E+07	1.76E+09
<i>Reduced</i>	<i>ULS</i>	0.27	1.00E+07	1.43E+09
	Factor:	0.75	0.78	0.81
<i>Original</i>	<i>ALS</i>	0.69	2.55E+07	2.91E+09
<i>Reduced</i>	<i>ALS</i>	0.52	1.98E+07	2.26E+09
	Factor:	0.75	0.78	0.78

The reduction factors listed in NORSOK N00-3 are based on an analysis of a jacket platform and thus might not be completely accurate for a roomier platform such as a jack-up. In Section 5.3.2 the irregular waves from a static time domain simulation was compared to Stokes 5th waves with equal crest height and period, both with their appropriate drag coefficients. The results showed that the Stokes 5th wave had an increased response of up to 20% for base shear and more than 10 % for both deck displacement and reaction overturning moment. This indicates that the drag increase cannot sufficiently account for higher order effects for time domain analyses of a jack-up. The drag coefficient should be increased even more for linear wave theory or second order kinematics should be required. This can be investigated further by comparing the kinematics underneath a quasi-static time domain simulation. Figure 5-24 shows the kinematics underneath a crest of 11.5 meters, with a wave period of 15.6 seconds, for both linear wave theory with Wheeler stretching and a Stokes 5th wave.

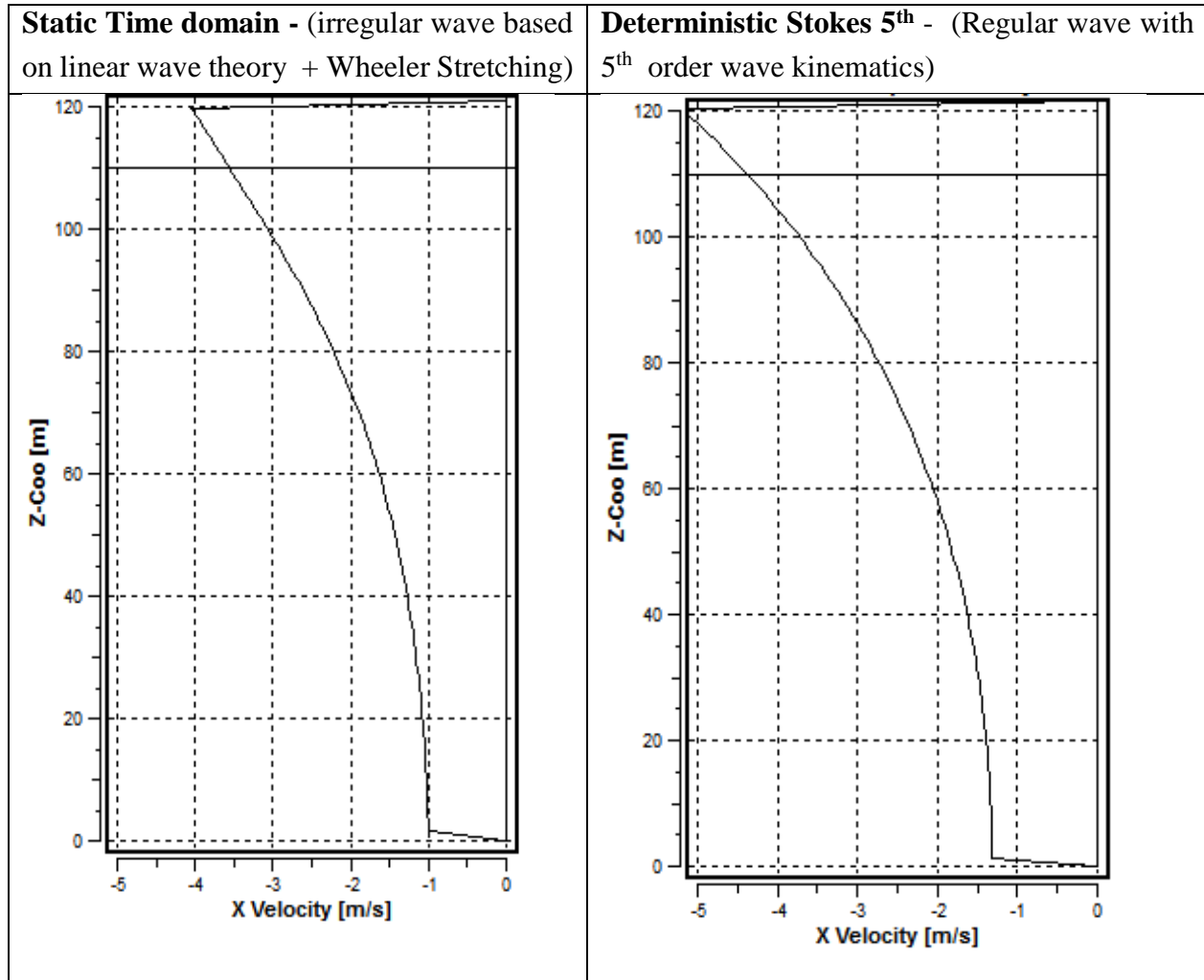


Figure 5-24: Comparison of horizontal velocity at a wave crest (11.5 meters and 15.6 second period) between stochastic time domain simulation and regular Stokes 5th order wave. Wave heading is in the negative x -direction.

The results show that the Stokes 5th wave has a maximum horizontal velocity of 5m/s while the irregular linear wave only has 4 m/s. This means that the drag forces, which depend on the square of velocity, is going to be roughly $\frac{5^2}{4^2} = \frac{25}{16} = 1.56$ times larger. The current NORSOK reduction only accounted for about 20-25%. There is a strong underestimation for extreme waves using linear wave theory and second order kinematics should be implemented to reduce the error of the estimation. It is also important to remember this has been tested only for a single case (wave) in this thesis and further analysis should be conducted. The results should be investigated further by using second order wave theory for both sea realization and wave kinematics in time domain simulations.

5.8 Summary

The extreme response was first calculated based on two different methods:

- Design wave method (Quasi static response using a deterministic Stokes 5th wave)
- Long-term response analysis (An all-sea states approach, with dynamic stochastic simulations in the time domain using linear wave theory with Wheeler stretching and increased drag coefficient according to N003)

The focus of the thesis has been on using the environmental contour method for extreme response. The Gumbel extreme distribution for static and dynamic has been created for deck displacement, base shear and overturning moment. The EDAFs were found for ULS and ALS using three different α -percentiles:

- By using the static response that equals the results of the Design Wave Method
- By using the dynamic response that equals the results of the Long-term response analysis.
- The 90-percentile

The resulting EDAFs are printed in Table 5-23.

Table 5-23: Resulting EDAFs and alpha-percentiles for the different methods

Alpha-percentile found from comparison with:		ULTIMATE LIMIT STATE			ACCIDENTAL LIMIT STATE		
		DD	BS	OTM	DD	BS	OTM
Design Wave	Alpha	0.966	0.993	0.984	0.964	0.986	0.974
(Quasi-static)	EDAF	1.85	1.53	1.60	1.32	1.14	1.25
Long-term	Alpha	0.88	0.81	0.89	0.97	0.93	0.96
(Dynamic)	EDAF	1.80	1.43	1.49	1.31	1.14	1.24
90-percentile	Alpha	0.90	0.90	0.90	0.90	0.90	0.90
(Static)	EDAF	1.81	1.46	1.50	1.33	1.15	1.25

The time domain simulations in USFOS are based on linear (Airy) wave theory and Wheeler stretching is used to account for wave kinematics up to the free surface. By comparing the static time domain simulations with Stokes 5th regular waves in USFOS, the results show that Wheeler stretching doesn't adequately account for higher order wave kinematics and hence cannot correctly predict the extreme response. This means that second order wave theory should be used for drag-dominated structures such as jack-ups in regard to extreme response estimation.

6 Conclusions and Further Work

6.1 Conclusion

In the beginning of this thesis the long-term variation of the wave climate at the Ekofisk-field was described based on 57 years of hindcast data. The Lonowe-model proved to give a good fit for the distribution of significant wave heights, but caused extra work for both the joint probability distribution of H_s and T_p and the environmental contour lines. The distributions and extreme wave crest and wave height values in the metocean report are in close agreement with the recommended values of NORSOK.

The second part of the thesis was the extreme response estimation for the CJ70 jack-up. The analysis showed that dynamics must be accounted for when analyzing drag dominated structures. The analysis has been based on the base shear and deck displacement of the platform since there was some problems in calculating the reaction overturning moment for CJ70 in USFOS.

The Environmental Contour Method can be used to estimate the extreme distribution for both static and dynamic response and then calculate the EDAF. The EDAF describes the difference between the platform's static and dynamic extreme response and depends on the α -percentile. The α -percentiles were found by comparing the extreme distribution with the resulting responses from the Design Wave Method and the Long-Term Analysis. The EDAF for deck displacement is between 1.80-1.85 for ULS and 1.32-1.33 for ALS. For Base Share it is between 1.43-1.53 for ULS and 1.14-1.15 for ALS.

The Design Wave Method based on using the q-probability largest wave crest showed to give higher results than the current NORSOK recommendation. The response based on the largest crest is between 7-10% larger and for ULS and for ALS the difference was between 3-13%, depending on the response. It is recommended to use the q-probability crests for the Design Wave Method since it gives a larger response and therefore should be the governing design criteria.

A comparison between the static time domain simulation and a Stokes 5th wave showed that the response is too low when using linear wave theory with Wheeler stretching and increased drag coefficient and thus second order wave theory should be used when calculating the extreme response on a drag-dominated structure.

6.2 Recommendations for Further Work

Metocean loads include current, waves and wind. This thesis has only investigated the jack-up's response due to wave loads, by adding current in the same direction as the waves, the resulting response could increase significantly since the load is dependent on the horizontal velocity squared. Wind will probably not have a very large impact for extreme response.

Conclusions and Further Work

The next step would be to do a study using second order wave theory and see the impact this has on the results. This theses has shown that linear wave theory isn't sufficient for extreme response calculation of this jack-up. The increased drag coefficient from NORSOK was based on a jack-up type platform and applying second order surface elevation and wave kinematics is a better solution than finding a new drag correction for every type of platform.

The comparison between a regular Stokes 5th and a similar wave from the static time domain simulation (Section 5.3.2) showed some differences that could be investigated further. The two waves were completely similar when the surface elevation at a certain point was measured in time, but the response of the structure showed a different curve. The wave from the static simulation is irregular and thus doesn't have the same shape along the whole structure. An improvement would be to find a wave that is similar to Stokes 5th in the x-z plane instead of z-time plane. This could be done by measuring the wave elevation along the platform

There are various USFOS-parameters that should be investigated further to validate the results. The spool-wave investigation in Section 5.3.5 revealed that the 5th largest wave accounted for the maximum response 5% of the time. This indicates that using only the five largest waves might have underestimated the maximum compared to doing the full 3-hour time domain simulation for some of the seeds. By running a large number of 3-hour time domain simulations it would be possible to find out how many waves should be used for the Spool-wave method. Structures that are highly sensitive to dynamics also need a large number of seconds before the wave impact and the study might show that using spool-wave isn't efficient for this kind of analysis. The number of seconds before the spool-wave is also an interesting study. The number of frequencies used for the sea surface generation with the EAP method should also be validated by comparison with fast Fourier transform.

The assumption that Gumbel is good fit for the 3-hour maximum is not necessarily true and the comparison with the extreme response population was not as nice as expected in the upper tail. There were 60 seeds in the sample that was investigated in this report and the method of moments was used to find the Gumbel-parameters. A fit using more simulations should generated and other methods of parameter-estimation could give better results.

The damping was set at 4% of critical, plus relative velocity to account for the hydrodynamic damping. Using relative velocity proved to decrease the extreme response of about 15- 20 % for all responses. Generally, the damping should be conservative, but an as accurate result as possible is always desired. The correct damping could be found from e.g. modelling tests.

7 References

- ANDERSEN, O. J. 2009. Statoil memo describing why and how tp should be corrected.
- BAARHOLM, G. S., HAVER, S. & ØKLAND, O. D. 2010. Combining contours of significant wave height and peak period with platform response distributions for predicting design response. *Marine Structures*, 23, 147-163.
- BÆKKEDAL, E. 2014. Alternative methods of realizing the sea spectrum for time-domain simulations of marine structures in irregular seas.
- BURY, K. V. 1975. Statistical models in applied science.
- DNV, D. N. V. 1996. Guidelines for Offshore Structural Reliability Analysis: Application to Jackup Platforms. *Joint Industry Project*, Report No 95-3203.
- DNV, D. N. V. 2010. DNV-RP-C205 Environmental conditions and environmental loads. *Norway: Det Norske Veritas*.
- DNV, D. N. V. 2012. DNV-RP-C104 Self-elevating units. *Recommended Practice*.
- DNV, D. N. V. 2013. Assessment of second order wave kinematics.
- FALTINSEN, O. 1993. *Sea loads on ships and offshore structures*, Cambridge university press.
- FENTON, J. D. 1985. A fifth-order Stokes theory for steady waves. *Journal of waterway, port, coastal, and ocean engineering*, 111, 216-234.
- FORRISTALL, G. 1978. On the statistical distribution of wave heights in a storm. *Journal of Geophysical Research: Oceans (1978–2012)*, 83, 2353-2358.
- FORRISTALL, G. Z. 2000. Wave crest distributions: Observations and second-order theory. *Journal of physical oceanography*, 30, 1931-1943.
- HARING, R., OSBORNE, A. & SPENCER, L. 1976. Extreme wave parameters based on continental shelf storm wave records. *Coastal Engineering Proceedings*, 1.
- HASSELMANN, K., BARNETT, T., BOUWS, E., CARLSON, H., CARTWRIGHT, D., ENKE, K., EWING, J., GIENAPP, H., HASSELMANN, D. & KRUSEMAN, P. 1973. Measurements of wind-wave growth and swell decay during the Joint North Sea Wave Project (JONSWAP). Deutches Hydrographisches Institut.

References

- HAYER, S. On the prediction of extreme wave crest heights. 7th Int. Workshop on Wave Hindcasting and Forecasting, Banff, Canada, 2002. Citeseer.
- HAYER, S. & NYHUS, K. A wave climate description for long term response calculations. 5th International OMAE Symposium, Tokyo, 1986. 27-34.
- HAYER, S. & WINTERSTEIN, S. R. 2009. Environmental contour lines: A method for estimating long term extremes by a short term analysis. *Transactions of the Society of Naval Architects and Marine Engineers*, 116, 116-127.
- HAYER, S. K. 2012. Recipe for estimating characteristic environmental load effect of drag governed structures significantly influenced by dynamics. *STATOIL*.
- HAYER, S. K. 2013. Prediction of Characteristic Response for Design Purposes (PRELIMINARY VERSION). *STATOIL*.
- JAHNS, H. & WHEELER, J. Long-term probabilities based on hindcasting of severe storms. Offshore Technology Conference, Houston, OTC, 1972.
- JAHNS, H. & WHEELER, J. 1973. Long-term wave probabilities based on hindcasting of severe storms. *J. Pet. Technol*, 473-486.
- JOHANNESSEN, T. B. On the Use of Linear and Weakly Nonlinear Wave Theory in Continuous Ocean Wave Spectra: Convergence With Respect to Frequency. ASME 2008 27th International Conference on Offshore Mechanics and Arctic Engineering, 2008. American Society of Mechanical Engineers, 211-217.
- LANGEN, I. & SIGBJØRNSSON, R. 1979. *Dynamisk analyse av konstruksjoner: Dynamic analysis of structures*, Tapir.
- LEIRA, B. J. 2014. TMR 4235 Stochastic Theory of Sea Loads, Probabilistic modelling and estimation.
- LONGUET-HIGGINS, M. S. 1963. The effect of non-linearities on statistical distributions in the theory of sea waves. *Journal of fluid mechanics*, 17, 459-480.
- MARTHINSEN, T. & WINTERSTEIN, S. R. On the skewness of random surface waves. Proc, 1992. 472-478.
- MYRHAUG, D. 2005. TMR4235 Stochastic Theory of Sea Loads. *Department of Marine Technology*.
- MYRHAUG, D. 2007. Marin Dynamikk–uregelmessig sjø. *Department of Marine Technology, NTNU*.
- NÆSS, A. 1985. The joint crossing frequency of stochastic processes and its application to wave theory. *Applied ocean research*, 7, 35-50.

References

- NORSOK, N. 2007. N003, Actions and Action Effects. *Norwegian Technology Standards Institution, Oslo, Norway, n-003*.
- ORR, M. J. 1996. Introduction to radial basis function networks. Technical Report, Center for Cognitive Science, University of Edinburgh.
- PIERSON, W. J. & MOSKOWITZ, L. 1964. A proposed spectral form for fully developed wind seas based on the similarity theory of SA Kitaigorodskii. *Journal of geophysical research*, 69, 5181-5190.
- SHARMA, J. & DEAN, R. 1981. Second-order directional seas and associated wave forces. *Society of Petroleum Engineers Journal*, 21, 129-140.
- SINTEF, M. 2010. USFOS Hydrodynamics: Theory Description of use Verification.
- STANSBERG, C. T. Non-Gaussian extremes in numerically generated second-order random waves on deep water. The Eighth International Offshore and Polar Engineering Conference, 1998. International Society of Offshore and Polar Engineers.
- TORSETHAUGEN, K. & HAVER, S. Simplified double peak spectral model for ocean waves. Proceedings of the 14th International Offshore and Polar Engineering Conference, Toulon, France, May, 2004. 23-28.
- WAMDI, T. G. 1988. The WAM model-a third generation ocean wave prediction model. *Journal of Physical Oceanography*, 18, 1775-1810.

References

A Results from Analyses

A.1 Scatter diagram

HS	SPECTRAL PEAK PERIOD																				SUM
	<2	2-3	3-4	4-5	5-6	6-7	7-8	8-9	9-10	10-11	11-12	12-13	13-14	14-15	15-16	16-17	17-18	18-19	19-20	>20	
0-1	0	84	2440	9795	8508	4072	2487	1958	1335	846	473	302	159	75	66	43	18	13	5	2	32681
1-2	0	0	109	3925	14361	18546	11615	5862	4112	3278	1846	865	299	183	96	59	19	9	1	0	65185
2-3	0	0	0	7	641	7358	13621	7142	2828	1662	1439	993	412	155	83	18	7	4	0	0	36370
3-4	0	0	0	0	1	256	3121	8071	3685	1239	546	363	246	125	62	27	11	4	0	0	17757
4-5	0	0	0	0	0	1	55	2120	3936	1505	512	185	63	46	48	8	5	0	1	0	8485
5-6	0	0	0	0	0	0	1	172	1135	1455	582	189	29	24	11	8	1	0	0	0	3607
6-7	0	0	0	0	0	0	0	0	142	449	417	221	42	13	7	0	1	0	0	0	1292
7-8	0	0	0	0	0	0	0	0	7	70	143	112	44	19	6	0	1	0	0	0	402
8-9	0	0	0	0	0	0	0	0	0	8	29	61	31	12	8	3	0	0	0	0	152
9-10	0	0	0	0	0	0	0	0	0	1	6	17	25	14	13	1	0	0	0	0	77
10-11	0	0	0	0	0	0	0	0	0	0	1	7	9	7	7	1	0	0	0	0	32
11-12	0	0	0	0	0	0	0	0	0	0	0	0	3	5	4	0	0	0	0	0	12
12-13	0	0	0	0	0	0	0	0	0	0	0	0	0	0	0	1	0	0	0	0	1
>13	0	0	0	0	0	0	0	0	0	0	0	0	0	0	0	0	0	0	0	0	0
SUM	0	84	2549	13727	23511	30233	30900	25325	17180	10513	5994	3315	1362	678	411	169	63	30	7	2	166053

Appendix 1: Scatter diagram of Hs and Tp for the Ekofisk-field

A.2 Stokes 5th of unchanged drag coefficient

Results of Stokes 5th analysis before the drag coefficient was reduced according to NORSOK.

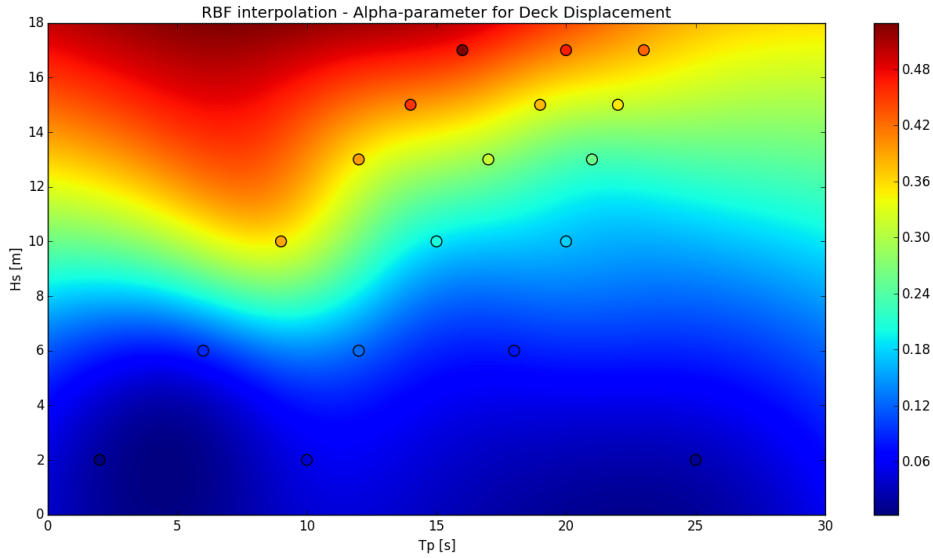
Appendix 2: : Resulting responses calculated with Design Wave Method using Stokes 5th wave with ordinary (time simulation) drag coefficients based on crest height from Forristall Crest distribution mean conditional period

Profile from Crest Height:	<i>Crest height</i> [m]	<i>Period, T</i> [s]	<i>Deck Displacement</i> [m]	<i>Base Shear</i> [N]	<i>Overturning Moment</i> [Nm]
ULS	15.1	16.4	0.36	1.29E+07	1.76E+09
ALS	19.6	19.2	0.69	2.55E+07	2.91E+09

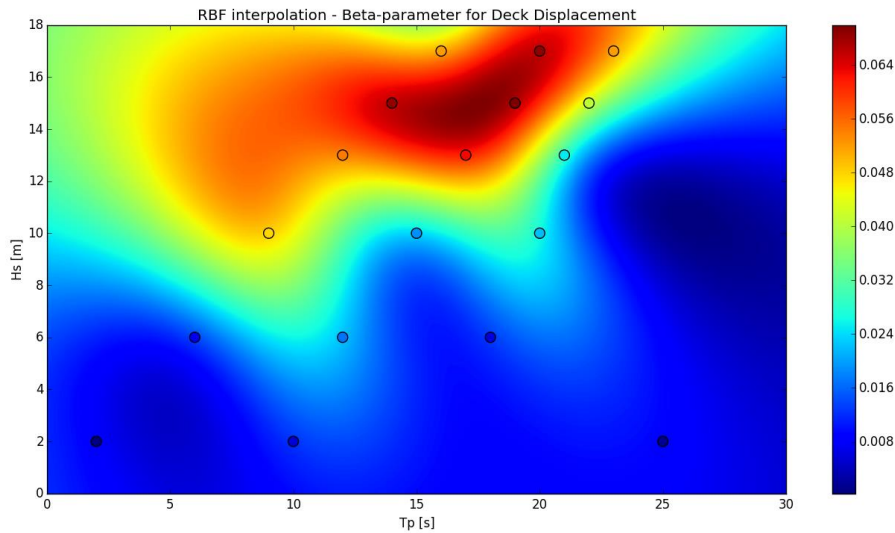
Appendix 3: Resulting responses calculated with Design Wave Method using Stokes 5th wave with ordinary (time simulation) drag coefficients based on wave height from Forristall Wave Height distribution and 90% confidence band of period

Profile decided by Wave Height	<i>Deck Displacement</i> [m]		<i>Base Shear</i> [N]	<i>Overturning Moment</i> [Nm]
ULS: Wave height 24.6 m				
<i>T [s]</i>	14.5	0.25	9.53E+06	1.49E+09
<i>T [s]</i>	16.4	0.30	1.07E+07	1.53E+09
<i>T [s]</i>	18.5	0.33	1.21E+07	1.61E+09
ALS: Wave height 31.7 m				
<i>T [s]</i>	17	0.57	1.99E+07	2.47E+09
<i>T [s]</i>	19.2	0.60	2.23E+07	2.58E+09
<i>T [s]</i>	21.7	0.61	2.47E+07	2.71E+09

A.3 Gumbel Parameters for Long-term Analysis

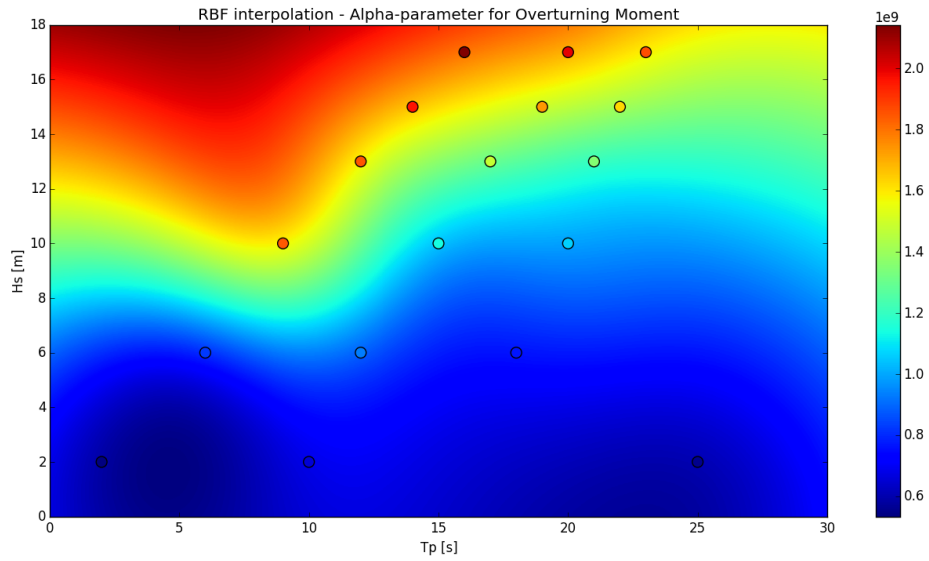


Appendix 4: The scale parameter, $\alpha(h_s, t_p)$, for the Gumbel distribution of extreme response for every value of H_s and T_p for Deck Displacement [m]. Created by interpolation, using the radial basis function with 18 selected sea states (circles) as input. Teal and Red con

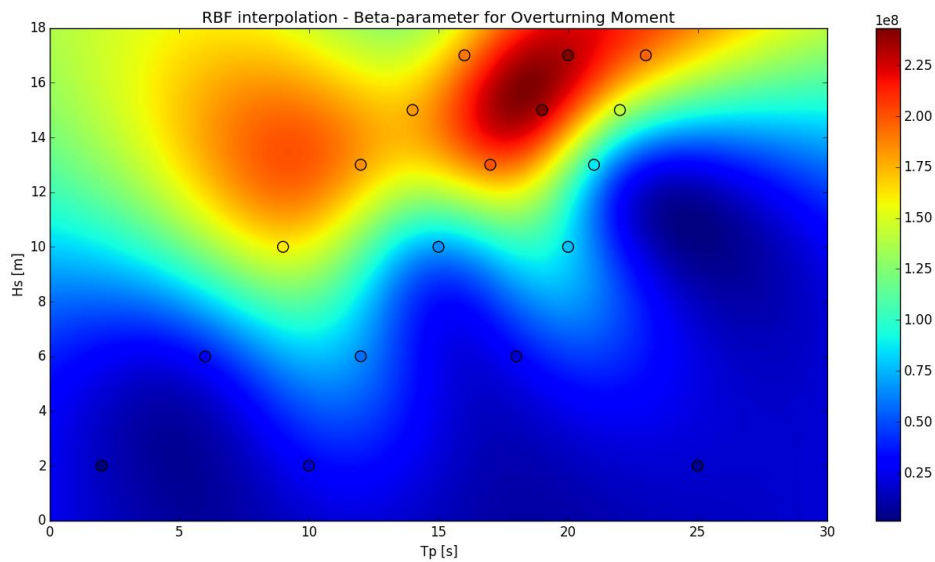


Appendix 5: The scale parameter, $\beta(h_s, t_p)$, for the Gumbel distribution of extreme response for every value of H_s and T_p for Deck Displacement [m]. Created by interpolation, using the radial basis function with 18 selected sea states (circles) as input. Teal and Red con

Results from Analyses

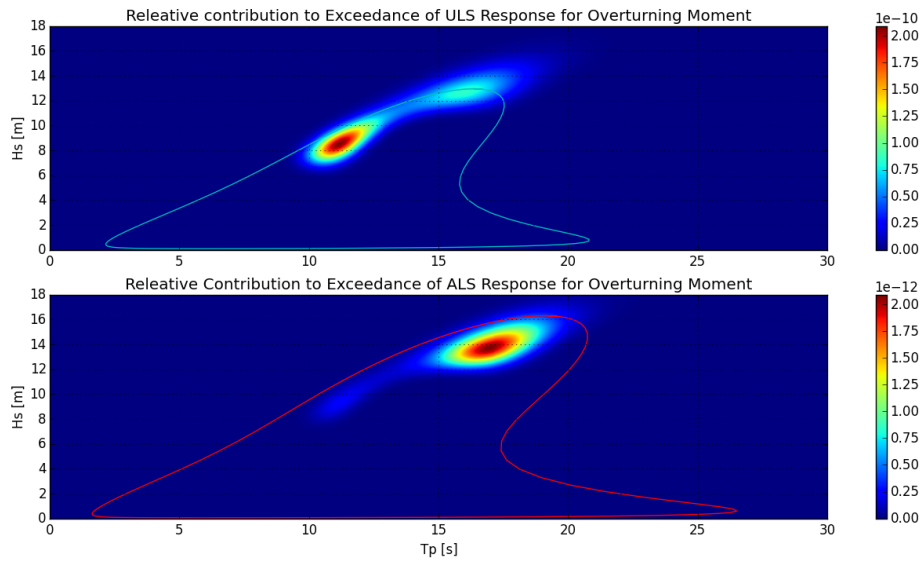


Appendix 6: The scale parameter, $\alpha(h_s, t_p)$, for the Gumbel distribution of extreme response for every value of H_s and T_p for Overturning Moment [Nm]. Created by interpolation, using the radial basis function with 18 selected sea states (circles) as input. Teal and Red con



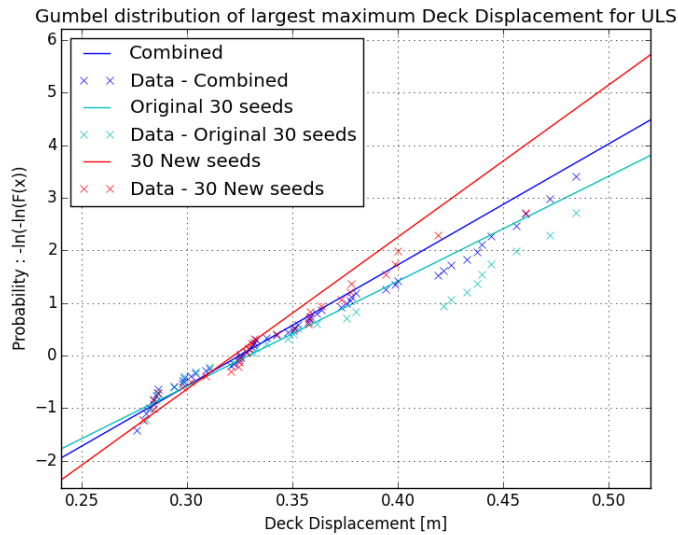
Appendix 7: The scale parameter, $\beta(h_s, t_p)$, for the Gumbel distribution of extreme response for every value of H_s and T_p for Overturning Moment [Nm]. Created by interpolation, using the radial basis function with 18 selected sea states (circles) as input. Teal and Red con

A.4 Relative Contribution to Extreme Response

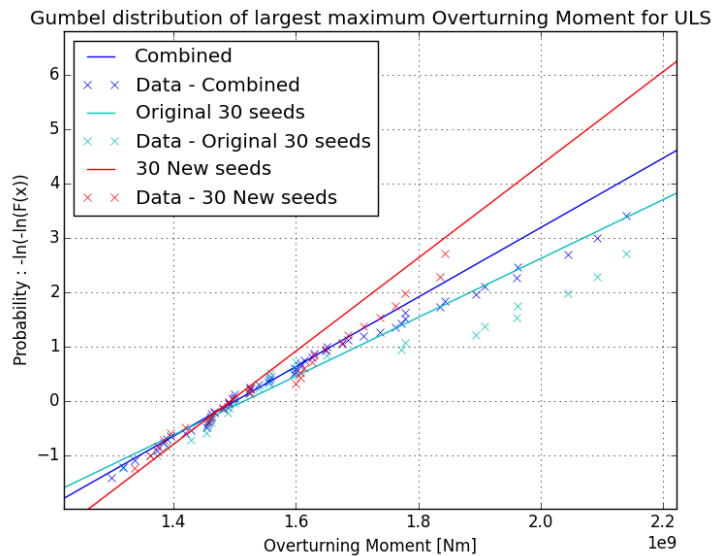


Appendix 8: Relative contribution to the probability of the response exceeding the limit states for Reaction Overturning Moment given the sea states parameters of H_s and T_p . Shown together with the respective environmental contours for ULS (upper) and ALS(lower

A.5 Number of Seeds in the Worst Sea State



Appendix 9: Comparison of resulting Gumbel extreme deck displacement distribution for the worst sea state for ULS using the original 30 seeds (teal), 30 new seeds (red) and the two samples combined into of containing 60 seeds (blue).



Appendix 10: Comparison of resulting Gumbel extreme overturning moment distribution for the worst sea state for ULS using the original 30 seeds (teal), 30 new seeds (red) and the two samples combined into of containing 60 seeds (blue).

B SOFTWARE

The programming language *Python* has been used to calculate all the statistical properties, using self-made scripts implemented with functions from open source *Python* packages. The output from these scripts have been used as input in the finite element software *USFOS*. Post-processing of *USFOS* results was also done in *Python*. All figures in this thesis have been plotted by self-written python scripts, unless stated otherwise. Some tables have been processed in *Excel* for better readability.

B.1 USFOS

USFOS is a computer program for nonlinear static and dynamic analysis of 3-dimensional structures in the time domain. It has been used to find the extreme responses on the jack-up investigated in this thesis. There are various modules in USFOS used for the computations. For time domain simulations, DYNRES, is a tool that processes the results and prints to file so that the data can be post-processed. In *DYNRES* the wave height, base shear and overturning moment is written to file for every time step, together with the deck displacements and time. The *USFOS* input consists of two files, the model file (cj70.fem) and head file (head.fem). The model file consists the nodes and elements of the structures FEM model, while the head file describes the loading and desired method of analysis. *USFOS* operates with *UNIX* commands, so a script to coordinate the simulations have been created in *Python*. When running a simulation, one must decide if it is to be static or dynamic and one can also look at design waves instead of whole time domain analysis of a sea state. This different methods of analysis are described in the USFOS Hydrodynamics manual. The different input for each simulation is defined in the head-file, while the model is described in the cj70.fem file.

To efficiently use *USFOS* it is important to use some kind of scripting to coordinate the different simulations. I decided to initiate USFOS using *python* to give commands directly to the windows command window. Python was also used to do changes in the head-file automatically so that every sea state could be run at once without any “manual” labor.

B.2 Python

Python is completely free, high-level programming language with a simple syntax that supports modules and packages which are available for free online. The scripts in this report were made

SOFTWARE

using *WinPython* version 2.7.9.1. *WinPython* is a free, open-source distribution of *Python 2.7* for *Windows 8*, especially designed for scientists and thus integrates libraries such as *NumPy*, *SciPy* and *Matplotlib*. The scripts have been written and run from the editor *Sublime Text 3*, but any text editor could be used.

Python, with all its included libraries and packages, is a great mathematical tool with similar capabilities to e.g. *MATLAB*. An advantage with *Python* is that it is also attractive for scripting, file-handling and connecting existing components together, and is also free to download. *Python* has no compilation step, which means debugging is extremely fast and the program can be run directly from the command window (*cmd*) or *Windows PowerShell*. Since scripting and file-handling is easy in *Python*, it has been used to give direct input and commands to *USFOS* for the time domain simulations. Every script and function is extensively commented to describe how it operates.

In this report *Python* has been used for:

- Creating Metocean Report, including reading of hindcast data, all calculations, plotting of results and generating input for *USFOS*.
- Scripting and file-handling for efficient use of *USFOS* with multiple simulations.
- Post-processing output from *USFOS*.
- Visualizations and plots in this report